doi.org/10.26434/chemrxiv.7877987.v1

Evaluation of Potent Isoquinoline-Based Thiosemicarbazone Antiproliferatives Against Solid Tumor Models

Daniel Sun, Soumya Poddar, Roy D. Pan, Juno Van Valkenburgh, Ethan Rosser, Evan Abt, Vincent Lok, Joseph Capri, Selena Hernandez, Janet Song, Joanna Li, Laurent Vergnes, Anthony Cabebe, Wesley Armstrong, Sheba Plamthottam, Dalton Steele, Corey Osto, Andreea Stuparu, Thuc Le, Karen Reue, Robert Damoiseaux, Johanes Czernin, Michael Jung, Caius Radu

Submitted date: 22/03/2019 • Posted date: 25/03/2019

Citation information: Sun, Daniel; Poddar, Soumya; Pan, Roy D.; Van Valkenburgh, Juno; Rosser, Ethan; Abt, Evan; et al. (2019): Evaluation of Potent Isoquinoline-Based Thiosemicarbazone Antiproliferatives Against Solid Tumor Models. ChemRxiv. Preprint.

The lead compound, an □-N-heterocyclic carboxaldehyde thiosemicarbazone HCT-13, was highly potent against a panel of pancreatic, small cell lung carcinoma, and prostate cancer models, with IC_{90} values in the low-to-mid nanomolar range. We show that the cytotoxicity of HCT-13 is copper-dependent, that it acts as a copper ionophore, induces production of reactive oxygen species (ROS), and promotes mitochondrial dysfunction and S-phase arrest. Lastly, DNA damage response/replication stress response (DDR/RSR) pathways, specifically Ataxia-Telangiectasia Mutated (ATM) and Rad3-related protein kinase (ATR), were identified as actionable adaptive resistance mechanisms following HCT-13 treatment. Taken together, HCT-13 is potent against solid tumor models and warrants in vivo evaluation against aggressive tumor models, either as a single agent or as part of a combination therapy.

File list (2)

Evaluation of potent isoquinoline-based thiosemicarbazone antiproliferatives against solid tumor models

Daniel L. Sun[†1,2,3], Soumya Poddar[†1,2], Roy D. Pan[1,2,3], Juno Van Valkenburgh[1,2,3], Ethan W. Rosser[1,2,3], Evan R. Abt[1,2], Vincent Lok[1], Joseph Capri[1,2], Selena P. Hernandez[3], Janet Song[1], Joanna Li[1], Laurent Vergnes[5], Anthony E. Cabebe[1], Wesley R. Armstrong[1], Sheba Plamthottam[3], Dalton Steele[3], Corey Osto[1], Andreea D. Stuparu[1,2], Thuc M. Le[1,2], Karen Reue[5,6], Robert Damoiseaux[4], Johannes Czernin[1,2], Michael E. Jung[3], and Caius G. Radu*[1,2]

[1]Department of Molecular and Medical Pharmacology, [2]Ahmanson Translational Imaging Division, University of California, Los Angeles, California 90095, United States, [3]Department of Chemistry and Biochemistry, University of California, Los Angeles, California 90095, United States, [4]UCLA Metabolomic Center, University of California, Los Angeles, Los Angeles, CA 90095, USA, [5]Department of Human Genetics, David Geffen School of Medicine, University of California, Los Angeles, California 90095, United States, [6]Molecular Biology Institute, University of California, Los Angeles, California 90095, United States.

[†] Contributed equally to this work

*Correspondence and requests for materials should be addressed to C.G.R. (email: cradu@mednet.ucla.edu)

ABSTRACT: A potent class of isoquinoline-based α-N-heterocyclic carboxaldehyde thiosemicarbazone (HCT) compounds has been re-discovered; based on this scaffold we have synthesized three series of antiproliferative agents through iterative rounds of methylation and fluorination modifications. Synergy between isoquinoline fluorination and 4' amine methylation was identified, and incubation of the compounds with physiologically relevant levels of $CuCl_2$ was shown to further potentiate their activity. The lead compound, **HCT-13**, was highly potent against a panel of pancreatic, small cell lung carcinoma, and prostate cancer models, with IC_{90} values in the low-to-mid nanomolar range. We show that the cytotoxicity of **HCT-13** is copper-dependent, that it acts as a copper ionophore, induces production of reactive oxygen species (ROS), and promotes mitochondrial dysfunction and S-phase arrest. Lastly, DNA damage response/replication stress response (DDR/RSR) pathways, specifically Ataxia-Telangiectasia Mutated (ATM) and Rad3-related protein kinase (ATR), were identified as actionable adaptive resistance mechanisms following **HCT-13** treatment. Taken together, **HCT-13** is potent against solid tumor models and warrants *in vivo* evaluation against aggressive tumor models, either as a single agent or as part of a combination therapy.

INTRODUCTION

The diverse therapeutic potential of α-N-heterocyclic carboxaldehyde thiosemicarbazones (HCTs) have been investigated since the 1940s, with tuberculostatic activity being first observed *in vivo* as early as 1946.[1] This class of compounds was subsequently shown to possess antitumor, antiviral, antibacterial, and antifungal activities, prompting decades of research and development.[2–7] In particular, isoquinoline-based HCTs such as IQ-1 (**HCT-1**)[3] were the subject of early interest due to their efficacy, particularly in terms of 50-day survival rates of tumor-bearing mice (**Figure 1**).[5] The research groups of Sartorelli and French spent decades developing isoquinoline HCTs and investigating other HCT scaffolds, eventually turning their attention to pyridyl-based HCT analogs. Notably, in 1992 Sartorelli and coworkers developed 3-aminopyridine-2-carboxaldehyde thiosemicarbazone (3-AP, also known as Triapine), a pyridyl-based HCT. It has since undergone multiple clinical trials for the treatment of various cancers, and it is widely accepted to inhibit ribonucleotide reductase (RNR), a critical enzyme for rapidly proliferating cells such as bacteria and cancer cells.[8–14] Two other HCT compounds, namely di-2-pyridylketone 4-cyclohexyl-4-methyl-3-thiosemicarbazone (DpC) hydrochloride and 4-(2-pyridinyl)-2-(6,7-dihydro-8(5*H*)-quinolinylidene)hydrazide-1-piperazinecarbothioic acid (COTI-2)[15,16], have been investigated in the clinic. However, despite the early promise, no HCT compounds have yet advanced beyond phase II clinical trials.[13]

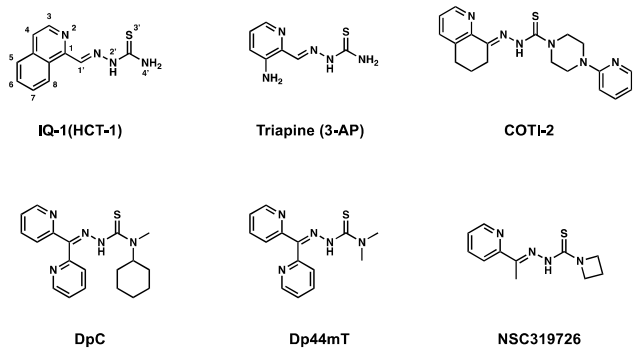

Figure 1. Structures of α-N-heterocyclic carboxaldehyde thiosemicarbazone (HCT) compounds of clinical and research significance.

While the mechanisms of action of HCTs are multi-modal and have not yet been fully defined[17–25], their biological activities generally stem from the ability to chelate transition metals through their heterocyclic nitrogen, Schiff base nitrogen, and thiosemicarbazone sulfur. The resulting HCT-metal complexes can undergo redox cycles, a property that generates cytotoxic reactive oxygen species (ROS) through Fenton and/or Haber-Weiss processes.[26] HCTs are particularly adept at binding copper[27], which can be either detrimental or beneficial to the compound's biological activity. For instance, physiological concentrations of copper in human plasma (11-18 μM)[28,29] strongly interfere with the RNR-inhibitory activity of 3-AP[27], while the cytotoxicities of Dp44mT[30,31] and NSC-319726[32] against glioblastoma and other cancer models are potentiated by copper. Binding of this transition metal is intriguing from an anticancer therapy standpoint, as cancers rely upon higher intracellular levels of copper, relative to healthy cells, to promote angiogenesis, tumor growth, and metastasis.[33,34] Indeed, several therapeutic strategies have employed small molecules to disrupt copper homeostasis in cancers, either through chelation-mediated copper sequestration, or by increasing intracellular copper to cytotoxic levels through ionophoric modalities.[32,35]

The antiproliferative effects of HCTs coupled with their ability to bind copper make them a compelling scaffold from which to develop copper-mediated therapeutics. We have identified isoquinoline-based HCTs as a viable scaffold for this purpose, as previously reported analogs demonstrated both *in vitro* and *in vivo* efficacy. Additionally, studies investigating the isoquinoline HCT chemical space have not emerged for years, as focus shifted away from this scaffold following the report of 3-AP.[3,5,6] Therefore, we aimed to develop novel isoquinoline-based HCTs which leverage copper against malignancies. Herein, the design and synthesis of such a series of molecules is reported, with identification of a lead compound (**HCT-13**) which inhibits proliferation of pancreatic ductal adenocarcinoma (PDAC), small cell lung carcinoma (SCLC), and prostate cancer (PC) models at nanomolar concentrations in the presence of physiologically relevant levels of copper. We further demonstrate that **HCT-13** increases intracellular copper levels, generates reactive oxygen species (ROS), and interferes with the mitochondrial electron transport chain. Additionally, we have identified actionable adaptive resistance mechanisms which could be exploited in combination therapies.

RESULTS

Synthesis of isoquinoline-based α-N-heterocyclic carboxaldehyde thiosemicarbazone (HCT) compounds

Among the previously reported isoquinoline HCTs, the 5-, 7-, and 8-fluoro analogs of **HCT-1** were of particular interest to our group. These compounds varied in terms of potency and toxicity[5], demonstrating that the effects of fluorination were dependent upon the position of isoquinoline substitution. The benefits that fluorination endows upon small-molecule drugs are well documented[36,37], and are also reflected in the marketplace, since approximately 20% of all pharmaceuticals are fluorinated.[38] Therefore, it was important to investigate how the previously unreported 4- and 6-fluoro analogs of **HCT-1** would perform in antiproliferative assays against cancer models. Additionally, we were intrigued as to whether fluorination at these positions would synergize with 4' amine alkylation, as Kowol et al. discovered that 4' amine alkylation potentiated the cytotoxicity of 3-AP analogs.[39]

Scheme 1. Synthesis HCT compounds 1-15 from simple isoquinolines[a,b]

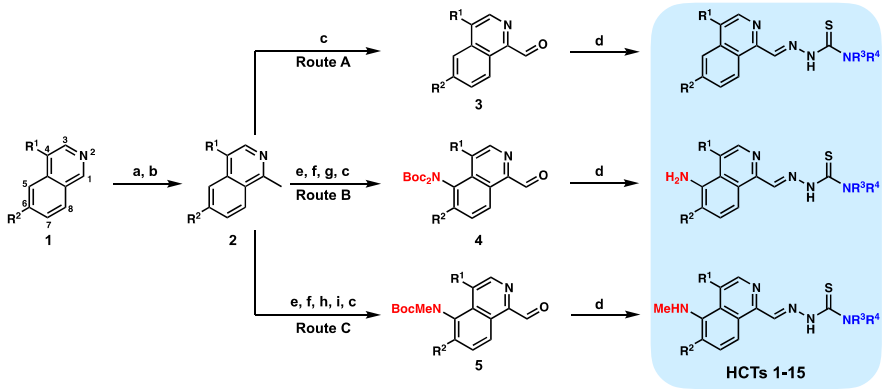

[a](a) allyl chloroformate, MeMgBr, THF; (b) $Pd(PPh_3)_4$, morpholine; DDQ, CH_2Cl_2; (c) SeO_2, 1,4-dioxane, 60 °C; (d) appropriate thiosemicarbazide, HCl, EtOH, reflux or microwave 50 °C; (e) KNO_3, H_2SO_4; (f) Fe, HCl, MeOH, reflux; (g) Boc_2O, DMAP, TEA, THF; (h) Boc_2O, DMAP, TEA, THF; $NaHCO_3$, MeOH, reflux or K_2CO_3, MeOH, reflux; (i) NaH, THF; MeI. [b]HCTs 1-3, 6-8, and 11-13 synthesized through Route A; HCTs 5 and 10 synthesized through Route B; HCTs 4, 9, 14, and 15 synthesized through Route C. See Supporting Information for full synthetic details.

Table 1. Substitution patterns of HCTs 1-15

	HCT-1	HCT-2	HCT-3	HCT-4	HCT-5	HCT-6	HCT-7	HCT-8	HCT-9	HCT-10	HCT-11	HCT-12	HCT-13	HCT-14	HCT-15
R^1	H	F	H	H	H	H	F	H	H	H	H	F	H	H	F
R^2	H	H	F	H	H	H	H	F	H	H	H	H	F	F	H
R^3	H	H	H	H	H	Me	Me	Me	Me	Me	Me	Me	Me	Me	Me
R^4	H	H	H	H	H	H	H	H	H	H	Me	Me	Me	Me	Me
5-Pos	H	H	H	NHMe	NH_2	H	H	H	NH_2	NHMe	H	H	H	NHMe	NHMe

A total of 15 isoquinoline-based HCTs – four known compounds (**HCT-1, HCT-4, HCT-5, HCT-6**) and 11 novel compounds – were synthesized and tested for antiproliferative potency against cancer models (**Scheme 1, Table 1**). The synthetic approach began with methylation of the appropriate isoquinoline **1** to generate **2** (**Scheme 1**). Depending upon the desired 5-position substituent, **2** was then subjected to either Route A (5-hydrido), Route B (5-amino), or Route C (5-methylamino). Syntheses of **HCTs 1-3**, **HCTs 6-8**, and **HCTs 11-13** were carried out by Route A, wherein the methyl substituent of **2** was oxidized using selenium dioxide (SeO_2) to furnish the carboxaldehyde **3**. Condensation with the appropriate thiosemicarbazide under acidic conditions yielded the desired HCT. **HCT-5** and **HCT-10** were synthesized *via* Route B, which began with nitration of **2** followed by an iron-mediated reduction to the amine, which was subsequently Boc-protected and oxidized to produce carboxaldehyde **4**. This intermediate was then simultaneously Boc-deprotected and condensed with the appropriate thiosemicarbazide under acidic conditions to furnish the target HCT. Syntheses of **HCT-4**, **HCT-9**, **HCT-14**, and **HCT-15** *via* Route C proceeded from **2** with installation of a nitro group, subsequent conversion to the mono-Boc-methylamine, and SeO_2-mediated oxidation to furnish **5**. Concurrent Boc-deprotection and thiosemicarbazide condensation were again achieved under acidic conditions to provide the desired HCT compound. While characterizing the HCTs, we occasionally observed the presence of a minor Z-isomeric product, particularly for **HCTs 11-15**. This isomer arose from an intramolecular hydrogen bond between the 2' amine of the thiosemicarbazone and the heterocyclic isoquinoline nitrogen, forming a stable 6-membered hydrogen bonded species.[40] The E and Z isomers were inseparable by reversed-phase HPLC purification and were used as a mixture *in vitro*, as previous studies reported no significant difference in potency.[40]

Fluorination and dimethylation display synergistic effects further potentiated by copper supplementation

IC_{90} values against MIAPACA2 cells for all compounds were first determined in normal cell culture conditions (DMEM media and 10% FBS) (**Figure 2**). Compounds were separated into three series – 4' primary amines, 4' secondary amines, and 4' tertiary amines – to reflect the relative degrees of 4' amine methylation. A series of non-methylated 4' primary amine compounds was first synthesized, with known compounds **HCT-1**, **HCT-4**, and **HCT-5** included to gauge whether fluorination of the isoquinoline proved

beneficial for biological activity.[41,42] Within the 4' primary amine series, fluorination at the isoquinoline 4-position (**HCT-2)** did not show an increase in potency relative to unsubstituted analog **HCT-1**. However, fluorination at the 6-position (**HCT-3)** showed a 3-fold increase in potency, demonstrating that the fluorine position impacts the potency of these compounds.

In the 4' secondary amine series, synergistic effect was observed when combining isoquinoline fluorination with 4' amine methylation. The 4-fluorine substituted **HCT-7** and the 6-fluorine substituted **HCT-8** were each significantly more potent than their non-fluorinated analog **HCT-6**, as well more potent than their 4' primary amine analogs (**HCT-2** and **HCT-3**, respectively). The trend of isoquinoline substitution and 4' secondary amine combining to enhance potency held for 5-methylamino substituted **HCT-9** and 5-amino substituted **HCT-10**. Taken together, these results suggested that combining isoquinoline substitution, particularly 4- or 6-fluorination, with 4' amine methylation produced synergistic antiproliferative effects when compared with either modification alone.

The effects of fluorine substitution became significantly more pronounced for the di-methylated 4'-tertiary amine compounds **HCT-12** and **HCT-13**, whose IC_{90} values were in the nM range and were roughly 110- and 270-fold more potent, respectively, when compared to their non-fluorinated analog **HCT-11**. Fluorination at the 6-position (**HCT-13**) was found to be a superior modification when compared to fluorination at the 4-position (**HCT-12**), a trend which also held for the fluorine-substituted 5-methylamino compounds **HCT-14** and **HCT-15**.

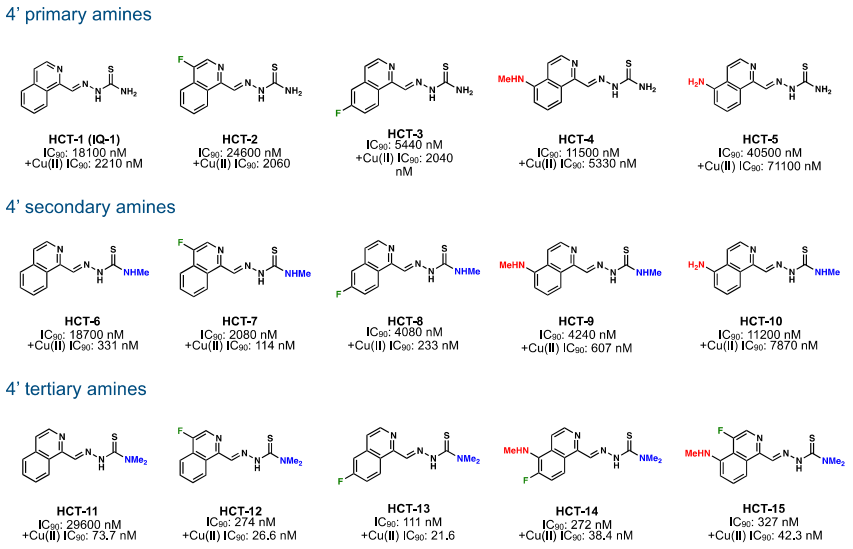

Figure 2 | Cu(II) supplementation potentiates the activity of isoquinoline HCTs. MIAPACA2 cells were treated with the indicated HCT ± 20 µM Cu(II) for 72 h, then cell viability was measured with CellTiter-Glo to determine IC_{90} values.

HCT compounds are known to be copper chelators, and a recent publication by Stockwell and coworkers demonstrated that the activity of a known 4' tertiary amine HCT (NSC-319726) was significantly potentiated by the addition of copper.[32] To test whether our compounds were similarly potentiated, IC_{90} (+Cu IC_{90}) values were determined against MIAPACA2 cells in media supplemented with physiologically relevant levels of copper (DMEM media + 10% FBS + 20 µM $CuCl_2$) (**Fig. 2)**. While the activity of **HCT-5** was attenuated, all other compounds displayed a significant increase in potency under copper-supplemented conditions. For non-fluorinated isoquinoline compounds **HCT-1**, **HCT-6**, and **HCT-11**, the +Cu IC_{90} values improved as the degree of methylation at the 4' amine increased (10-fold, 60-fold, and 400-fold increase in potency, respectively, versus non-copper-supplemented IC_{90} values). Copper supplementation was similarly beneficial for fluorinated isoquinolines – all such compounds displayed significant improvements in antiproliferative potency in presence of copper, and fluorine substitution led to greater potency when compared with corresponding non-fluorinated analogs. Compounds bearing 4' tertiary amines were the most active, achieving +Cu IC_{90} values as low as 21.6 nM (**HCT-13**). The results demonstrated that physiologically relevant levels of copper potentiated the activity of

isoquinoline HCTs, and that 4' amine methylation synergized with fluorine substitution. Due to its potency and straightforward synthesis, we chose **HCT-13** as a lead compound for in-depth mechanism of action studies.

HCT-13 highly potent against a panel of solid tumor models and induces copper-dependent cytotoxicity

Serum copper levels are elevated (>20 µM) in individuals with solid tumor types such as pancreatic ductal adenocarcinoma (PDAC), small cell lung carcinoma (SCLC), and prostate cancer (PC).[43–48] These cancers rely upon elevated copper levels to sustain growth, making this transition metal a viable target for therapeutic modulation.[34] In a panel of PDAC, SCLC, and PC cancer models cultured in media supplemented with physiologically relevant levels of copper (20 µM $CuCl_2$), **HCT-13** was a highly potent growth inhibitor, with +Cu IC_{90} values ranging from 1 nM to 200 nM (**Figure 3a**). The MIAPACA2 cell line, a well-characterized PDAC model that was highly sensitive to **HCT-13** treatment, was used to further investigate the mechanism of action of the lead compound.

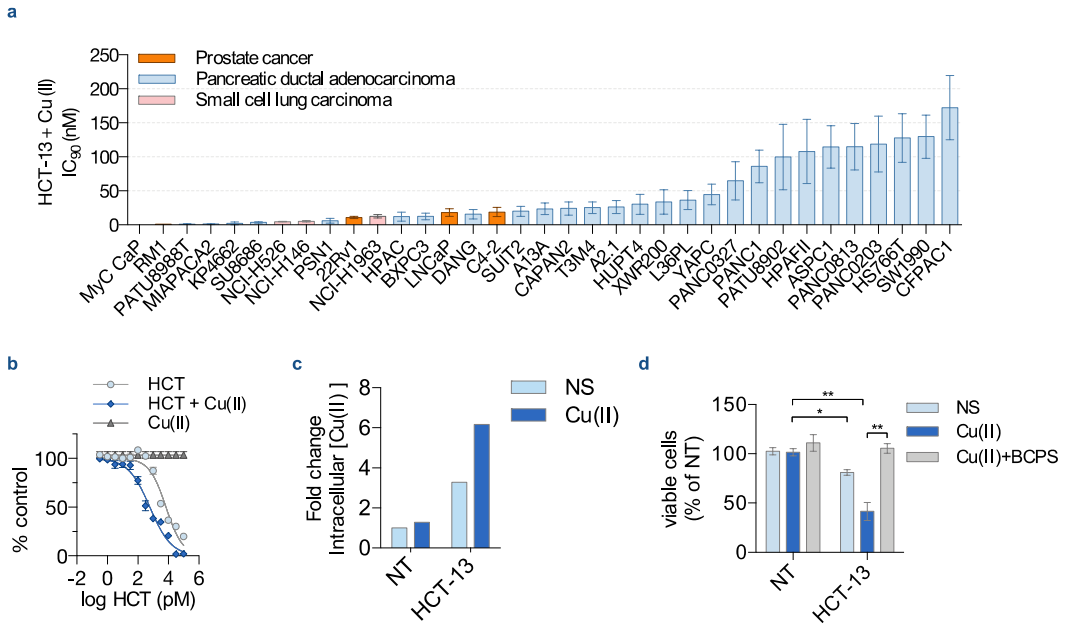

Fig. 3 | Copper potentiates HCT-13 toxicity against a panel of cancer models. (**a**) IC_{90} in a panel of human and mouse prostate cancer (PC), small cell lung carcinoma (SCLC) and pancreatic ductal adenocarcinoma (PDAC) models treated with HCT-13 + Cu(II) (20 µM) for 72h measured by CellTiterGlo. (**b**) Proliferation rate of MIAPACA2 PDAC cells measured by CellTiterGlo following HCT-13 treatment for 72h ± Cu(II) (20 µM), and with Cu(II) alone. (**c**) Intracellular concentrations of copper measured by inductively coupled plasma mass spectrometry (ICP-MS) in MIAPACA2 PDAC cells treated with HCT-13 (25nM) for 24h ± Cu(II) (20 µM). (**d**) Inhibition of proliferation of MIAPACA2 cells treated with HCT-13 (25nM) + Cu(II) (20 µM) for 24h ± bathocuproine disulfonate (BCPS, 300 µM) measured by trypan blue exclusion.

(mean ± SD, n = 2, one-way ANOVA corrected for multiple comparisons by Bonferroni adjustment, * $P < 0.05$; ** $P < 0.01$; *** $P < 0.001$).

MIAPACA2 proliferation was measured in response to **HCT-13** in the presence and absence of 20 µM $CuCl_2$ (Cu(II)), as well as in response to 20 µM Cu(II) alone (**Figure 3b**). The potency of **HCT-13** improved by greater than 5-fold under Cu(II) supplemented conditions, with its IC_{90} decreasing from 110 nM to 21 nM. Importantly, Cu(II) supplementation alone did not affect proliferation at all. To probe whether **HCT-13** was acting as an ionophore, intracellular copper levels were measured using inductively coupled plasma mass spectrometry (ICP-MS). In the presence of **HCT-13**, intracellular copper levels increased both with and without Cu(II) supplementation (**Figure 3c**). Additionally, treatment with bathocuproine disulfonate (BCPS), a membrane impermeable Cu(II) chelator, abrogated the cytotoxicity of **HCT-13** in the presence of Cu(II), suggesting that the growth inhibitory effect of our lead compound is largely dependent upon the availability of copper (**Figure 3d**). Collectively, this data suggests that **HCT-13** is a Cu(II) ionophore which increases intracellular copper concentration, and whose cytotoxicity is copper-dependent.

HCT-13 induces oxidative stress and ROS production

While **HCT-13** in the presence of Cu(II) exhibited nanomolar potency against a panel of solid cancer models, the underlying reasons remained unknown as the canonical mechanism of HCT cytotoxicity is poorly defined in the literature. Cu(II)-supplemented MIAPACA2 cells treated with **HCT-13** showed induction of AMPK phosphorylation (T172) at 24 h, demonstrating suppression of mitochondrial oxidative phosphorylation (**Figure 4a**). Further, **HCT-13** treatment increased heme oxygenase-1 (HO-1) levels in MIAPACA2 cells, indicative of ROS induction (**Figure 4a**). Based on the immunoblot results, we set out to determine whether **HCT-13** treatment was leading to ROS generation. We found that treatment with our lead compound induced ROS generation detectable by CM-H_2DCFDA staining (**Figure 4b**). Interestingly, ROS generation resulting from **HCT-13** treatment of MIAPACA2 cells was also observed in the mitochondria, as measured by mitochondria-specific dye MitoSOX (**Figure 4c**).

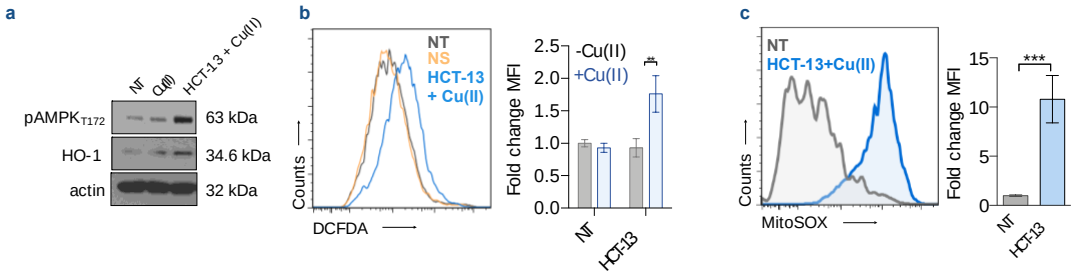

Figure 4 | Induction of ROS by HCT-13. (**a**) Representative immunoblots of MIAPACA2 PDAC cells treated as indicated for 24h. (**b**) Reactive oxygen species (ROS) measurement using CM-H2DCFDA staining after HCT-13 (25nM) + Cu(II) (20 µM) treatment for 24h. (**c**) Mitochondrial ROS detection using MitoSOX staining in MIAPACA2 PDAC cells treated with HCT-13 (25 nM) + Cu(II) (20 µM) for 24h.

(mean ± SD, n = 2, Student t-test, ***$P < 0.001$).

HCT-13 induces mitochondrial dysfunction and displays mitochondria-dependent cytotoxicity

Considering the canonical role AMPK plays in energy homeostasis, and the implication that AMPK activation may signal mitochondrial dysfunction[49], we compared the metabolic status of MIAPACA2 cells treated with **HCT-13** for 24 hr with and without 20 µM Cu(II) using a Seahorse Bioscience XFe24 analyzer. In the presence of Cu(II), **HCT-13** significantly reduced both the basal respiration and maximum respiratory capacities of MIAPACA2 cells, indicating mitochondrial electron transport chain (mtETC) impairment (**Figure 5a**). *In vitro* mitochondrial complex activity following **HCT-13** treatment was dissected by an electron flow assay in isolated mitochondria, which showed decreased activity of complexes I and II (**Figure 5b**).

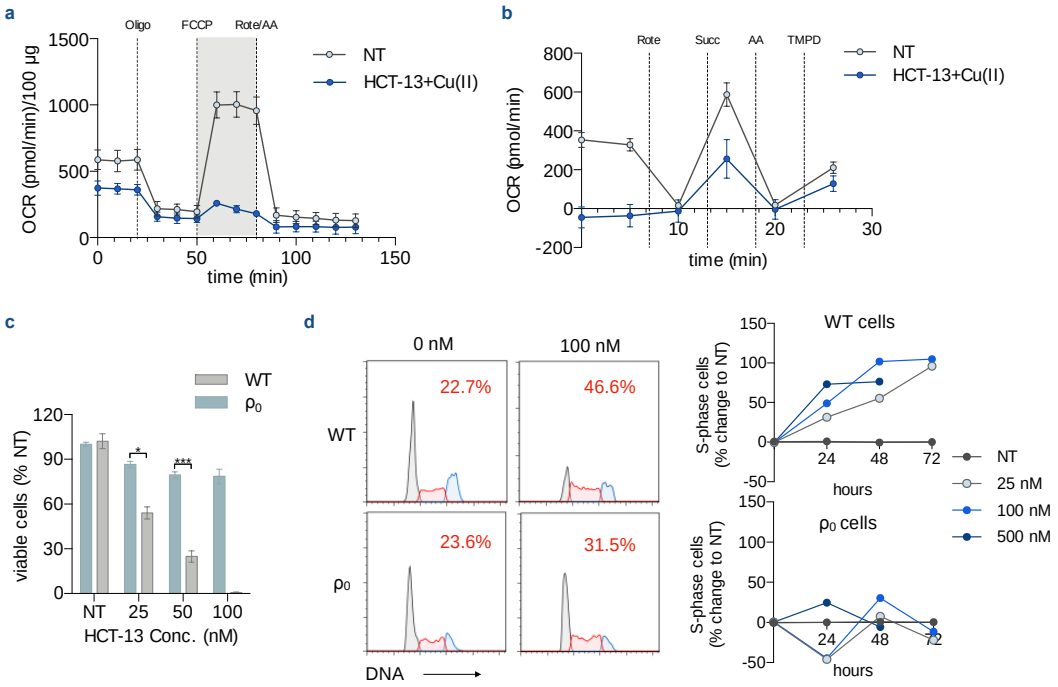

Figure 5 | HCT-13 alters cellular energetics through inhibition of electron transport chain and has selective mitochondrial toxicity. (a) Mito Stress Test of MIAPACA2 PDAC cells treated with HCT-13 (25 nM) + Cu(II) (20 µM) for 24h. (b) Electron flow assay in isolated mitochondria treated with HCT-13 (100 nM) + Cu(II) (20 µM) for 1h. (c) Viability of 143 BTK parental (wild type, WT) and ρ_0 cells after 48h of the indicated HCT-13 concentration + Cu(II) (20 µM) treatment, assessed with Trypan Blue Staining. (d) 48h cell cycle histogram and plots of S-phase arrest plots in 143 BTK WT and 143 BTK ρ_0 cells at 24, 48 and 72h following treatment with indicated concentrations of HCT-13 + Cu(II) (20 µM).

(mean ± SD, n = 2, one-way ANOVA corrected for multiple comparisons by Bonferroni adjustment, * $P < 0.05$; ** $P < 0.01$; *** $P < 0.001$).

These findings suggested that **HCT-13** inhibited mtETC activity but did not indicate whether the lead compound's cytotoxicity stemmed from effects independent of mitochondrial function. Another HCT compound, Dp44mT, was reported to increase AMPK expression and induce ROS, although its cytotoxicity was not attributed to the functionality of the mitochondria.[50] To determine whether the cytotoxicity of **HCT-13** was mitochondria-dependent, its effects upon 143 BTK ρ_0, an mtDNA-deficient fibroblast cell line, were examined. Both 143 BTK ρ_0 and parental (wild type, WT) cells were treated with **HCT-13** + 20 µM Cu(II) for 48 h, after which cell viability was determined through trypan blue staining (**Figure 5c**). Compared to WT, the ρ_0 cells were significantly less sensitive to the treatment. The cytotoxicity of **HCT-13** was partially abolished by supplementation with uridine (rU) but not by pyruvate, suggesting disruption to the supply of pyrimidine nucleotides in addition to impaired mitochondria (**Supplementary Figure S2a**). Proper mitochondrial function is necessary for the action of dihydroorotate dehydrogenase, an enzyme critical for the *de novo* production of pyrimidine nucleotides, and one for which **HCT-13** did not demonstrate affinity (**Supplementary Figure S2b**). Additionally, cell cycle analysis revealed marked S-phase arrest in 143 BTK WT cells but not in 143 BTK ρ_0 (**Figure 5d**). Taken together, these results indicate that the cytotoxic effects of **HCT-13** are mitochondria-dependent and suggest that **HCT-13** may be indirectly targeting DHODH, and thus *de novo* pyrimidine nucleotide production, through induction of mitochondrial dysfunction.

Small molecule kinase inhibitor screen with HCT-13 identifies the DNA-damage pathway as a resistance mechanism

To identify potential resistance mechanisms and synergistic interactions with **HCT-13**, we performed an unbiased pharmacological inhibition screen using a chemical genomics platform consisting of 430 kinase inhibitors (Selleckchem, Cat. L1200). MIAPACA2 cells were treated with the 430-member library, covering a 7-point concentration range spanning between 6.5 nM and 5 µM, with and without 25 nM **HCT-13** in presence of 20 µM $CuCl_2$. After 72 h of incubation, ATP content was measured using CellTiter-Glo (**Figure 6a**). A composite synergy score was calculated for each combination, defined as the sum of the Bliss Additivity Score (%

proliferation inhibition observed - % proliferation inhibition expected). A positive synergy score indicates greater-than-additive interaction, and a negative score indicates less-than-additive interaction i.e. antagonism.

The ten highest scoring compounds were kinase inhibitors contained in the DNA damage response/replication stress response (DDR/RSR) module, with the ATM/ATR/CHK pathway featuring as the most prominent codependency (**Figure 6b, 6c**). All six ATM, ATR and CHEK1 inhibitors included in the library scored positively in the screen, indicating synergy with our lead compound. Upon **HCT-13** + Cu(II) treatment, we consistently observed phosphorylation of the downstream targets of ATR and ATM, CHEK1 and CHEK2, respectively, indicating activation of this pathway as an adaptive resistance mechanism. This phosphorylation was accompanied by induction of DNA damage marker pH2AX and by cleavage of apoptotic marker caspase 3 (**Figure 6d**). The synergistic interaction between **HCT-13** and ATR inhibition was further validated using cell death assays measured by Annexin V/PI and Trypan Blue Viability Staining in PDAC (MIAPACA2, CFPAC-1) and PC (C4-2) cell lines (**Figure 6E, 6F, and Supplementary Figure S3b, S3c**).

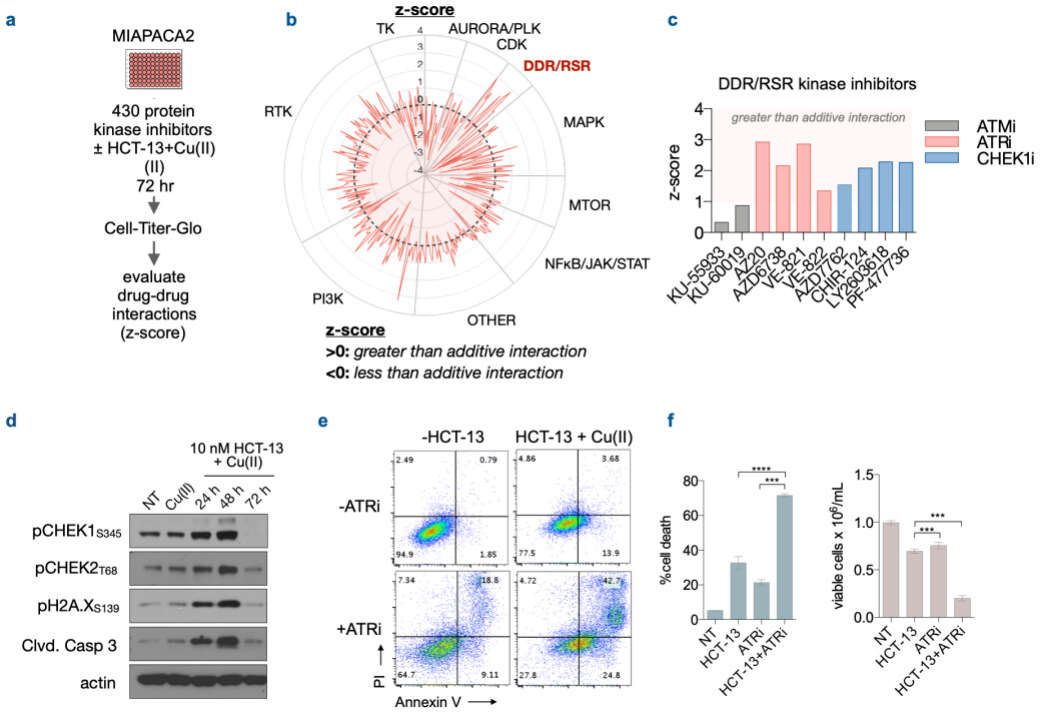

Figure 6 | A chemical genomics screen identifies the replication stress response pathway as an actionable co-dependency of HCT-13-treated cells. (a) Experimental design of a synthetic lethality screen using a library of protein kinase inhibitors against HCT-13-treated cells in the presence of Cu(II) (20 µM). (b) Radar plot of screen results. (c) z-score values for kinase inhibitors within the DNA damage response/replication stress response (DDR/RSR) pathway module. (d) Representative immunoblot of replication stress and cell death biomarkers in MIAPACA2 PDAC cells treated with HCT-13 (10 nM) + Cu(II) (20 µM). (e) Annexin V/PI staining in MIAPACA2 cells to validate the synergistic interaction of HCT-13 (25nM) + Cu(II) (20 µM) with ATRi (250nM VE-822) treated for 72h. (f) Trypan Blue Viability staining in MIAPACA2 cells to validate the synergistic interaction of HCT-13 (25nM) with ATRi (250nM VE-822) treated for 72h in presence of Cu(II) (20 µM).

(mean ± SD, n = 2, one-way ANOVA corrected for multiple comparisons by Bonferroni adjustment, * $P < 0.05$; ** $P < 0.01$; *** $P < 0.001$; **** $P < 0.0001$).

DISCUSSION

We primarily focused on two modifications of the **HCT-1** (IQ-1) scaffold during our synthetic planning: fluorination of the isoquinoline ring, and sequential methylation of the 4' amine. Though the 5-, 7-, and 8-fluoro-substituted analogs of **HCT-1** were previously reported, and while it was apparent that fluorine position could influence a compound's toxicity and produce differential antiproliferative effects upon various cell lines, no trends had previously emerged regarding the effects of fluorine position.[5] Additionally, multiple groups have shown that 4' amine methylation potentiates the activity HCTs such as pyridine 2-carboxyaldehyde thiosemicarbazones and 2-acetylpyridine thiosemicarbazones.[24,39,40] We therefore sought to synthesize the novel 4- and 6-fluoro analogs of **HCT-1** and investigate what effects sequential 4' amine methylation had upon antiproliferative activity. Following our isoquinoline HCT synthetic campaign, analysis of the antiproliferative data revealed several trends. Without copper supplementation, fluorination at either the 4- or 6-position of the isoquinoline ring led to an increase in potency for five out of six compounds, when compared with their corresponding non-fluorinated analogs (**Figure 2**). In some cases, the change was dramatic – for example, the IC_{90} of **HCT-13** was nearly 270-fold lower than its non-fluorinated analog **HCT-11**. Secondly, 4' amine methylation in the absence of isoquinoline substitution or copper supplementation was detrimental to activity, as demonstrated by the decrease in potencies for **HCT**s **6** and **11** when compared with 4' primary amine **HCT-1** (**Figure 2**). However, combining 4' amine methylation and isoquinoline substitution in a single compound, as in **HCT**s **7-10**, **12** and **13**, produced synergistic antiproliferative effects when compared with either their 4' primary amine or unsubstituted isoquinoline analogs. **HCT-13** again exemplified this trend, with potency nearly 270-fold greater than its non-substituted isoquinoline analog **HCT-11** and nearly 50-fold greater than its non-methylated analog **HCT-3** (**Figure 2**). The underlying mechanisms responsible for this synergy remain under study by our group. Finally, the antiproliferative activities of all but one of our isoquinoline HCTs were potentiated by supplementation with physiologically relevant levels of copper, with **HCT-5** being the exception. The observed trends culminated with identification of our lead compound as **HCT-13**, which was uncomplicated in its synthesis and potent both in the absence and presence of copper supplementation.

The potency of **HCT-13** is highlighted by its nanomolar IC_{90} values against a panel of PDAC, SCLC, and PC cancer models in the presence of physiologically relevant levels of copper (**Figure 3a**). The use of copper-chelating small molecules in anticancer therapy is an established strategy which is executed either through sequestration of copper from tumor tissue, or through increasing intracellular copper to cytotoxic levels.[51] **HCT-13** behaved as an ionophore and increased intracellular levels of copper, both in the presence and absence of copper supplementation. This property is essential for the cytotoxicity of **HCT-13**, as sequestration of copper via BCPS-chelation negated our lead compound's growth inhibitory effects (**Figure 3d**). We further demonstrated that **HCT-13** leverages copper to effect its cytotoxicity in a mitochondria-dependent manner. Specifically, the data indicate that **HCT-13** induces mitochondrial dysfunction and mitochondria-dependent S-phase arrest, and generates ROS and oxidative stress in different cancer models. Strikingly, mitochondria-deficient 143 BTK ρ_0 cells were significantly less sensitive to **HCT-13** in the presence of copper compared to their parental 143 BTK WT counterpart, providing further evidence of mitochondria-dependent cytotoxicity (**Fig 5c**). It is possible that the observed S-phase arrest results from disruption of the *de novo* pathway (DNP) for pyrimidine nucleotide biosynthesis, which supplies cells with the pyrimidine nucleotides necessary for replication. The lone oxidation step of the pyrimidine DNP is carried out by dihydroorotate dehydrogenase (DHODH), an enzyme located in the inner mitochondrial membrane, which utilizes ubiquinone as a redox partner. Without a properly functioning mitochondrial ETC, DHODH does not have access to the levels of ubiquinone necessary for the oxidative enzyme to adequately turn-over, leading to shortages in pyrimidine nucleotides and corresponding S-phase arrest.[52–57]

In general, cancer cells exhibit higher levels of ROS and higher baseline oxidative stress than healthy cells, which may imbue our lead compound with selectivity towards them. The ROS and mitochondrial dysfunction produced in MIAPACA2 cells by **HCT-13** lead to an increase in DNA damage marker pH2AX, which may explain why our compound synergized with inhibitors of ATR (Ataxia-Telangiectasia Mutated (ATM) and Rad3-related protein kinase), the most upstream kinase in the DNA-damage response/replication stress response (DDR/RSR) pathway. Synergy with DDR/RSR inhibitors may increase the therapeutic window of our lead compound, should it be administered in combination therapy. The observed mechanisms of action of **HCT-13** suggest that

it may also synergize with radiotherapy, as therapeutic ionizing radiation increases ROS, thereby increasing oxidative stress and DNA damage in the targeted area(s). Therefore, **HCT-13** could also function as a radiosensitizer by further increasing the load of ROS, oxidative stress, and DNA damage when administered in combination with radiation therapy. Taken together, the potency of **HCT-13** as a single-agent therapeutic against aggressive solid tumor models, its mechanism of action, and the observed synergy with ATR inhibitors warrant further testing *in vivo.*

CONCLUSION

A class of isoquinoline-based HCTs has been expanded upon to produce a set of novel antiproliferative compounds. The synergistic effects of combining 4' amine methylation with isoquinoline substitution were demonstrated, and **HCT-13** was identified as a highly potent antiproliferative which is active against a panel of PDAC, SCLC, and PC cancer models. The presence of physiologically-relevant levels of Cu(II) greatly potentiated our lead compound's activity, and subsequent investigation into **HCT-13**'s mechanism of action revealed that it acts as a copper ionophore and requires copper to effect its cytotoxicity. Furthermore, **HCT-13** induces ROS production, oxidative stress, S-phase arrest, and mitochondrial dysfunction which may contribute to indirect inhibition of DHODH. Lastly, a high-throughput phenotypic screen of protein kinase inhibitors was used to identify actionable adaptive resistance mechanisms of **HCT-13**-treated cells, and the DDR/RSR pathways were revealed as actionable vulnerabilities. Specifically, we show that ATR inhibition synergizes with **HCT-13** in presence of physiologically-relevant levels of Cu(II). Taken together, this study demonstrates the potential of **HCT-13** for use in anti-cancer therapy, either as a single agent or as part of a larger combination therapy.

ACKNOWLEDGEMENTS

We thank Dr. Nagichettiar Satyamurthy for his expert chemistry advice, and Dr. Kym Faull at the Pasarow Mass Spectrometry Laboratory for continued tutelage regarding mass spectrometry. This work was supported by the National Cancer Institute [Grant R01CA187678-01 administered by the National Institutes of Health, Trethera Coporation [Contract Number 20162965]. This material is additionally based upon work supported by the National Science Foundation Graduate Research Fellowship Program [Grant No. DGE-1650504 to E.W.R].

REFERENCES

(1) Brockman, R. W.; Thomson, J. R.; Bell, M. J.; Skipper, H. E. Observations on the Antileukemic Activity of Pyridine-2-carboxaldehyde Thiosemicarbazones and Thiocarbohydrazone*. *Cancer Res.* **1956**, *16*, 167-170.

(2) Beraldo, H.; Gambino, D. The Wide Pharmacological Versatility of Semicarbazones, Thiosemicarbazones, and Their Metal Complexes. *Mini Rev. Med. Chem.* **2004**, *4*, 31-39.

(3) Sartorelli, A. C. Effect of Chelating Agents Upon the Synthesis of Nucleic Acids and Protein: Inhibition of DNA Synthesis by 1-Formylisoquinoline Thiosemicarbazone. *Biochem. Biophys. Res. Commun.* **1967**, *27*, 26-32.

(4) Liu, M. C.; Lin, T. S.; Sartorelli, A. C. Synthesis and Antitumor Activity of Amino Derivatives of Pyridine-2-carboxaldehyde Thiosemicarbazone. *J. Med. Chem.* **1992**, *35*, 3672-3677.

(5) Agrawal, K. C.; Mooney, P. D.; Sartorelli, A. C. Potential Antitumor Agents. 13. 4-Methyl-5-amino-1-formylisoquinoline Thiosemicarbazone. *J. Med. Chem.* **1976**, *19*, 970-972.

(6) French, F. A.; Blanz, E. J.; DoAmaral, J. R.; French, D. A. Carcinostatic Activity of Thiosemicarbazones of Formyl Heteroaromatic Compounds. VI. 1-Formylisoquinoline Derivatives Bearing Additional Ring Substituents, with Notes on Mechanism of Action. *J. Med. Chem.* **1970**, *13*, 1117-1124.

(7) French, F. A.; Blanz, E. J. The Carcinostatic Activity of α-(N) Heterocyclic Carboxaldehyde Thiosemicarbazone. *Cancer Res.* **1965**, *25*, 1454-1458.

(8) Karp, J. E.; Giles, F. J.; Gojo, I.; Morris, L.; Greer, J.; Johnson, B.; Thein, M.; Sznol, M.; Low, J. A Phase I study of the novel ribonucleotide reductase inhibitor 3-aminopyridine-2-carboxaldehyde thiosemicarbazone (3-AP, Triapine®) in combination with the nucleoside analog fludarabine for patients with refractory acute leukemias and aggressive myeloproliferative disorders. *Leuk. Res.* **2008**, *32*, 71-77.

(9) Le, T. M.; Poddar, S.; Capri, J. R.; Abt, E. R.; Kim, W.; Wei, L.; Uong, N. T.; Cheng, C. M.; Braas, D.; Nikanjam, M.; Rix, P.; Merkurjev, D.; Zaretsky, J.; Kornblum, H. I.; Ribas, A.; Herschman, H. R.; Whitelegge, J.; Faull, K. F.; Donahue, T. R.; Czernin, J.; Radu, C. G. ATR Inhibition Facilitates Targeting of Leukemia Dependence on Convergent Nucleotide Biosynthetic Pathways. *Nat. Commun.* **2017**, *8*, 241.

(10) Ohui, K.; Afanasenko, E.; Bacher, F.; Ting, R. L. X.; Zafar, A.; Blanco-Cabra, N.; Torrents, E.; Dömötör, O.; May, N. V.; Darvasiova, D.; Enyedy, É. A.; Popović-Bijelić, A. Reynisson, J.; Rapta, P.; Babak, M. V.; Pastorin, G.; Arion, V. B. New Water-Soluble Copper(II) Complexes with Morpholine-Thiosemicarbazone Hybrids: Insights into the Anticancer and Antibacterial Mode of Action. *J. Med. Chem.* **2018**, 62(2), 512-530.

(11) Aye, Y.; Long, M. J.; Stubbe, J. Mechanistic Studies of Semicarbazone Triapine Targeting Human Ribonucleotide Reductase *in Vitro* and in Mammalian Cells. *J. Biol. Chem.* **2012**, *287*, 35768-35778.

(12) Ma, B.; Goh, B. C.; Tan, E. H.; Lam, K. C.; Soo, R.; Leong, S. S.; Wang, L. Z.; Mo, F.; Chan, A. T.; Zee, B.; Mok, T. A multicenter phase II trial of 3-aminopyridine-2-carboxaldehyde thiosemicarbazone (3-AP, Triapine®) and gemicitabine in advanced non-small-cell lung cancer with pharmacokinetic evaluation using peripheral blood mononuclear cells. *Invest. New Drugs* **2008**, *26*, 169-173.

(13) Knox, J. J.; Hotte, S. J.; Kollmannsberger, C.; Winquist, E.; Fisher, B.; Eisenhauer, E. A. Phase II study of Triapine® in patients with metastatic renal cell carcinoma: a trial of the National Cancer Institute of Canada Clinical Trials Group (NCIC IND.161). *Invest. New Drugs* **2007**, *25*, 471-477.

(14) Yu, Y.; Kalinowski, D. S.; Kovacevic, Z.; Siafakas, A. R.; Jansson, P. J.; Stefani, C.; Lovejoy, D. B.; Sharpe, P. C.; Bernhardt, P. V.; Richardson, D. R. Thiosemicarbazone from the Old to New: Iron Chelators That are More Than Just Ribonucleotide Reductase Inhibitors. *J. Med. Chem.* **2009**, *52*, 5271-5294.

(15) Salim, K. Y.; Maleki Vareki, S.; Danter, W. R.; Koropatnick, J. COTI-2, a novel small molecule that is active against multiple human cancer cells in lines *in vitro* and *in vivo*. *Oncotarget* **2016**, *7*, 41363-41379.

(16) Guo, Z. L.; Richardson, D. R.; Kalinowski, D. S.; Kovacevic, Z.; Tan-Un, K. C.; Chan, G. C. *J.* The novel thiosemicarbazone, di-2-pyridylketone 4-cyclohexyl-4-methyl-3-thiosemicarbazone (DpC), inhibits neuroblastoma growth in vitro and in vivo multiple mechanisms. *Hematol. Oncol.* **2016**, *9*, 98.

(17) Malarz, K.; Mrozek-Wilczkiewicz, A.; Serda, M.; Rejmund, M.; Polanski, J.; Musiol, R. The role of oxidative stress in activity of anticancer thiosemicarbazones. *Oncotarget* **2018**, *9*, 17689-17710.

(18) Finch, R. A.; Liu, M. C.; Cory, A. H.; Cory, J. G.; Sartorelli, A. C. Triapine (3-aminopyridine-2-carboxaldehyde thiosemicarbazone; 3-AP): an inhibitor of ribonucleotide reductase with antineoplastic activity. *Adv. Enzyme Regul.* **1999**, *39*, 3-12.

(19) Yu, Y.; Wong, J.; Lovejoy, D. B.; Kalinowski, D. S.; Richardson, D. R. Chelators at the Cancer Coalface: Desferrioxamine to Triapine and Beyond. *Clin. Cancer. Res.* **2006**, *12*, 6876-6883.

(20) Alvero, A. B.; Chen, W.; Sartorelli, A. C.; Schwartz, P.; Rutherford, T.; Mor, G. Triapine (3-aminopyridine-2-carboxaldehyde thiosemicarbazone) Induces Apoptosis in Ovarian Cancer Cells. *J. Soc. Gynecol. Investig.* **2006**, *13*, 145-152.

(21) Yu, Y.; Gutierrez, E.; Kovacevic, Z.; Saletta, F.; Obeidy, P.; Suryo Rahmanto, Y.; Richardson, D. R. Iron Chelators for the Treatment of Cancer. *Curr. Med. Chem.* **2012**, *19*, 2689-2702.

(22) Merlot, A. M.; Kalinowski, D. S.; Richardson, D. R. Novel Chelators Treatment: Where Are We Now? *Antioxid. Redox Signal.* **2013**, *18*, 973-1006.

(23) Chaston, T. B.; Lovejoy, D. B.; Watts, R. N.; Richardson, D. R. Examination of the Antiproliferative Activity of Iron Chelators: Multiple Cellular Targets and the Different Mechanism of Action of Triapine Compared with Desferrioxamine and the Potent Pyridoxal Isonicotinoyl Hydrazone Analogue 311. *Clin. Cancer Res.* **2003**, *9*, 402-414.

(24) Cory, J. G.; Cory, A. H.; Rappa, G.; Lorico, A.; Liu, M. C.; Lin, T. S.; Sartorelli, A. C. Inhibitors of ribonucleotide reductase: comparative effects of amino- and hydroxy-substituted pyridine-2-carboxaldehyde thiosemicarbazones. *Biochem. Pharmacol.* **1994**, *48*, 335-344.

(25) Richardson, D. R.; Kalinowski, D. S.; Richardson, V.; Sharpe, P. C.; Lovejoy, D. B.; Islam, M.; Bernhardt, P. V. 2-Acetylpyridine Thiosemicarbazones are Potent Iron Chelators and Antiproliferative Agents: Redox Activity, Iron Complexation and Charaterization of their Antitumor Activity. *J. Med. Chem.* **2009**, *52*, 1459-1470.

(26) Popović-Bijelić, A.; Kowol, C. R.; Lind, M. E.; Luo, J.; Himo, F.; Enyedy, E. A.; Arion, V. B.; Gräslund, A. Ribonucleotide reductase inhibition by metal complexes of Triapine (3-aminopyridine-2-carboxaldehyde thiosemicarbazone): A combined experimental and theoretical study. *J. Inorg. Biochem.* **2011**, *105*, 1422-1431.

(27) Ishiguro, K.; Lin, Z. P.; Penketh, P. G.; Shyam, K.; Zhu, R.; Baumann, R. P.; Zhu, Y. L.; Sartorelli, A. C.; Rutherford, T. J.; Ratner, E. S. Distinct mechanisms of cell-kill by triapine and its terminally dimethylated derivative Dp44mT due to a loss or gain of activity of their copper(II) complexes. *Biochem. Pharmacol.* **2014**, *91*, 312-322.

(28) Denoyer, D.; Clatworthy, S. A.; Masaldan, S.; Meggyesy, P. M.; Cater, M. A. Heterogeneous copper concentrations in cancerous human prostate tissues. *Prostate* **2015**, *75*, 1510-1517.

(29) Madsen, E.; Gitlin, J. D. Copper and Iron Disorders of the Brain. *Annu. Rev. Neurosci.* **2007**, *30*, 317-337.

(30) Jansson, P. J.; Yamagishi, T.; Arvind, A.; Seebacher, N.; Gutierrez, E.; Stacy, A.; Maleki, S.; Sharp, D.; Sahni, S.; Richardson, D. R. Di-2-pyridylketone 4,4-Dimethyl-3-thiosemicarbazone Overcomes Multidrug-Resistance by Novel Mechanism Involving the Hijacking of Lysosomal P-Glycoprotein (Pgp). *J. Biol. Chem.* **2015**, *290*, 9588-9603.

(31) Whitnall, M.; Howard, J.; Ponka, P.; Richardson, D. R. A class of iron chelators with a wide spectrum of potent antitumor activity that overcomes resistance to chemotherapeutics. *Proc. Natl. Acad. Sci. USA* **2006**, *103*, 14901-14906.

(32) Shimada, K.; Reznik, E.; Stokes, M. E.; Krishnamoorthy, L.; Bos, P. H.; Song, Y.; Quartararo, C. E.; Pagano, N. C.; Carpizo, D. R.; deCarvalho, A. C.; Lo, D. C.; Stockwell, B. R. Copper-Binding Small Molecule Induces Oxidative Stress and Cell-Cycle Arrest in Glioblastoma-Patient-Derived Cells. *Cell Chem. Biol.* **2018**, *25*, 585-594.

(33) Chen, D.; Cui, Q. C.; Yang, H.; Dou, Q. P. Disulfiram, a Clinically Used Anti-Alcoholism Drug and Copper-Binding Agent, Induces Apoptotic Cell Death in Breast Cancer Cultures and Xenografts via Inhibition of the Proteasome Activity. *Cancer Res.* **2006**, *66*, 10425-10433.

(34) Brewer, G. J.; Dick, R. D.; Grover, D. K.; LeClaire, V.; Tseng, M.; Wicha, M.; Pienta, K.; Redman, B. G.; Jahan, T.; Sondak, V. K.; Strawderman, M.; LeCarpentier, G.; Merajver, S. D. Treatment of Metastatic Cancer with Tetrathiomolybdate, an Anticopper, Antiangiogenic Agent: Phase I Study. *Clin. Cancer Res.* **2000**, *6*, 1-10.

(35) Cen, D.; Gonzalez, R. I.; Buckmeier, J. A.; Kahlon, R. S.; Tohidian, N. B.; Meyskens, F. L. Disulfiram Induces Apoptosis in Human Melanoma Cells: A Redox-related Process. *Mol. Cancer Ther.* **2002**, *1*, 197-204.

(36) Müller, K.; Faeh, C.; Diederich, F. Fluorine in Pharmaceuticals: Looking Beyond Intuition. *Science.* **2007**, *317*, 1881-1886.

(37) Purser, S.; Moore, P. R.; Swallow, S.; Gouverneur, V. Fluorine in Medicinal Chemistry. *Chem. Soc. Rev.* **2008**, *37*, 320-330.

(38) Zhou, Y.; Wang, J.; Gu, Z.; Wang, S.; Zhu, W.; Aceña, J. L.; Soloshonok, V. A.; Izawa, K.; Liu, H. Next Generation of Fluorine-Containing Pharmaceuticals, Compounds Currently in Phase II-III Clinical Trials of Major Pharmaceutical Companies: New Structural Trends and Therapeutic Areas. *Chem. Rev.* **2016**, *116*, 422-518.

(39) Kowol, C. R.; Trondl, R.; Heffeter, P.; Arion, V. B.; Jakupec, M. A.; Roller, A.; Galanski, M.; Berger, W.; Keppler, B. K. Impact of Metal Coordination on Cytotoxicity of 3-Aminopyridine-2-carboxaldehyde Thiosemicarbazone and Novel Insights into Terminal Dimethylation. *J. Med. Chem.* **2009**, *52*, 5032-5043.

(40) Kowol, C. R.; Miklos, W.; Pfaff, S.; Hager, S.; Kallus, S.; Pelivan, K.; Kubanik, M.; Enyedy, É. A.; Berger, W.; Heffeter, P.; Keppler, B. K. Impact of Stepwise NH_2-Methylation of Triapine on the Physicochemical Properties, Anticancer Activity, and Resistance Circumvention. *J. Med. Chem.* **2016**, *59*, 6739-6752.

(41) Agrawal, K. C.; Booth, B. A.; Sartorelli, A. C. Potential Antitumor Agents. I. A series of 5-Substituted 1-Formylisoquinoline Thiosemicarbazones. *J. Med. Chem.* **1968**, *11*, 700-703.

(42) Mooney, P. D.; Booth, B. A.; Moore, E. C.; Agrawal, K. C.; Sartorelli, A. C. Potential Antitumor Agents. 10. Synthesis and Biochemical Properties of 5-N-Alkylamino-, N,N-Dialkylamino-, and N-Alkylacetamido-1-formylisoquinoline Thiosemicarbazones. J. *Med. Chem.* **1974**, *17*, 1145-1150.

(43) Denoyer, D.; Pearson, H. B.; Clatworthy, S. A.; Smith, Z. M.; Francis, P. S.; Llanos, R. M.; Volitakis, I.; Phillips, W. A.; Meggyesy, P. M.; Masaldan, S.; Cater, M. A. Copper as a target for prostate cancer therapeutics: copper-ionophore pharmacology and altering systemic copper distribution. *Oncotarget* **2016**, *7*, 37064-37080.

(44) Cater, M. A.; Pearson, H. B.; Wolyniec, K.; Klaver, P.; Bilandzic, M.; Paterson, B. M.; Bush, A. I.; Humbert, P. O.; La Fontaine, S.; Donnelly, P. S.; Haupt, Y. Increasing Intracellular Bioavailable Copper Selectivity Targets Prostate Cancer Cells. *ACS Chem. Biol.* **2013**, *8*, 1621-1631.

(45) Safi, R.; Nelson, E. R.; Chitneni, S. K.; Franz, K. J.; George, D. J.; Zalutsky, M. R.; McDonnell, D. P. Copper signaling axis as a target for prostate cancer therapeutics. *Cancer Res.* **2014**, *74*, 5819-5831.

(46) Kodydkova, J.; Vavrova, L.; Stankova, B.; Macasek, J.; Krechler, T.; Zak, A. Antioxidant Status and Oxidative Stress Markers in Pancreatic Cancer and Chronic Pancreatitis. *Pancreas* **2013**, *42*, 614-621.

(47) Lener, M. R.; Scott, R. J.; Wiechowska-Kozłowska, A.; Serrano-Fernández, P.; Baszuk, P.; Jaworska-Bieniek, K.; Sukiennicki, G.; Marciniak, W.; Muszyńska, M.; Kładny, J.; Gromowski, T.; Kaczmarek, K.; Jakubowska, A.; Lubiński. Serum concentration of selenium and copper in patients diagnosed with pancreatic cancer. *Cancer Res. Treat.* **2016**, *48*, 1056-1064.

(48) Zhang, X.; Yang, Q. Association between serum copper levels and lung cancer risk: A meta-analysis. *J. Int. Med. Res.* **2018**, 46(12), 4863-4873.

(49) Herzig, S.; Shaw, R. AMPK: guardian of metabolism and mitochondrial homeostasis. *Nat. Rev. Mol. Cell Biol.* **2018**, *19*, 121-135.

(50) Krishan, S.; Richardson, D. R.; Sahni, S. The Anticancer Agent, Di-2-Pyridylketone 4,4-Dimethyl-3-Thiosemicarbazone (Dp44mT), Up-Regulates the AMPK-Dependent Energy Homeostasis Pathway in Cancer Cells. *Biochem. Biophys. Acta.* **2016**, *1863*, 2916-2933.

(51) Englinger, B.; Pirker, C.; Heffeter, P.; Terenzi, A.; Kowol, C. R.; Keppler, B. K.; Berger, W. Metal Drugs and the Anticancer Immune Response. Metal Drugs and the Anticancer Immune Response. *Chem. Rev.* **2019**, 119, 1519-1624.

(52) Madak, J. T.; Bankhead, A.; Cuthbertson, C. R.; Showalter, H. D.; Neamati, N. Revisiting the role of dihydroorotate dehydrogenase as a therapeutic target for cancer. *Pharmacol. Ther.* [Online early access, in press]. DOI: https://doi.org/10.1016/j.pharmthera.2018.10.012. Published online: October 19, **2018**.

(53) Löffler, M.; Jöckel, J.; Schuster, G. & Becker, C. Dihydroorotat-ubiquinone oxidoreductase links mitochondria in the biosynthesis of pyrimidine nucleotides. *Mol. Cell Biochem.* **1997**, *174*, 125-129.

(54) Rawls, J.; Knecht, W.; Diekert, K.; Lill, R.; Löffler, M. Requirements for the mitochondrial import and localization of dihydroorotate dehydrogenase. *Eur. J. Biochem.* **2000**, *267*, 2079-2087.

(55) Zameitat, E.; Freymark, G.; Dietz, C. D.; Löffler, M.; Bölker, M. Functional Expression of Human Dihydroorotate Dehydrogenase (DHODH) in *pyr4* Mutants of *Ustilago maydis* Allows Target Validation of DHODH Inhibitors In Vivo. *Appl. Environ. Microbiol.* **2007**, *73*, 3371-3379.

(56) Lane, A. N.; Fan, T. W. Regulation of mammalian nucleotide metabolism and biosynthesis. *Nucleic Acids Res.* **2015**, *43*, 2466-2485.

(57) Morais, R.; Desjardins, P.; Turmel, C.; Zinkewich-Péotti, K. Development and Characterization of continuous avian cell lines depleted of mitochondrial DNA. *In Vitro Cell. Dev. Biol.* **1988**, *24*, 649-658.

Supplementary Information

Materials and Methods

General

All chemicals, reagents and solvents were obtained from commercial sources and were used without further purification. Unless otherwise noted, reactions were carried out in oven-dried glassware under an atmosphere of argon using commercially available anhydrous solvents. Tetrahydrofuran (THF) was distilled from sodium under an argon atmosphere. Dichloromethane was distilled from calcium hydride. Solvents used for extractions and chromatography were not anhydrous. Analytical TLC was carried out on precoated silica gel (Merck silica gel 60, F254) and visualized with UV light. Column chromatography was performed with silica (Fisher, 230-400 mesh). ^{1}H NMR, ^{13}C NMR, and ^{19}F NMR spectra were measured in $CDCl_3$ or DMSO-d_6 on Bruker AV spectrometers at 400 or 500 MHz. Chemical shifts were reported in parts per million (δ) relative to residual solvent signals. The signals observed were described as follows: s (singlet), d (doublet), t (triplet), q (quartet), dd (doublet of doublets), dt (doublet of triplets), ddd (doublet of doublet of doublets), tt (triplet of triplets), tdd (triplet of doublet of doublets), m (multiplet), br s (broad singlet). Mass spectra were obtained on a Waters LCT Premier with ACQUITY UPLC mass spectrometer under electrospray ionization (ESI) or Thermo Fisher Scientific Exactive Plus with direct analysis in real time (DART) ionization. Purity of all compounds used in biological assays was determined on a Hewlett Packard 1090 HPLC system using an Aquasil C18 column (250 mm × 2 mm, 5 μm, Keystone Scientific) with an acetonitrile/water solvent system containing 0.1% TFA with detection performed at 254 nm (minute/%acetonitrile: 0/0, 8/0, 35/95, 43/95, 45/0, 55/0). HPLC purification was performed on a Hewlett Packard 1090 HPLC system with Hypersil Gold column (250 mm × 10 mm, 5 μm, Thermo Scientific) with and acetonitrile/water solvent system containing 0.05% formic acid and 10 mM ammonium formate. All microwave-assisted reactions were carried out in a CEM Discover 908005 Microwave synthesizer system.

Cell culture and culture conditions

Pancreatic adenocarcinoma cell lines: PATU8988T, MIAPACA2, SU8686, PSN1, HPAC, BXPC3, DANG, SUIT2, A13A, CAPAN2, T3M4, A2.1, HUPT4, XWR200, L36PL, YAPC, PANC0327, PANC1, PATU8902, HPAF11, ASPC1, PANC0813, PANC0203, HS766T, SW1990, and CFPAC1; prostate cancer cell lines: 22Rv1, LNCaP, RM1 and C4-2; and small cell lung carcinoma cell lines: NCI-H526, NCI-H146, and NCI-H1963 were obtained from American Type Culture Collection (ATCC). 143 BTK WT and 143 BTK ρ_0, BJ WT and BJ ρ_0 cells were gifts from Prof. Michael Teitell in UCLA. Murine Prostate cancer cell line MyC CaP was a kind gift from Prof. DLJ Thorek at WUSTL. Murine Pancreatic cancer cells KP4662 was a kind gift from Prof. Robert Vonderheide at UPenn. With a few exceptions, cell lines were cultured in DMEM (Corning) or RPMI (Corning) containing 10% fetal bovine serum (FBS, Omega Scientific) and were grown at 37 °C, 20% O_2 and 5% CO_2. All cultured cells were incubated in antibiotic free media and were regularly tested for mycoplasma contamination using MycoAlert kit (Lonza) following the manufacturer's instructions, except that the reagents were diluted 1:4 from their recommended amount.

Proliferation assay

Cells were plated in 384-well plates (500 cells/well for adherent cell lines in 30 μl volume). Drugs were serially diluted to the desired concentrations and an equivalent volume of DMSO was added to vehicle control. Following 72 h incubation, ATP content was measured using CellTiter-Glo reagent according to manufacturer's instructions (Promega, CellTiter-Glo Luminescent Cell Viability Assay), and analyzed by SpectraMax luminometer (Molecular Devices). IC_{50} and IC_{90} values, concentrations required to inhibit

proliferation by 50% and 90% respectively compared to DMSO treated cells, were calculated using Prism 6.0 h (Graphpad Software).

Western blot

Cells were lysed using RIPA buffer supplemented with protease (ThermoFisher, 78,430) and phosphatase (ThermoFisher, 78,420) inhibitors, scraped, sonicated, and centrifuged (20,000 × *g* at 4 °C). Protein concentrations in the supernatant were determined using the Micro BCA Protein Assay kit (Thermo), and equal amounts of protein were resolved on pre-made Bis-Tris polyacrylamide gels (Life Technologies). Primary antibodies: $pAMPK_{T172}$ (Cell signaling, #2535, 1:1000), HO-1 (Cell signaling, #5061S, 1:1000), pS345 CHEK1(Cell signaling, #2348L, 1:1000), pT68 CHEK2 (Cell signaling, #2197 S, 1:1000), pS139 H2A.X (Millipore, 05-636, 1:1000), clvd. Casp3 (Cell signaling, #9662, 1:1000), and anti-actin (Cell Signaling Technology, 9470, 1:10,000). Primary antibodies were stored in 5% BSA (Sigma-Aldrich) and 0.1% NaN_3 in TBST solution. Anti-rabbit IgG HRP-linked (Cell Signaling Technology, 7074, 1:2500) and anti-mouse IgG HRP-linked (Cell Signaling Technology, 7076, 1:2500) were used as secondary antibodies. Chemiluminescent substrates (ThermoFisher Scientific, 34,077 and 34,095) and autoradiography film (Denville) were used for detection.

Viability/Apoptosis assay

Viable cells were measured by Trypan blue staining using vi-cell counter (Beckman Coulter, CA, USA). Apoptosis and cell death were assayed using Annexin V-FITC and PI according to manufacturer's instructions (FITC Annexin V Apoptosis Detection Kit, BD Sciences, #556570).

Cell cycle

Cell cycle was assessed using Propidium iodide staining at indicated timepoints. Cells were pulsed with EdU 1 h before collection at different time points. Cells were fixed 4% paraformaldehyde, permeabilized with perm/wash reagent (Invitrogen), stained with Azide-AF647 (using click-chemistry, Invitrogen; Click-iT EdU Flow cytometry kit, #C10634) and FxCycle-Violet (Invitrogen), and then analyzed by flow cytometry (a detailed description is available in the Supplementary Information).

ROS Measurements

Cellular ROS measurement was assayed with CM-H2DCFDA staining after treatment according to manufacturer's instructions (Reactive Oxygen Species (ROS) Detection Reagents, Invitrogen, #D399). The cells were then incubated with 5 μM of CM-H2DCFDA for 30 min, spun down at 450 x g for 4 mins, and the supernatant was replaced with fresh media containing lethal compounds and/or Cu(II). Then, the cells were incubated for 30 mins, spun down, and the supernatant was replaced with PBS. The samples were analyzed using flow cytometry.

Mitochondrial ROS was measured using MitoSOX staining according to manufacturer's instructions (MitoSOX, Invitrogen, #M36008). Cells were treated with HCT-13, washed and treated with MitoSOX. Cells were then incubated for 30 minutes at 37°C. After incubation, media is aspirated and cells are washed with PBS and analyzed by flow cytometry.

Mito Stress Test and Electron Flow Assay

Oxygen consumption rate (OCR) was measured using a XF24 Analyzer (Agilent) and normalized per μg protein. For cellular OCR, cells were incubated in unbuffered DMEM containing 25 mM glucose, 1 mM pyruvate and 2 mM glutamine. OCR was measured before (total respiration) and after the sequential injection of 1 μM oligomycin (complex V inhibitor), 0.75 μM FCCP (uncoupler), and 1 μM of rotenone and myxothiazol (complex I and III inhibitors, respectively), as described previously.[1] Mitochondrial respiration was calculated by subtracting the non-mitochondrial respiration left after rotenone and myxothiazol injection. Oligomycin-sensitive respiration represents ATP-linked respiration (coupled respiration).

To measure electron transport chain complex activity from cells, cells were incubated in MAS buffer with 10 mM pyruvate (complex I substrate), 2 mM malate, 4 μM FCCP, 4 mM ADP, and 1 nM of XF Plasma Membrane Permeabilizer (PMP) reagent (Agilent). OCR was measured before and after the sequential injection of 2 μM rotenone, 10 mM succinate (complex II substrate), 4 μM antimycin A (complex III inhibitor), and a mix of 10 mM ascorbate and 100 μM TMPD (complex IV substrates), as described previously (2). Antimycin A-sensitive respiration represents the complex III respiration.

To measure OCR directly from mitochondria, mitochondria were isolated from fresh mouse liver by dual centrifugation at 800g and 8000g and seeded by centrifugation (2). Mitochondria were incubated with 1 mM pyruvate (complex I), 2 mM malate, 4 μM FCCP in MAS buffer, as well as the "corresponding drugs" for 30 min at 37ºC. OCR was measured before and after the sequential injections described in the previous paragraph.

Intracellular Cu(II) measurement

Cells were plated in 6-well plates and cultured for one day. Vehicle of **HCT13** were added to the cells the following day and incubated for 24 hours. The plates were then washed 2 times with PBS containing 1 mM EDTA and 2 times with PBS alone. The concentration of Cu(II) was measured using Inductive Coupled Plasma Mass Spectrometry (ICP-MS) using standard procedure.

DHODH activity

Recombinant protein was incubated in an aqueous solution (total volume, 1.0 mL) containing 500 μM DHO (Sigma, D1728), 200 mM K_2CO_3-HCl (pH 8.0), 0.2% triton x-100, and 100 μM coenzyme Q10 (Sigma, C9538) at 37 °C for 0, 15, 30, 45, or 60 min. An aliquot (100 μL) of the mixture of enzyme reaction mixture or cell/tissue lysate was mixed with 100 μL of 0, 0.5, or 1.0 μM orotic acid, 50 μL of H2O, 250 μL of 4.0 mM 4-TFMBAO (Sigma, 422231), 250 μL of 8.0 mM $K_3[Fe(CN)_6]$ (Sigma, 244023), and 250 μL of 80 mM K_2CO_3 (Sigma, P5833) and then heated at 80 °C for 4.0 min. The reaction was stopped by cooling in an ice-water bath and the absorbance was measured with a spectrofluorometer (FP-6300 Jasco, Tokyo, Japan): excitation and emission wavelengths were 340 nm and 460 nm, respectively.

FACS analyses

All flow cytometry data were acquired on a five-laser LSRII cytometer (BD), and analyzed using the FlowJo software (Tree Star).

Supplementary Figures

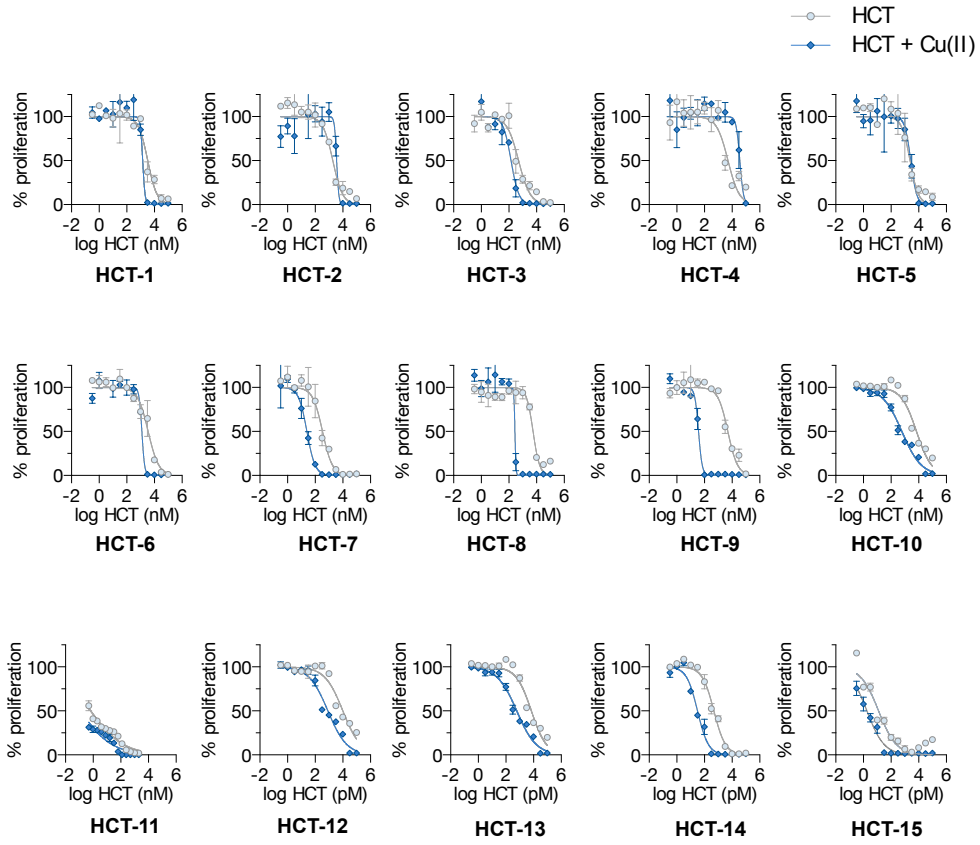

Fig. S1 | Summary of HCT compound dose response curves. Viability curves measured with CellTiterGlo in MIAPACA2 cells treated with each HCT ± Cu(II) (20 µM) for 72h.

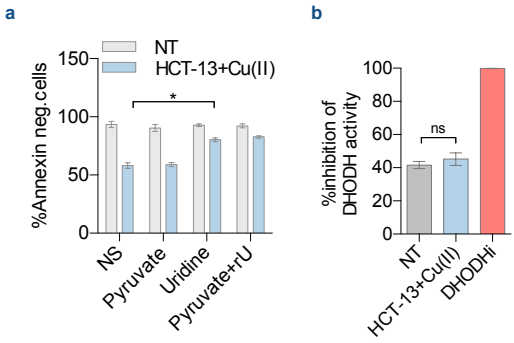

Fig. S2 | Cell proliferation inhibition induced by HCT-13 is partially rescued by uridine supplementation. (**a**) Rescue of HCT-13 (25 nM)-induced cell death by Uridine (rU) (200 µM), Pyruvate (1 mM), or both following 48h of treatment (**b**) Measurement of DHODH activity using recombinant DHODH assay following treatment with indicated perturbations for 2 min. DHODH inhibitor used: NITD-982 - 1 µM; HCT-13 - 100 nM, 1 µM, (100 nM data shown); Cu(II) - 20 µM.

(mean ± SD, n = 2, Student t-test, * $P < 0.05$).

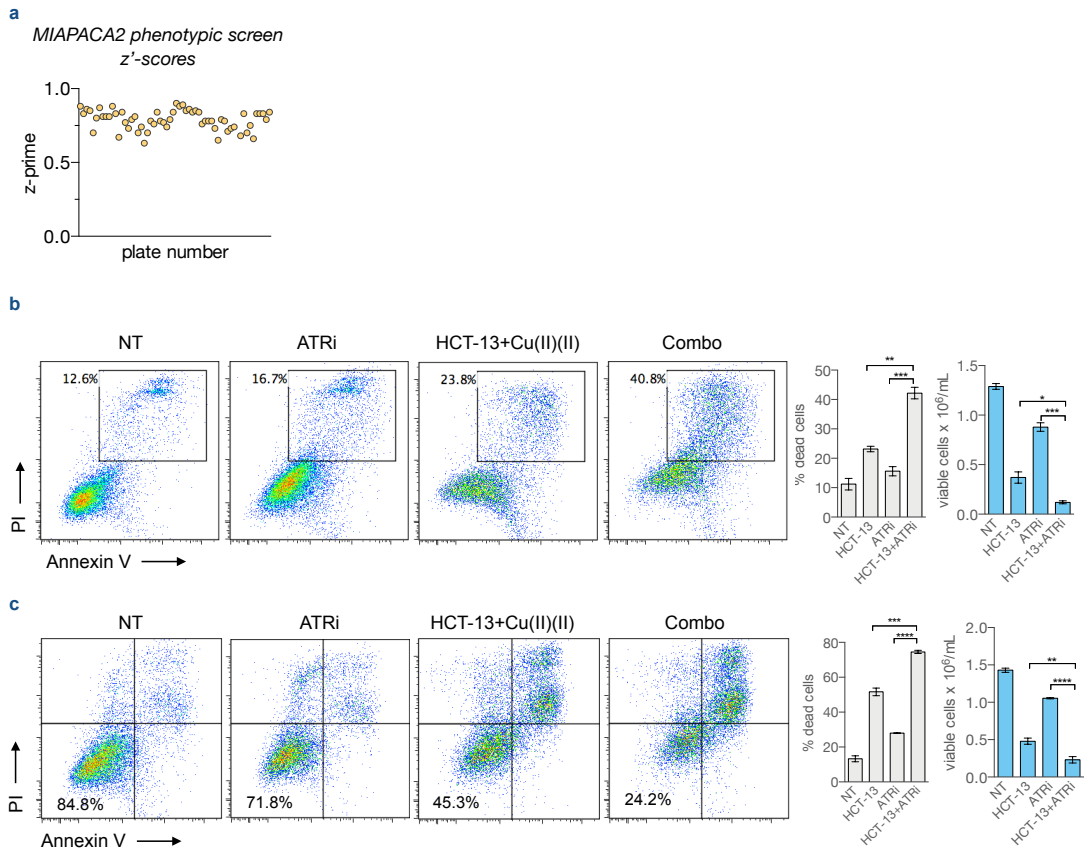

Fig. S3 | Identification of resistance mechanisms to HCT-13 using a synthetic lethality screen (**a**) Assay quality, as measured by Z-factor (Z') scores (**b and c**) Annexin V/PI staining and Trypan Blue staining in CFPAC-1 PDAC cells and C4-2 PC cells to validate the synergistic interaction of HCT-13 with ATRi (250 nM VE-822) treated for 72h in presence of Cu(II) (20 µM).

(mean ± SD, n = 2, one-way ANOVA corrected for multiple comparisons by Bonferroni adjustment, * $P < 0.05$; ** $P < 0.01$; *** $P < 0.001$; **** $P < 0.0001$).

Synthesis of compounds S1-S22 and HCT1-HCT16

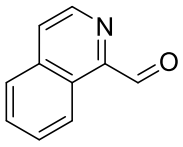

Isoquinoline-1-carboxaldehyde (S1). To a solution of 1-methylisoquinoline (1.0 g, 6.98 mmol) in 1,4-dioxane (10 mL) was added selenium dioxide (0.930 g, 8.38 mmol) and the mixture was refluxed for 4 h. The mixture was filtered, then concentrated *in vacuo*. The crude residue was purified by column chromatography (25% DCM:Hexanes) to give the product **S1** as a taupe powder (0.840 g, 69% yield). ^{1}H NMR (500 MHz, DMSO-d_6) δ 10.28 (s, 1H), 9.15 (ddd, J = 7.7, 1.9, 0.8 Hz, 1H), 8.82 (d, J = 5.5 Hz, 1H), 8.21 (dd, J = 5.6, 0.9 Hz, 1H), 8.17–8.12 (m, 1H), 7.93–7.84 (m, 2H). ^{13}C NMR (125 MHz, DMSO-d_6) δ 195.64, 149.38, 142.47, 136.49, 131.00, 130.30, 127.45, 125.77, 125.41, 124.73. DART-MS: *m/z* calcd. for $C_{10}H_8NO$ $(M+H)^+$ 158.06004, found 158.05977.

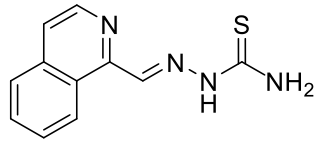

(*E*)-2-(isoquinolin-1-ylmethylene)hydrazine-1-carbothioamide (HCT1): Synthesized from **S1** as previously reported.[1] ^{1}H NMR (500 MHz, DMSO-d_6) δ 11.74 (s, 1H), 9.19 (d, J = 8.5 Hz, 1H), 8.60–8.54 (m, 2H) 8.49 (br s, 1H), 8.02 (d, J = 8.1 Hz, 1H), 7.86 (d, J = 5.6 Hz, 1H), 7.84–7.78 (m, 2H), 7.75 (ddd, J = 8.3, 6.8, 1.4 Hz, 1H). ^{13}C NMR (125 MHz, DMSO-d_6) δ 178.41, 150.78, 145.99, 142.13, 136.24, 130.47, 129.08, 127.22, 126.94, 125.58, 121.77. DART-MS: m/z calcd. for $C_{11}H_{10}N_4S$ $(M+H)^+$ 231.06989, found 231.06938.

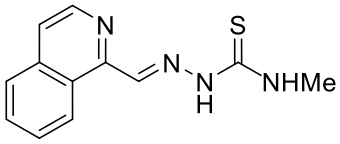

(*E*)-2-(isoquinolin-1-ylmethylene)-*N*-methylhydrazine-1-carbothioamide (HCT6): To a solution of **S1** (0.060 g, 0.382 mmol) in ethanol (3 mL) was added 4-methyl-3-thiosemicarbazide (0.040g, 0.382 mmol) and HCl (0.318 mL, 12 M in H_2O). The mixture was refluxed for 4 h. The solid that formed was collected by filtration, washed with water, and recrystallized from EtOH to yield **HCT6** as a yellow powder (0.058 g, 62% yield). ^{1}H NMR (500 MHz, DMSO-d_6) δ 11.78 (br s, 1H), 9.11 (br s, 1H), 8.61 (s, 1H), 8.56 (d, J = 5.6 Hz, 1H), 8.31 (br s, 1H), 8.02 (d, J = 8.1 Hz, 1H), 7.89–7.79 (m, 2H), 7.76 (t, J = 7.7 Hz, 1H), 3.07 (s, 3H). ^{13}C NMR (125 MHz, DMSO-d_6) δ 178.36, 151.06, 144.76, 142.15, 136.25, 130.42, 128.86, 127.21, 126.82, 125.64, 121.48, 31.34. DART-MS: m/z calcd. for $C_{12}H_{13}N_4S$ $(M+H)^+$ 245.08554, found 245.08505.

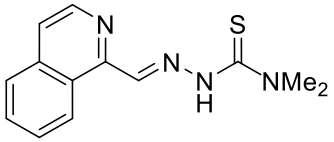

and
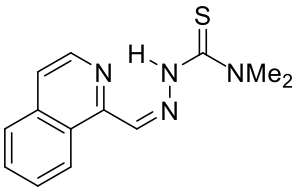

(*E*)-2-(Isoquinolin-1-ylmethylene)-*N*,*N*-dimethylhydrazine-1-carbothioamide and (*Z*)-2-(Isoquinolin-1-ylmethylene)-*N*,*N*-dimethylhydrazine-1-carbothioamide (HCT11). To a solution of **S1** (0.060 g, 0.382 mmol) in ethanol (3 mL) was added 4,4-dimethyl-3-thiosemicarbazide (0.046g, 0.382 mmol) and HCl (0.318 mL, 12 M in H_2O). The mixture was refluxed for 4 h. The solid that formed was collected by filtration, washed with water, and recrystallized from EtOH to yield **HCT11** as a yellow powder (0.056 g, 57% yield) (mixture of E and Z isomers). ^{1}H NMR (500 MHz, DMSO-*d*6) δ 15.99 (s, 0.33H), 11.26 (br s, 1H), 9.77 (dd, *J* = 8.8, 5.1 Hz, 1H), 8.81 (d, *J* = 8.6 Hz, 0.33H), 8.70 (d, *J* = 1.7 Hz, 1H), 8.69 (d, *J* = 1.2 Hz, 0.33H), 8.63 (s, 0.33H), 8.55 (d, *J* = 5.5 Hz, 1H), 8.12 (d, *J* = 8.2 Hz, 0.33H), 8.01–7.96 (m, 1.33H), 7.92 (ddd, *J* = 8.1, 7.0, 1.1 Hz, 0.33H), 7.88–7.76 (m, 2.33H), 7.72 (ddd, *J* = 8.4, 6.8, 1.4 Hz, 1H), 3.43 (s, 1.98H), 3.35 (s, 6H). ^{13}C NMR (125 MHz, DMSO-d_6) δ 180.88, 180.81, 151.94, 150.58, 147.81, 142.50, 140.45, 136.86, 136.82, 131.80, 130.77, 129.48, 129.16, 128.21, 128.17 (2C), 127.68, 126.83, 125.87, 124.60, 122.53, 121.93, 42.08 (4C). DART-MS: m/z calcd. for $C_{13}H_{15}N_4S$ $(M+H)^+$ 259.10119, found 259.10080.

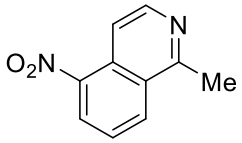

1-Methyl-5-nitroisoquinoline (S2). To a solution of 1-methylisoquinoline (28.80 g, 201.2 mmol) in sulfuric acid (92.4 mL) at 0℃ was added KNO_3 (20.4 g, 201.2 mmol) in sulfuric acid (78.0 mL). The mixture was heated at 60℃ for 2 h and then poured slowly over crushed ice. The solution was made alkaline with NH_4OH; the resulting tan precipitate was filtered, washed with water, and dried to afford **S2** as a tan solid (20.00 g, 53%). ^{1}H NMR (500 MHz, $CDCl_3$) δ 8.61 (d, *J* = 6.2 Hz, 1H), 8.47–8.50 (m, 2H), 8.28 (d, *J* = 6.3 Hz, 1H), 7.71 (t, *J* = 8.1 Hz, 1H), 3.05 (s, 3H). ^{13}C NMR (125 MHz, $CDCl_3$) δ 159.53, 145.38, 132.53, 128.65, 128.23, 127.79, 125.58, 114.26 (2C), 23.38. DART-MS: *m/z* calcd. for $C_{10}H_9N_2O_2$ $(M+H)^+$ 189.06585, found 189.06544.

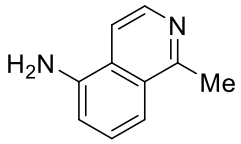

1-Methylisoquinolin-5-amine (S3). To a solution of **S2** (20.00 g, 106.28 mmol) in MeOH (530 mL) and iron powder (44.40 g, 795.05 mmol) was added concentrated HCl (1 mL, 12 M in H_2O). The mixture was refluxed for 2 h and then a solution of sodium hydroxide (6 mL, 2 M in H_2O) was added. The mixture was filtered, then concentrated *in vacuo*, and resuspended in EtOAc (200 mL) and water (200 mL). The organic layer was separated and the aqueous layer was extracted with EtOAc (3 × 200 mL). The organic

layers were combined and dried over Na_2SO_4, filtered, and then concentrated *in vacuo*. The crude residue was purified by flash column chromatography (gradient, 10–30% EtOAc:hexanes). The isoquinoline **S3** was obtained as a brown solid (15.0 g, 90%). ^{1}H NMR (500 MHz, $CDCl_3$) δ 8.36 (d, J = 6.1 Hz, 1H), 7.55 (dt, J = 8.4, 1.0 Hz, 1H), 7.45 (d, J = 5.7 Hz, 1H), 7.39 (dd, J = 8.5, 7.4 Hz, 1H), 6.95 (dd, J = 7.5, 0.9 Hz, 1H), 4.18 (br s, 2H), 2.93 (s, 3H). ^{13}C NMR (125 MHz, $CDCl_3$) δ 165.39, 159.15, 141.94, 128.35, 127.51, 126.16, 116.19, 113.09, 112.73, 23.06. DART-MS: *m/z* calcd. for $C_{10}H_{11}N_2$ $(M+H)^+$ 159.09167, found 159.09136.

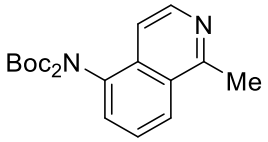

***tert*-Butyl (*tert*-butoxycarbonyl)(1-methylisoquinolin-5-yl)carbamate (S4).** To a solution of **S3** (360.0 mg, 2.28 mmol) in THF (10 mL) was added Boc_2O (1.68 g, 6.83 mmol), DMAP (28.0 mg, 0.23 mmol), and TEA (0.69 g, 3.65 mmol) and the mixture was stirred at 22 °C overnight. The reaction was quenched with water (10 mL) and the organic layers were separated. The aqueous layer was extracted with EtOAc (3 × 10 mL). The organic layers were combined and dried over Na_2SO_4, filtered, and then concentrated *in vacuo*. The crude residue was purified by flash column chromatography (gradient, 10–30% EtOAc:hexanes). The isoquinoline **S4** was obtained as a brown solid (420.0 mg, 51%). ^{1}H NMR (500 MHz, $CDCl_3$) δ 8.43 (d, J = 6.0 Hz, 1H), 8.11 (d, J = 8.5 Hz, 1H), 7.58 (t, J = 7.9 Hz, 1H), 7.51 (dd, J = 7.3, 1.1 Hz, 1H), 7.46 (d, J = 5.9 Hz, 1H), 2.99 (s, 3H), 1.31 (s, 18H). ^{13}C NMR (125 MHz, $CDCl_3$) δ 159.16, 151.59, 142.73, 135.74, 133.82, 129.64, 128.20, 126.55, 125.86, 113.74, 83.19 (2C), 27.90 (6C), 22.90. DART-MS: *m/z* calcd. for $C_{20}H_{27}N_2O_4$ $(M+H)^+$ 359.19653, found 359.19540.

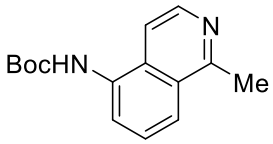

***tert*-Butyl (1-methylisoquinolin-5-yl)carbamate (S5).** To a solution of **S3** (10.00 g, 63.21 mmol) in THF (250 mL) was added Boc_2O (34.38 g, 158.0 mmol), DMAP (772.2 mg, 6.32 mmol), and TEA (15.96 g, 158.0 mmol) and the mixture was stirred at 22 °C overnight. After completion of the reaction as judged by TLC, $NaHCO_3$ (15.93 g, 189.6 mmol) and MeOH (100 mL) were added to the reaction mixture and it was refluxed overnight. After completion of the reaction (monitored by TLC), the mixture was concentrated *in vacuo* and then resuspended in EtOAc (200 mL) and water (200 mL). The organic layer was separated and the aqueous layer was extracted with EtOAc (3 × 200 mL). The organic layers were combined and dried over Na_2SO_4, filtered, and then concentrated *in vacuo*. The crude residue was purified by flash column chromatography (gradient, 10–30% EtOAc:hexanes). The isoquinoline **S5** was obtained as a brown oil (4.73 g, 29%). ^{1}H NMR (500 MHz, $CDCl_3$) δ 8.37 (d, J = 6.1 Hz, 1H), 7.56 (dt, J = 8.3, 1.0 Hz, 1H), 7.46 (d, J = 6.7 Hz, 1H), 7.40 (dd, J = 8.5, 7.4 Hz, 1H), 6.95 (dd, J = 7.5, 0.9 Hz, 1H), 2.94 (s, 4H), 1.56 (s, 9H). ^{13}C NMR (125 MHz, $CDCl_3$) δ 165.39, 159.15, 141.94, 128.35, 127.51, 126.16, 116.19, 113.09, 112.73, 76.91, 29.86 (3C), 23.06, one low-field carbon were either not observed or is overlapping

with another low- field carbon. DART-MS: *m/z* calcd. for $C_{15}H_{19}N_2O_2$ $(M+H)^+$ 259.14410, found 259.14349.

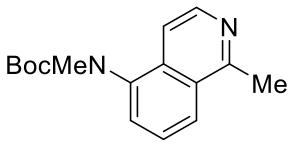

***tert*-Butyl methyl(1-methylisoquinolin-5-yl)carbamate (S6).** To a solution of **S5** (1.99 g, 7.68 mmol) in THF (50 mL) was added NaH 60% in mineral oil (399.6 mg, 9.99 mmol). After effervescence ceased, the resulting solution was refluxed for 30 min. To the reaction mixture was then added MeI (622 µL, 9.99 mmol) in THF (2 mL) and the solution was subsequently refluxed overnight. The mixture was concentrated *in vacuo* and the crude residue was purified by flash column chromatography (gradient, 10–30% EtOAc:hexanes). The isoquinoline **S6** was obtained as an amber oil (4.73 g, 29%). ^{1}H NMR (500 MHz, $CDCl_3$) δ 8.42 (d, J = 6.0 Hz, 1H), 8.08 (d, J = 8.4 Hz, 1H), 7.46–7.61 (m, 3H), 3.31 (s, 3H), 3.01 (s, 3H), 1.23 (s, 9H). ^{13}C NMR (125 MHz, $CDCl_3$) δ 159.01, 155.21, 140.21, 133.54, 128.35, 126.95, 124.96, 121.52, 114.65, 76.15, 29.71, 28.06 (3C), 22.51, one low-field carbon were either not observed or is overlapping with another low-field carbon. DART-MS: *m/z* calcd. for $C_{16}H_{21}N_2O_2$ $(M+H)^+$ 273.15975, found 273.15891.

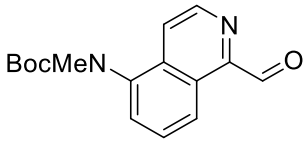

***tert*-Butyl (1-formylisoquinolin-5-yl)(methyl)carbamate (S7).** To a solution of **S6** (1.50 g, 5.51 mmol) in 1,4-dioxane (60 mL) was added SeO_2 (1.22 g, 11.0 mmol). The mixture was stirred at 60 °C overnight then cooled to 22 °C. The mixture was concentrated *in vacuo* and the crude residue was purified by flash column chromatography (gradient, 5–25% EtOAc:hexanes). The isoquinoline **S7** was obtained as a white solid (711.9 mg, 45%). ^{1}H NMR (500 MHz, $CDCl_3$) δ 10.39, 9.28 (d, J = 8.6 Hz, 1H), 8.80 (d, J = 5.7 Hz, 1H), 7.88 (d, J = 5.1 Hz, 1H), 7.74 (d, J = 8.0 Hz, 1H), 7.61 (m, 1H), 3.33 (s, 3H), 1.22 (s, 9H). ^{13}C NMR (125 MHz, $CDCl_3$) δ 195.44, 155.05, 150.18, 142.85, 139.95, 134.55, 129.90, 128.96, 127.08, 124.99, 120.65, 80.72, 37.85, 28.08 (3C). DART-MS: *m/z* calcd. for $C_{16}H_{19}N_2O_3$ $(M+H)^+$ 287.13902, found 287.13812.

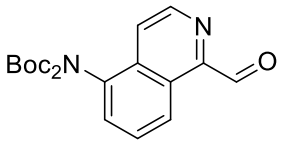

***tert*-Butyl (*tert*-butoxycarbonyl)(1-formylisoquinolin-5-yl)carbamate (S8).** To a solution of **S4** (200.0 mg, 0.558 mmol) in 1,4-dioxane (5.5 mL) was added SeO_2 (123.8 mg, 1.12 mmol). The mixture was

stirred at 60 °C overnight then cooled to 22 °C. The mixture was concentrated *in vacuo* and the crude residue was purified by flash column chromatography (gradient, 5–25% EtOAc:hexanes). The isoquinoline **S8** was obtained as a white solid (63.2 mg, 30%). ^{1}H NMR (500 MHz, $CDCl_3$) δ 10.40 (s, 1H), 9.34 (dt, *J* = 8.7, 1.0 Hz, 1H), 8.81 (d, *J* = 5.7 Hz, 1H), 7.89 (dd, *J* = 5.7, 1.0 Hz, 1H), 7.76 (dd, *J* = 8.7, 7.4 Hz, 1H), 7.61 (dd, *J* = 7.3, 1.1 Hz, 1H), 1.32 (s, 18H). ^{13}C NMR (125 MHz, $CDCl_3$) δ 195.59, 151.36, 150.23, 143.31, 134.94, 130.49, 129.74, 126.88, 126.00, 119.90, 83.60 (2C), 27.91 (6C), two low-field carbon were either not observed or is overlapping with another low-field carbon . DART-MS: *m/z* calcd. for $C_{20}H_{25}N_2O_5$ $(M+H)^+$ 373.17580, found 373.17496.

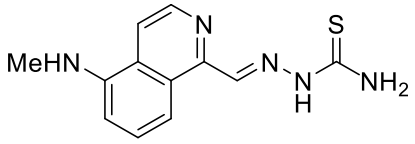

(*E*)-2-((5-(Methylamino)isoquinolin-1-yl)methylene)hydrazine-1-carbothioamide (HCT4). To a solution of **S7** (100.0 mg, 0.3492 mmol) in EtOH (1.75 mL) was added thiosemicarbazide (31.8 mg, 0.3492 mmol) and HCl (350 µL, 6 M in H_2O). The mixture was stirred and refluxed for 1.5 h and then cooled to 22 °C. The hydrochloride salt that formed was neutralized with 1.4 mL of a saturated aqueous $NaHCO_3$ solution. The precipitate of the desired compound was collected by filtration, washed with water, EtOH and then dried to yield the isoquinoline **HCT4** as a black solid (622.4 mg, 97%). ^{1}H NMR (500 MHz, DMSO- d_6) δ 12.32 (s, 1H), 9.07 (br s, 1H), 8.92 (s, 1H), 8.90 (s, 1H), 8.57 (d, *J* = 6.6 Hz, 1H), 8.52 (d, *J* = 6.7 Hz, 1H), 7.85 (t, *J* = 8.2 Hz, 1H), 7.56 (d, *J* = 8.3 Hz, 1H), 7.30 (br s, 1H), 7.01 (d, *J* = 8.0 Hz, 1H), 2.91 (s, 3H). ^{13}C NMR (125 MHz, DMSO-d_6) δ 179.40, 146.25, 146.00, 133.09, 130.09, 128.72, 126.75 (2C), 119.38, 111.17, 110.66, 30.39. DART-MS: *m/z* calcd. for $C_{12}H_{14}N_5S$ $(M+H)^+$ 260.09644, found 260.09501.

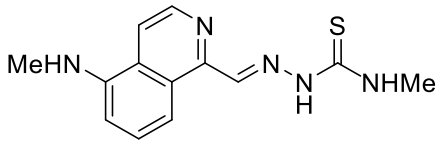

and

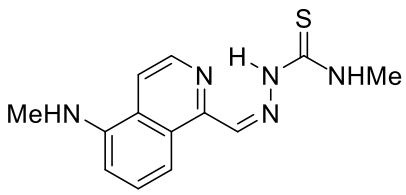

(*E*)-*N*-Methyl-2-((5-(methylamino)isoquinolin-1-yl)methylene)hydrazine-1-carbothioamide and (*Z*)-*N*-Methyl-2-((5-(methylamino)isoquinolin-1-yl)methylene)hydrazine-1-carbothioamide (HCT9). To a solution of **S7** (51.4 mg, 0.18 mmol) in EtOH (0.88 mL) was added 4-methyl-3-thiosemicarbazide (18.9 mg, 0.18 mmol) and HCl (0.18 mL, 6 M in H_2O). The mixture was stirred and refluxed for 1.5 h then cooled to 22 °C. The hydrochloride salt that formed was neutralized with saturated aqueous $NaHCO_3$ solution (0.88 mL). The precipitate of the desired compound was collected by filtration, washed with water, EtOH and then dried to yield the isoquinoline **HCT9** as a black solid (49.0 mg, 94%) (mixture of *E* and *Z* isomers). ^{1}H NMR (500 MHz, DMSO-d_6) δ 14.74 (s, 0.15H), 12.22 (s, 1H), 9.39 (br s, 1H), 8.93 (q, *J* = 4.7 Hz, 0.15H), 8.78 (s, 1H), 8.54 (d, *J* = 5.9 Hz, 0.15H), 8.50 (d, *J* = 6.5 Hz, 1H), 8.38 (s, 1H), 8.17 (s, 0.15H), 8.12 (d, *J* = 5.9 Hz, 0.15H), 7.82 (d, *J* = 8.6 Hz, 0.15H), 7.76 (t, *J* = 8.1 Hz, 1H), 7.69 (s, 1H), 7.56 (t, *J* = 8.1 Hz, 0.15H), 7.08 (br s, 1H), 6.92 (d, *J* = 7.7 Hz, 1.15H), 6.72 (d, *J* = 7.8 Hz, 0.15H), 3.07 (d, *J* = 4.6 Hz, 3H), 3.02 (d, *J* = 4.6 Hz, 0.45 H), 2.88 (s, 3H), 2.86 (s, 0.45H). ^{13}C NMR (125 MHz, DMSO-d_6) δ 178.84, 178.38, 150.11, 147.37, 145.83 (2C), 145.56, 138.94, 132.45, 130.58, 129.19,

128.23, 128.22, 126.87 (2C), 126.80, 118.47, 117.04, 111.57, 110.13, 109.63, 106.57, 31.59, 31.42, 30.42 (2C). DART- MS: *m/z* calcd. for $C_{13}H_{16}N_5S$ $(M+H)^+$ 274.11209, found 274.11104.

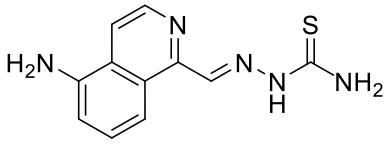

(*E*)-2-((5-Aminoisoquinolin-1-yl)methylene)hydrazine-1-carbothioamide (HCT5). To a solution of **S8** (30.0 mg, 0.081 mmol) in EtOH (0.39 mL) was added thiosemicarbazide (7.3 mg, 0.802 mmol) and HCl (80.6 μL, 6 M in H_2O). The mixture was stirred and refluxed for 1.5 h then cooled to 22 °C. The hydrochloride salt that formed was neutralized with saturated aqueous $NaHCO_3$ solution (0.39 mL). The precipitate of the desired compound was collected by filtration, washed with water, EtOH and then dried to yield the isoquinoline **HCT5** as a green solid (19.6 mg, 99%). ^{1}H NMR (500 MHz, DMSO-d_6) δ 11.66 (br s, 1H), 8.57 (s, 1H), 8.42 (d, J = 5.8 Hz, 1H), 8.31 (br s, 1H), 8.25 (d, J = 8.5 Hz, 1H), 7.98 (d, J = 5.8 Hz, 1H), 7.60 (br s, 1H), 7.42 (t, J = 8.1 Hz, 1H), 6.89 (d, J = 7.1 Hz, 1H), 6.02 (s, 2H). ^{13}C NMR (125 MHz, DMSO-d_6) δ 178.46, 150.36, 145.86, 144.62, 140.01, 129.74, 126.78. 125.83. 116.50, 113.12, 110.74. DART-MS: *m/z* calcd. for $C_{11}H_{11}N_5S$ $(M+H)^+$ 246.08079, found 246.08020.

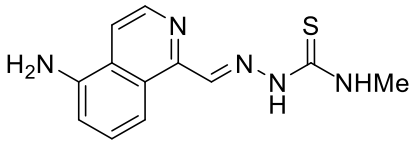

and

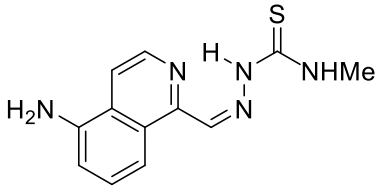

(*E*)-2-((5-Aminoisoquinolin-1-yl)methylene)-*N*-methylhydrazine-1-carbothioamide and (*Z*)- 2-((5-Aminoisoquinolin-1-yl)methylene)-*N*-methylhydrazine-1-carbothioamide (HCT10). To a solution of **S8** (27.1 mg, 0.0728 mmol) in EtOH (0.73 mL) was added 4-methyl-3-thiosemicarbazide (7.7 mg, 0.0732 mmol) and HCl (72.8 μL, 6 M in H_2O). The mixture was stirred and refluxed for 1.5 h then cooled to 22 °C. The hydrochloride salt that formed was neutralized with saturated aqueous $NaHCO_3$ solution (0.73 mL). The precipitate of the desired compound was collected by filtration, washed with water, EtOH and then dried to yield the isoquinoline **HCT10** as a yellow solid (5.1 mg, 27%) (mixture of *E* and *Z* isomers). ^{1}H NMR (500 MHz, DMSO-d_6) δ 14.80 (s, 0.08H), 11.66 (br s, 1H), 8.95 (d, J = 4.9 Hz, 0.08H), 8.62 (s, 1H), 8.52 (d, J = 5.9 Hz, 0.8H), 8.42 (d, J = 5.8 Hz, 1H), 8.25 (d, J = 3.3 Hz, 1H), 8.18 (s, 0.08H), 8.11–8.15 (m, 1.08H), 7.99 (d, J = 5.9 Hz, 1H), 7.83 (d, J = 8.4 Hz, 0.08H), 7.48 (t, J = 7.9 Hz, 0.08H), 7.43 (t, J = 8.0 Hz, 1H), 6.97 (d, J = 7.6 Hz, 0.08H), 6.91 (dd, J = 7.6, 0.9 Hz, 1H), 6.21 (s, 0.16H), 6.04 (s, 2H), 3.05– 3.07 (m, 3.24H). ^{13}C NMR (125 MHz, DMSO-d_6) δ 178.85, 178.52, 150.83, 150.19, 145.53, 145.20, 145.10, 140.49, 138.40, 130.28, 130.10, 129.16, 128.41, 127.36, 126.27, 126.16, 117.81, 116.96, 113.24, 111.66, 111.18, 110.61, 31.74, 31.59. DART-MS: *m/z* calcd. for $C_{12}H_{14}N_5S$ $(M+H)^+$ 260.09644, found 260.09563.

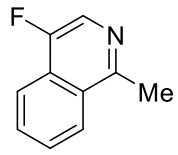

4-Fluoro-1-methylisoquinoline (S9). To a solution of 4-fluoroisoquinoline (1.50 g, 10.19 mmol) in THF (102 mL) was added allyl chloroformate (2.17 mL, 20.38 mmol). MeMgBr (10.19 mL, 2 M in diethyl ether) was then added dropwise to the reaction mixture at 0 °C with stirring. The reaction mixture was gradually warmed to 22 °C over a period of 2 h. The mixture was quenched with saturated aqueous NH_4Cl (10 mL) and water (100 mL) was added. The organic layer was separated and the aqueous layer was extracted with EtOAc (3 × 100 mL). The organic layers were combined and dried over $MgSO_4$, filtered, and then concentrated *in vacuo*. The crude residue in EtOAc was filtered through a silica plug, concentrated *in vacuo* and the residue was subjected to the next reaction without further purification. To a solution of the crude residue and $Pd(PPh_3)_4$ (70.1 mg, 0.061 mmol) in DCM (60 mL) at 0 °C was added morpholine (523.1 uL, 6.07 mmol). The reaction mixture was stirred and slowly warmed to 22 °C over a period of 3 h. The mixture was cooled to 0 °C and DDQ (1.38 g, 6.07 mmol) was added in portions. After the reaction mixture stirred at 0 °C for 30 min, the reaction was slowly poured into a solution of saturated $NaHCO_3$ solution (60 mL) and extracted with DCM (3 × 60). The combined extracts are washed with brine, dried over Na_2SO_4, and concentrated *in vacuo*. The crude residue was purified by flash column chromatography (gradient, 5–25% EtOAc:hexanes). The isoquinoline **S9** was obtained as a brown oil (241.9 mg, 15% over three steps). ^{1}H NMR (500 MHz, $CDCl_3$) δ 8.23 (d, J = 1.7 Hz, 1H), 8.06–8.09 (m, 2H), 7.73-7.76 (m, 1H), 7.64-7.67 (m, 1H), 2.90 (s, 3H). ^{13}C NMR (125 MHz, $CDCl_3$) δ 154.48 (d, $^1J_{C\text{-}F}$ = 257.5 Hz), 154.24 (d, $^3J_{C\text{-}F}$ = 4.9 Hz), 130.14 (d, $^4J_{C\text{-}F}$ = 1.6 Hz), 128.35 (d, $^4J_{C\text{-}F}$ = 2.4 Hz), 127.83, 126.64 (d, $^2J_{C\text{-}F}$ = 15.3 Hz), 126.57 (d, $^2J_{C\text{-}F}$ = 22.3 Hz), 125.60 (d, $^4J_{C\text{-}F}$ = 2.1 Hz), 120.09 (d, $^3J_{C\text{-}F}$ = 4.5 Hz), 22.10. ^{19}F NMR (376 MHz, $CDCl_3$) δ –143.11, extraneous peak found at –139.82. DART-MS: *m/z* calcd. for $C_{10}H_9FN$ $(M+H)^+$ 162.07135, found 162.07092.

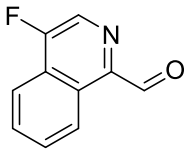

4-Fluoroisoquinoline-1-carboxaldehyde (S10). To a solution of **S9** (40.0 mg, 0.248 mmol) in 1,4-dioxane (2.5 mL) was added SeO_2 (55.1 mg, 0.496 mmol). The mixture was stirred at 60 °C overnight then cooled to 22 °C. The mixture was concentrated *in vacuo* and the crude residue was purified by flash column chromatography (gradient, 5–25% EtOAc:hexanes). The isoquinoline **S10** was obtained as a white solid (27.3 mg, 63%). ^{1}H NMR (500 MHz, DMSO-d_6) δ 10.32 (s, 1H), 9.37–9.41 (m, 1H), 8.59 (d, J = 1.5 Hz, 1H), 8.16–8.20 (m, 1H), 7.82-7.87 (m, 2H). ^{13}C NMR (125 MHz, DMSO-d_6) δ 194.23, 157.16 (d, $^1J_{C\text{-}F}$ = 270.3 Hz), 146.44 (d, $^3J_{C\text{-}F}$ = 5.6 Hz), 131.07 (d, $^4J_{C\text{-}F}$ = 2.2 Hz), 130.95 128.48 (d, $^2J_{C\text{-}F}$ = 24.6 Hz), 128.14 (d, $^4J_{C\text{-}F}$ = 4.1 Hz), 126.85 (d, $^2J_{C\text{-}F}$ = 14.4 Hz), 125.64 (d, $^4J_{C\text{-}F}$ = 1.8 Hz), 119.85 (d, $^3J_{C\text{-}F}$ = 4.7 Hz). ^{19}F NMR (376 MHz, $CDCl_3$) δ –129.02. DART-MS: *m/z* calcd. for $C_{10}H_6FNO$ $(M+H)^+$ 176.05062, found 176.05012.

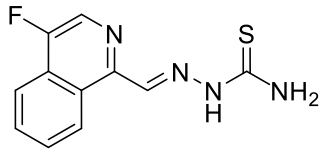

(*E*)-2-((4-Fluoroisoquinolin-1-yl)methylene)hydrazine-1-carbothioamide (HCT2). To a solution of **S10** (6.0 mg, 0.0343 mmol) in EtOH (0.5 mL) was added thiosemicarbazide (3.3 mg, 0.0343 mmol) and HCl (34 μL, 0.206 mmol, 6 M in H_2O). The mixture was stirred and refluxed for 1.5 h then cooled to 22 °C. The hydrochloride salt that formed was then neutralized with saturated aqueous $NaHCO_3$ solution (0.5 mL). The precipitate of the desired compound was collected by filtration, washed with water, EtOH and then dried to yield the isoquinoline **HCT2** as a pale-yellow solid (3.0 mg, 35%). ^{1}H NMR (500 MHz, DMSO-d_6) δ 11.70 (s, 1H), 9.28 (d, J = 8.5 Hz, 1H), 8.56 (d, J = 1.5 Hz, 1H), 8.53 (s, 1H), 8.48 (s, 1H), 8.13 (d, J = 8.2 Hz, 1H), 7.94 (ddd, J = 8.2, 7.0, 0.9 Hz, 1H), 7.85 (m, 2H). ^{13}C NMR (125 MHz, DMSO-d_6) δ 178.84, 154.73 (d, $^1J_{C\text{-}F}$ = 262.2 Hz), 148.03 (d, $^3J_{C\text{-}F}$ = 5.2 Hz), 145.84, 131.75, 130.69, 128.10 (d, $^2J_{C\text{-}F}$ = 23.3 Hz), 127.75, 127.35 (d, $^4J_{C\text{-}F}$ = 3.0 Hz), 126.51 (d, $^2J_{C\text{-}F}$ = 14.9 Hz), 119.79 (d, $^3J_{C\text{-}F}$ = 4.6 Hz). ^{19}F NMR (376 MHz, DMSO-d_6) δ –137.31. DART-MS: *m/z* calcd. for $C_{11}H_9FN_4S$ $(M+H)^+$ 249.06047, found 249.05042.

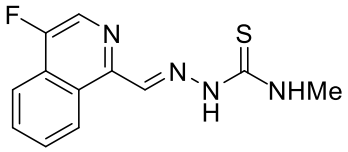

(*E*)-2-((4-Fluoroisoquinolin-1-yl)methylene)-*N*-methylhydrazine-1-carbothioamide (HCT7). To a solution of **S10** (6.0 mg, 0.0343 mmol) in EtOH (0.5 mL) was added 4-methyl-3-thiosemicarbazide (3.6 mg, 0.0343 mmol) and HCl (34 μL, 0.206 mmol, 6 M in H_2O). The mixture was stirred and refluxed for 1.5 h then cooled to 22 °C. The hydrochloride salt that formed was then neutralized with saturated aqueous $NaHCO_3$ solution (0.5 mL). The precipitate of the desired compound was collected by filtration, washed with water, EtOH and then dried to yield the isoquinoline **HCT7** as a pale-yellow solid (2.6 mg, 29%). ^{1}H NMR (500 MHz, DMSO-d_6) δ 11.76 (s, 1H), 9.19 (d, J = 8.6 Hz, 1H), 8.56 (d, J = 1.4 Hz, 1H), 8.56 (s, 1H), 8.34 (d, J = 4.4 Hz, 1H), 8.14 (d, J = 8.3 Hz, 1H), 7.94–7.97 (m, 1H), 7.85–7.89 (m, 1H), 3.06 (d, J = 4.6 Hz, 3H). ^{13}C NMR (125 MHz, DMSO-d_6) δ 178.84, 154.73 (d, $^1J_{C\text{-}F}$ = 262.2 Hz), 148.03 (d, $^3J_{C\text{-}F}$ = 5.2 Hz), 145.84, 131.75, 130.69, 128.10 (d, $^2J_{C\text{-}F}$ = 23.3 Hz), 127.75, 127.35 (d, $^4J_{C\text{-}F}$ = 3.0 Hz), 126.51 (d, $^2J_{C\text{-}F}$ = 14.9 Hz), 119.79 (d, $^3J_{C\text{-}F}$ = 4.6 Hz), 31.86. ^{19}F NMR (376 MHz, DMSO-d_6) δ –137.53, extraneous peak found at –134.32. DART-MS: *m/z* calcd. for $C_{12}H_{12}FN_4S$ $(M+H)^+$ 263.07612, found 263.07520.

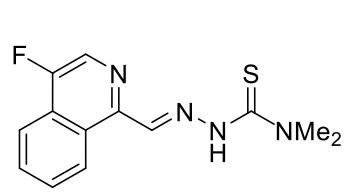

and
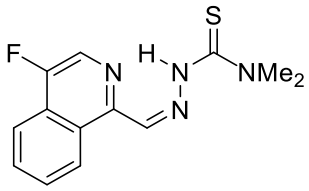

(*E*)-2-((4-Fluoroisoquinolin-1-yl)methylene)-*N*,*N*-dimethylhydrazine-1-carbothioamide and (*Z*)-2-((4-Fluoroisoquinolin-1-yl)methylene)-*N*,*N*-dimethylhydrazine-1-carbothioamide (HCT12). To a solution of **S10** (17.8 mg, 0.102 mmol) in MeOH (1.0 mL) was added 4,4-dimethyl-3-thiosemicarbazide (12.0 mg, 0.102 mmol) and HCl (101 μL, 0.610 mmol, 6 M in H_2O). The mixture was microwaved at 300 W and 50 °C for 1.0 h. The hydrochloride salt that formed was then neutralized with saturated aqueous $NaHCO_3$ solution (1.0 mL). The precipitate of the desired compound was collected by filtration, washed with water, EtOH and then dried to yield the isoquinoline **HCT12** as a pale-yellow solid (16.0 mg, 57%) (mixture of *E* and *Z* isomers). ^{1}H NMR (500 MHz, DMSO-d_6) δ 15.52 (s, 0.15H), 11.28 (s, 1H), 9.87 (d, J = 8.7 Hz, 1H), 8.87 (d, J = 9.0 Hz, 0.15H), 8.77 (d, J = 1.9 Hz, 0.15H), 8.69 (s, 1H), 8.57 (d, J = 1.6 Hz, 1.15H), 8.23 (d, J = 8.2 Hz, 0.15H), 8.15 (d, J = 8.2 Hz, 1H), 8.02–8.05 (m, 0.15H), 7.92–7.97 (m, 1.15H), 7.86 (ddd, J = 8.3, 6.9, 1.3 Hz, 1H), 3.42 (s, 0.90H), 3.36 (s, 6H). ^{13}C NMR (125 MHz, DMSO-d_6) δ 180.79, 180.73, 154.60 (d, $^1J_{C\text{-}F}$ = 261.7 Hz), 154.13 (d, $^1J_{C\text{-}F}$ = 261.8 Hz), 148.75 (d, $^3J_{C\text{-}F}$ = 5.1 Hz), 147.76 (d, $^3J_{C\text{-}F}$ = 5.7 Hz), 147.05, 132.52, 131.59 (d, $^4J_{C\text{-}F}$ = 5.1 Hz), 131.10, 130.49, 130.30, 128.60 (d, $^4J_{C\text{-}F}$ = 3.3 Hz), 128.41 (d, $^4J_{C\text{-}F}$ = 1.0 Hz), 127.90 (d, $^2J_{C\text{-}F}$ = 23.3 Hz), 127.19 (d, $^4J_{C\text{-}F}$ = 2.6 Hz), 126.88 (d, $^2J_{C\text{-}F}$ = 14.8 Hz), 126.71 (d, $^2J_{C\text{-}F}$ = 14.7 Hz), 126.35 (d, $^2J_{C\text{-}F}$ = 25.2 Hz),124.98, 120.23 (d, $^3J_{C\text{-}F}$ = 4.3 Hz), 119.79 (d, $^3J_{C\text{-}F}$ = 4.7 Hz), 42.04 (4C). ^{19}F NMR (376 MHz, DMSO-d_6) δ –134.93, –138.02. DART-MS: *m/z* calcd. for $C_{13}H_{14}FN_4S$ $(M+H)^+$ 277.09177, found 277.09096.

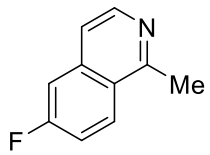

6-Fluoro-1-methylisoquinoline (S11). To a solution of 6-fluoroisoquinoline (1.00 g, 6.80 mmol) in THF (120 mL) was added allyl chloroformate (1.64 mL, 13.59 mmol). MeMgBr (6.98 mL, 13.59 mmol, 2 M in diethyl ether) was then added dropwise to the reaction mixture at 0 °C while stirring and the mixture was gradually warmed to 22 °C over a period of 2 h. The reaction was quenched with saturated aqueous NH_4Cl (12 mL) and water (120 mL) was added. The organic layer was separated and the aqueous layer was extracted with EtOAc (3 × 120 mL). The organic layers were combined and dried over $MgSO_4$, filtered, and then concentrated *in vacuo*. The crude residue in EtOAc was filtered through a silica plug, concentrated *in vacuo* and the crude residue was subjected to the next reaction without further purification. To a solution of the crude residue and $Pd(PPh_3)_4$ (293.4 mg, 0.254 mmol) in DCM (50 mL) at 0 °C was added morpholine (437.9 uL, 5.08 mmol). The reaction was stirred and slowly warmed to 22 °C over a period of 3 h. The mixture was cooled to 0 °C and DDQ (1.15 g, 5.08 mmol) was added portionwise. After the reaction mixture stirred at 0 °C for 30 min, the reaction was slowly poured into a solution of saturated $NaHCO_3$ solution (50 mL) and extracted with DCM (3 × 50). The combined extracts are washed with brine, dried over Na_2SO_4, and concentrated *in vacuo* and the crude residue was purified by flash column chromatography (gradient, 5–25% EtOAc:hexanes). The isoquinoline **S11** was obtained as a brown oil (583.9 mg, 53% over three steps). ^{1}H NMR (500 MHz, DMSO-d_6) δ 8.37 (d, J = 5.8 Hz,

1H), 8.13 (dd, J = 9.2, 5.5 Hz, 1H), 7.46 (d, J = 5.8 Hz, 1H), 7.40 (dd, J = 9.3, 2.6 Hz, 1H), 7.34 (td, J = 8.8, 2.6 Hz, 1H), 2.95 (s, 3H). ^{13}C NMR (125 MHz, DMSO-d_6) δ 162.94 (d, $^{1}J_{C\text{-}F}$ = 252.2 Hz), 158.53 (d, $^{5}J_{C\text{-}F}$ = 1.0 Hz), 142.77, 137.58 (d, $^{3}J_{C\text{-}F}$ = 10.4 Hz), 128.79 (d, $^{3}J_{C\text{-}F}$ = 9.6 Hz), 124.72 (d, $^{4}J_{C\text{-}F}$ = 1.0 Hz), 119.01 (d, $^{4}J_{C\text{-}F}$ = 5.0 Hz), 117.31 (d, $^{2}J_{C\text{-}F}$ = 25.0 Hz), 110.44 (d, $^{2}J_{C\text{-}F}$ = 20.6 Hz), 22.53. ^{19}F NMR (376 MHz, $CDCl_3$) δ –108.23. DART-MS: *m/z* calcd. for $C_{10}H_9FN$ $(M+H)^+$ 162.07135, found 162.07096.

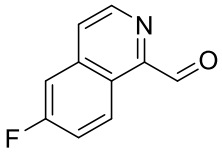

6-Fluoroisoquinoline-1-carboxaldehyde (S12). To a solution of **S11** (500.0 mg, 3.10 mmol) in 1,4-dioxane (19.0 mL) was added SeO_2 (688.4 mg, 6.20 mmol). The mixture was stirred at 60 °C overnight then cooled to 22 °C. The mixture was concentrated *in vacuo* and the crude residue was purified by flash column chromatography (gradient, 5–25% EtOAc:hexanes). The isoquinoline **S12** was obtained as a white solid (200.9 mg, 37%). ^{1}H NMR (500 MHz, DMSO-d_6) δ 10.35 (s, 1H), 9.39 (ddd, J = 10.1, 5.6, 0.9 Hz, 1H), 8.75 (dd, J = 5.6, 0.4 Hz, 1H), 7.85 (d, J = 5.5 Hz, 1H), 7.50–7.54 (m, 2H). ^{13}C NMR (125 MHz, DMSO-d_6) δ 195.51, 163.18 (d, $^{1}J_{C\text{-}F}$ = 255.1 Hz), 149.71 (d, $^{4}J_{C\text{-}F}$ = 1.8 Hz), 143.34 (d, $^{5}J_{C\text{-}F}$ = 1.0 Hz), 138.70 (d, $^{3}J_{C\text{-}F}$ = 10.4 Hz), 129.24 (d, $^{3}J_{C\text{-}F}$ = 9.2 Hz), 124.90 (d, $^{4}J_{C\text{-}F}$ = 5.4 Hz), 123.49 (d, $^{5}J_{C\text{-}F}$ = 1.0 Hz), 120.53 (d, $^{2}J_{C\text{-}F}$ = 24.8 Hz), 110.23 (d, $^{2}J_{C\text{-}F}$ = 20.9 Hz). ^{19}F NMR (376 MHz, $CDCl_3$) δ –105.46. DART- MS: *m/z* calcd. for $C_{10}H_7FNO$ $(M+H)^+$ 176.05062, found 176.05015.

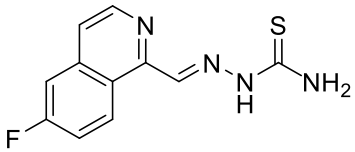

(*E*)-2-((6-Fluoroisoquinolin-1-yl)methylene)hydrazine-1-carbothioamide (HCT3). To a solution of **S12** (10.2 mg, 0.0582 mmol) in EtOH (0.5 mL) was added thiosemicarbazide (5.3 mg, 0.0582 mmol) and HCl (58 µL, 0.349 mmol, 6 M in H_2O). The mixture was stirred and refluxed for 1.5 h then cooled to 22 °C. The hydrochloride salt that formed was then neutralized with saturated aqueous $NaHCO_3$ solution (0.5 mL). The precipitate of the desired compound was collected by filtration, washed with water, EtOH and then dried to yield the isoquinoline **HCT3** as a pale-yellow solid (13.4 mg, 93%). ^{1}H NMR (500 MHz, DMSO-d_6) δ 11.74 (s, 1H), 9.30 (dd, J = 9.4, 5.8 Hz, 1H), 8.55 (d, J = 5.6 Hz, 1H), 8.51 (s, 2H), 7.80–7.85 (m, 3H), 7.57 (td, J = 9.0, 2.8 Hz, 1H). ^{13}C NMR (125 MHz, DMSO-d_6) δ 178.88, 162.70 (d, $^{1}J_{C\text{-}F}$ = 250.4 Hz), 151.35, 146.33, 143.50, 138.62 (d, $^{3}J_{C\text{-}F}$ = 10.7 Hz), 131.52 (d, $^{3}J_{C\text{-}F}$ = 9.5 Hz), 123.24, 121.79 (d, $^{4}J_{C\text{-}F}$ = 5.0 Hz), 119.36 (d, $^{2}J_{C\text{-}F}$ = 24.5 Hz), 110.86 (d, $^{2}J_{C\text{-}F}$ = 20.7 Hz). ^{19}F NMR (376 MHz, DMSO-d_6) δ – 107.79, extraneous peak found at –106.49. DART-MS: *m/z* calcd. for $C_{11}H_{10}FN_4S$ $(M+H)^+$ 249.06047, found 249.05984.

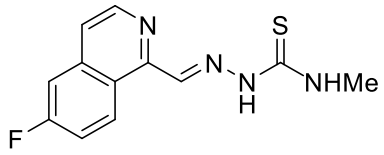

(*E*)-2-((6-Fluoroisoquinolin-1-yl)methylene)-*N*-methylhydrazine-1-carbothioamide (HCT8). To a solution of **S12** (8.8 mg, 0.0502 mmol) in EtOH (0.5 mL) was added 4-methyl-3-thiosemicarbazide (5.3 mg, 0.0502 mmol) and HCl (50 µL, 0.300 mmol, 6 M in H_2O). The mixture was stirred and refluxed for 1.5 h then cooled to 22 °C. The hydrochloride salt that formed was then neutralized with saturated aqueous $NaHCO_3$ solution (0.5 mL). The precipitate of the desired compound was collected by filtration, washed with water, EtOH and then dried to yield the isoquinoline **HCT8** as a pale-yellow solid (10.8 mg, 82%). ^{1}H NMR (500 MHz, DMSO-d_6) δ 11.80 (s, 1H), 9.20 (dd, J = 9.4, 5.7 Hz, 1H), 8.55 (d, J = 5.6 Hz, 1H), 8.54 (s, 1H), 8.35 (d, J = 4.7 Hz, 1H), 7.83 (dd, J = 9.2, 3.9 Hz, 2H) 7.60 (td, J = 9.0, 2.7 Hz, 1H), 3.06 (d, J = 4.5 Hz, 3H). ^{13}C NMR (125 MHz, DMSO-d_6) δ 178.56, 162.71 (d, $^1J_{C\text{-}F}$ = 250.4 Hz), 151.55, 145.22, 143.53, 138.62 (d, $^3J_{C\text{-}F}$ = 10.6 Hz), 131.28 (d, $^3J_{C\text{-}F}$ = 9.5 Hz), 123.29, 121.67 (d, $^4J_{C\text{-}F}$ = 5.1 Hz), 119.23 (d, $^2J_{C\text{-}F}$ = 24.8 Hz), 110.89 (d, $^2J_{C\text{-}F}$ = 20.8 Hz), 31.85. ^{19}F NMR (376 MHz, DMSO-d_6) δ –106.55, extraneous peak found at –107.74. DART-MS: *m/z* calcd. for $C_{12}H_{12}FN_4S$ $(M+H)^+$ 263.07612, found 263.07538.

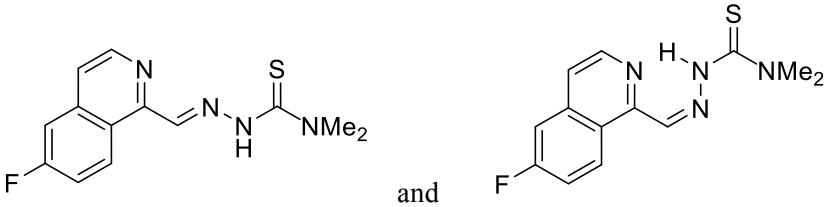

(*E*)-2-((6-Fluoroisoquinolin-1-yl)methylene)-*N*,*N*-dimethylhydrazine-1-carbothioamide and (*Z*)-2-((6-Fluoroisoquinolin-1-yl)methylene)-*N*,*N*-dimethylhydrazine-1-carbothioamide (HCT13). To a solution of **S12** (8.6 mg, 0.0491 mmol) in EtOH (0.5 mL) was added 4,4-dimethyl-3-thiosemicarbazide (5.9 mg, 0.0491 mmol) and HCl (49 µL, 0.294 mmol, 6 M in H_2O). The mixture was stirred and refluxed for 1.5 h then cooled to 22 °C. The hydrochloride salt that formed was then neutralized with saturated aqueous $NaHCO_3$ solution (0.5 mL). the precipitate of the desired compound was collected by filtration, washed with water, EtOH and then dried to yield the isoquinoline **HCT13** as a pale-yellow solid (7.4 mg, 55%). ^{1}H NMR (500 MHz, DMSO-d_6) δ 15.90 (s, 0.21H), 11.30 (s, 1H), 9.87 (dd, J = 9.5, 5.9 Hz, 1H), 8.91 (dd, J = 9.4, 5.4 Hz, 0.21H), 8.66 (m, 1.21H), 8.59 (s, 0.21H), 8.55 (d, J = 5.6 Hz, 1H), 7.97 (d, J = 5.6 Hz, 0.21H), 7.91 (dd, J = 9.6, 2.7 Hz, 0.21H), 7.79–7.82 (m, 2H), 7.73 (td, J = 9.1, 2.7 Hz, 0.21H), 7.62 (ddd, J = 9.6, 8.6, 2.8 Hz, 1H), 3.40 (s, 1.26H), 3.33 (s, 6H). ^{13}C NMR (125 MHz, DMSO-d_6) δ 180.78 (2C), 163.19 (d, $^1J_{C\text{-}F}$ = 251.7 Hz), 162.66 (d, $^1J_{C\text{-}F}$ = 250.6 Hz), 151.99 (d, $^5J_{C\text{-}F}$ = 1.2 Hz), 150.63 (d, $^5J_{C\text{-}F}$ = 0.9 Hz), 147.57, 143.42, 141.42, 138.83 (d, $^3J_{C\text{-}F}$ = 15.5 Hz), 138.76 (d, $^4J_{C\text{-}F}$ = 10.7 Hz), 132.08 (d, $^3J_{C\text{-}F}$ = 9.3 Hz), 131.62, 128.64 (d, $^3J_{C\text{-}F}$ = 9.9 Hz), 124.14, 123.10, 122.12 (d, $^4J_{C\text{-}F}$ = 5.2 Hz), 121.56 (d, $^4J_{C\text{-}F}$ = 5.1 Hz), 119.54 (d, $^2J_{C\text{-}F}$ = 25.6 Hz), 119.14 (d, $^2J_{C\text{-}F}$ = 24.4 Hz), 111.48 (d, $^2J_{C\text{-}F}$ = 20.8 Hz), 110.90 (d, $^2J_{C\text{-}F}$ = 20.7 Hz), 42.04 (4C). ^{19}F NMR (376 MHz, DMSO-d_6) δ –106.34, –107.95. DART-MS: *m/z* calcd. for $C_{13}H_{14}FN_4S$ $(M+H)^+$ 277.09177, found

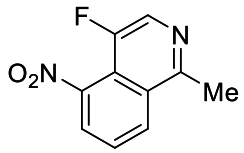

4-Fluoro-1-methyl-5-nitroisoquinoline (S13). To a solution of **S11** (0.376 g, 2.333 mmol) in sulfuric acid (0.4 mL) at 0 ℃ was added KNO_3 (0.234 g, 2.333 mmol) in sulfuric acid (0.6 mL). The mixture was heated at 60 ℃ for 2 h and then poured slowly over crushed ice. The solution was made alkaline with NH_4OH; the resulting tan precipitate was filtered, washed with water, and dried to afford **S13** as a tan solid (0.210 g, 44%). ^{1}H NMR (500 MHz, $CDCl_3$) δ 8.42 (d, J = 2.9 Hz, 1H), 8.36 (d, J = 8.3 Hz, 1H), 7.98 (d, J = 7.4 Hz, 1H), 7.77 (t, J = 7.8 Hz, 1H), 3.03 (s, 3H). ^{13}C NMR (125 MHz, $CDCl_3$) δ 155.10 (d, $^4J_{C\text{-}F}$ = 5.2 Hz), 151.08 (d, $^1J_{C\text{-}F}$ = 262.1 Hz), 144.92, 130.04 (d, $^2J_{C\text{-}F}$ = 25.2 Hz), 129.62, 128.88, 127.24, 125.53, 118.43 (d, $^3J_{C\text{-}F}$ = 12.1 Hz), 22.66. ^{19}F NMR (376 MHz, $CDCl_3$) δ -133.19. DART-MS: *m/z* calcd. for $C_{10}H_8FN_2O_2$ $(M+H)^+$ 207.05643, found 207.05705.

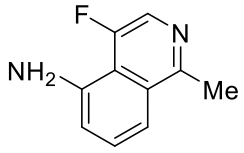

4-Fluoro-1-methylisoquinolin-5-amine (S14). To a solution of **S13** (0.210 g, 1.02 mmol) in MeOH (50 mL) iron powder (0.171 g, 3.06 mmol and HCl (1 mL, 12 M in H_2O). The mixture was refluxed for 2 h and then a solution of sodium hydroxide (2 mL, 6 M in H_2O) was added. The mixture was filtered and extracted with diethyl ether (200 mL). The organic layer was dried over Na_2SO_4, filtered, and then concentrated *in vacuo*. The crude residue was purified by flash column chromatography (gradient, 10–30% EtOAc:hexanes). The isoquinoline **S14** was obtained as a brown solid (0.173 g, 96%). ^{1}H NMR (500 MHz, $CDCl_3$) δ 8.09 (d, J = 5.1 Hz, 1H), 7.46–7.39 (m, 2H), 6.88 (dd, J = 6.9, 1.8 Hz, 1H), 4.83 (br s, 2H), 2.87 (d, J = 1.3, 3H). ^{13}C NMR (125 MHz, $CDCl_3$) δ 155.92 (d, $^1J_{C\text{-}F}$ = 253.3 Hz), 154.74 (d, $^4J_{C\text{-}F}$ = 4.9 Hz), 142.23 (d, $^4J_{C\text{-}F}$ = 3.0 Hz), 129.19, 115.79 (d, $^3J_{C\text{-}F}$ = 8.8 Hz), 114.77, 114.76, 113.81 (2C), 22.61. ^{19}F NMR (376 MHz, $CDCl_3$) δ -136.45. DART-MS: *m/z* calcd. for $C_{10}H_{10}FN_2$ $(M+H)^+$ 177.08225, found 177.08220.

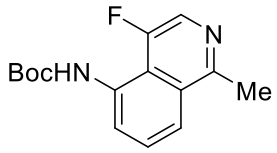

***tert*-butyl (4-fluoro-1-methylisoquinolin-5-yl)carbamate (S15).** To a solution of **S14** (1.14 g, 6.49 mmol) in THF (15 mL) was added DMAP (79.3 mg, 0.65 mmol) then Boc_2O (3.54 g, 16.23 mmol) and the mixture was stirred at 22 °C overnight. After completion of the reaction as judged by TLC, K_2CO_3 (2.69 g, 19.47 mmol) and MeOH (10 mL) were added to the reaction mixture and then refluxed overnight.

The mixture was then concentrated *in vacuo* and resuspended in EtOAc (20 mL) and water (20 mL). The organic layer was separated and the aqueous layer was extracted with EtOAc (3 × 20 mL). The organic layers were combined and dried over Na_2SO_4, filtered, and then concentrated *in vacuo*. The crude residue was purified by flash column chromatography (gradient, 5–20% EtOAc:hexanes). The isoquinoline **S15** was obtained as a brown oil (0.572 g, 33%). ^{1}H NMR (500 MHz, $CDCl_3$) δ 8.50 (dd, J = 7.9, 1.0 Hz, 1H), 8.17 (d, J = 5.7 Hz, 1H), 8.05 (d, J = 17.8 Hz, 1H), 7.73 (ddd, J = 8.4, 3.0, 1.0 Hz, 1H), 7.60 (t, J = 8.2 Hz, 1H), 2.88 (d, J = 1.3 Hz, 3H), 1.55 (s, 9H). ^{13}C NMR (125 MHz, $CDCl_3$) δ 158.37 (d, $^1J_{C\text{-}F}$ = 296.5 Hz), 153.19, 137.68, 131.10, 128.23 (d, $^3J_{C\text{-}F}$ = 10.7 Hz), 124.83, 124.45, 121.14 (d, $^2J_{C\text{-}F}$ = 22.3 Hz), 119.58, 82.72, 28.15 (3C), 17.84, one low-field carbon were either not observed or is overlapping with another low-field carbon. ^{19}F NMR (376 MHz, $CDCl_3$) δ -136.85. DART-MS: *m/z* calcd. for $C_{15}H_{18}FN_2O_2$ $(M+H)^+$ 277.13468, found 277.13425.

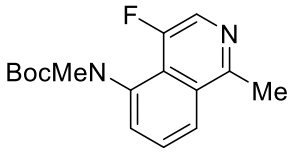

***tert*-Butyl methyl(4-fluoro-1-methylisoquinolin-5-yl)carbamate (S16).** To a solution of **S15** (0.524 g, 1.90 mmol) in THF (10 mL) was added NaH 60% in mineral oil (59.2 mg, 2.49 mmol). After effervescence ceased, the resulting solution was refluxed for 30 min. To the reaction mixture was then added MeI (0.350 g, 4.49 mmol) in THF (2 mL) and the solution refluxed overnight. The mixture was concentrated and passed through a silica plug (1:10-2:1 EtOAc:hexanes). The mixture was concentrated *in vacuo* and the crude residue was purified by flash column chromatography (gradient, 10–30% EtOAc:hexanes). The isoquinoline **S16** was obtained as an amber oil containing a mixture of rotamers (0.456 g, 82%). ^{1}H NMR (400 MHz, $CDCl_3$) δ 8.25–8.22 (m, 1.5H), 8.11–8.02 (m, 1.5H), 7.71–7.61 (m, 2H), 7.55 (dd, J = 7.3, 1.3 Hz, 1H), 3.28 (s, 3H), 3.27 (s, 1.5H), 2.96 (s, 3H), 2.95 (s, 1.5H), 1.53 (s, 4.5H), 1.21 (s, 9H). ^{13}C NMR (125 MHz, $CDCl_3$) δ 155.41, 154.92 (d, $^4J_{C\text{-}F}$ = 5.7 Hz), 154.90 (d, $^4J_{C\text{-}F}$ = 5.4 Hz), 154.63, 154.51, 153.54 (d, $^1J_{C\text{-}F}$ = 259.3 Hz), 137.94, 131.60, 130.52, 130.05, 129.74, 128.44, 128.19, 127.82 (d, $^2J_{C\text{-}F}$ = 27.6 Hz), 125.49, 125.08, 124.53, 124.34 (d, $^3J_{C\text{-}F}$ = 8.1 Hz), 80.79, 80.23, 38.52 (d, $^5J_{C\text{-}F}$ = 3.82 Hz), 37.81 (d, $^5J_{C\text{-}F}$ = 3.07 Hz), 28.38 (3C), 28.05 (3C), 22.46, 22.26, two low-field carbons were either not observed or is overlapping with another low-field carbon. ^{19}F NMR (376 MHz, $CDCl_3$) δ -140.37, -141.22. DART-MS: *m/z* calcd. for $C_{16}H_{20}FN_2O_2$ $(M+H)^+$ 291.15033, found 291.14981.

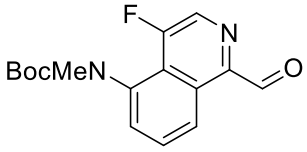

***tert*-Butyl methyl(4-fluoro-1-formylisoquinolin-5-yl)carbamate (S17).** To a solution of **S16** (0.40 g, 1.38 mmol) in 1,4-dioxane (10 mL) was added SeO_2 (0.183 g, 1.65 mmol). The mixture was stirred at 60 °C overnight then cooled to 22 °C. The mixture was concentrated *in vacuo* and the crude residue was purified by flash column chromatography (gradient, 5–25% EtOAc:hexanes). The isoquinoline **S17** was obtained as an off-white solid containing a mixture of rotamers (0.152 g, 36%). ^{1}H NMR (500 MHz, $CDCl_3$) δ 10.32 (d, J = 1.5 Hz, 1H), 10.29 (d, J = 1.6 Hz, 0.5H), 9.38 (tdd, J = 7.5, 2.7, 1.4 Hz, 1.5H),

8.58 (dd, J = 3.9, 1.1 Hz, 1H), 8.56 (dd, J = 4.0, 1.3 Hz, 0.5H), 7.80 (tt, J = 7.3, 1.4 Hz, 1.5H), 7.68 (dt, J = 7.5, 0.5Hz, 0.5H), 7.62 (dt, J = 7.4, 1.0 Hz, 1H), 3.31 (d, J = 1.1 Hz, 3H), 3.30 (d, J = 0.9 Hz, 1.5H), 1.54 (s, 4.5H), 1.21 (s, 9H). ^{13}C NMR (125 MHz, $CDCl_3$) 194.12, 194.09, 156.39 (d, $^1J_{C\text{-}F}$ = 272.5 Hz), 156.35 (d, $^1J_{C\text{-}F}$ = 255.9 Hz), 155.21, 154.41, 146.67 (d, $^3J_{C\text{-}F}$ = 6.1 Hz), 137.64 (d, $^4J_{C\text{-}F}$ = 1.7 Hz), 131.73 (d, $^4J_{C\text{-}F}$ = 1.9 Hz), 131.12 (d, $^4J_{C\text{-}F}$ = 1.9 Hz), 131.05, 130.95 (d, $^2J_{C\text{-}F}$ = 21.5 Hz), 130.85, 130.57 (d, $^2J_{C\text{-}F}$ = 28.5 Hz), 130.25 (d, $^2J_{C\text{-}F}$ = 28.2 Hz), 129.83 (d, $^4J_{C\text{-}F}$ = 2.4 Hz), 129.49 (d, $^4J_{C\text{-}F}$ = 2.5 Hz), 125.05, 124.68 (d, $^4J_{C\text{-}F}$ = 1.7 Hz), 124.56 ($^3J_{C\text{-}F}$, J = 7.4 Hz), 124.44 (d, $^3J_{C\text{-}F}$ = 7.1 Hz), 81.01, 80.49, 38.56 (d, $^5J_{C\text{-}F}$ = 3.3 Hz), 37.83 (d, $^5J_{C\text{-}F}$ = 2.6 Hz), 28.36 (3C), 28.03 (3C), one low-field carbon were either not observed or is overlapping with another low-field carbon. ^{19}F NMR (376 MHz, $CDCl_3$) δ -133.9. DART-MS: *m/z* calcd. for $C_{16}H_{18}FN_2O_3$ $(M+H)^+$ 305.12960, found 305.12824.

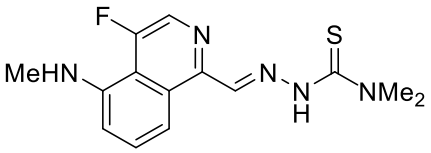

and

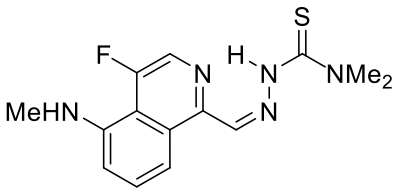

(*E*)-2-((4-Fluoro-5-(methylamino)isoquinolin-1-yl)methylene)-*N*,*N*-dimethylhydrazine-1-carbothioamide and (*Z*)-2-((4-Fluoro-5-(methylamino)isoquinolin-1-yl)methylene)-*N*,*N*-dimethylhydrazine-1-carbothioamide (HCT15). To a solution of **S17** (30.0 mg, 0.099 mmol) in MeOH (3.0 mL) was added 4,4-dimethyl-3-thiosemicarbazide (11.7 mg, 0.985 mmol) and HCl (98 µL, 0.59 mmol, 6 M in H_2O). The mixture was microwaved at 300 W and 50 °C for 1.0 h. The hydrochloride salt that formed was then neutralized with saturated aqueous $NaHCO_3$ solution (1.5 mL). The precipitate of the desired compound was collected by filtration, washed with water, EtOH and then dried to yield the isoquinoline **HCT15** as a pale-yellow solid containing a mixture of *E*- and *Z*-isomers (12.2 mg, 41%). ^{1}H NMR (500 MHz, DMSO-d_6) δ 15.46 (s, 0.33H), 11.13 (br s, 1H), 8.91 (dd, J = 8.4, 2.9 Hz, 1H), 8.62 (s, 1H), 8.50 (d, J = 5.1 Hz, 0.33H), 8.39 (s, 0.33H), 8.32 (d, J = 4.8 Hz, 1H), 7.89 (dd, J = 8.5, 2.9 Hz, 0.33H), 7.65 (t, J = 8.2 Hz, 0.33H), 7.57 (t, J = 8.2 Hz, 1H), 6.82 (d, J = 8.0 Hz, 0.33H), 6.73 (d, J = 7.9 Hz, 1H), 6.55 (dd, J = 11.9, 5.2 Hz, 0.33H), 6.39 (dd, J = 12.4, 5.0 Hz, 1H), 3.37 (s, 1.98H), 3.31 (s, 6H), 2.86–2.84 (m, 3.99H). ^{13}C NMR (125 MHz, DMSO-d_6) δ 180.95, 180.72, 156.41 (d, J = 260.4 Hz), 147.99 (d, $^4J_{C\text{-}F}$ = 4.3 Hz), 147.41, 147.16, 144.92, 144.61 (d, $^4J_{C\text{-}F}$ = 3.7 Hz), 131.90, 131.69, 130.83, 130.78, 129.29 (d, $^4J_{C\text{-}F}$ = 2.4 Hz), 127.41 (d, $^2J_{C\text{-}F}$ = 28.8 Hz), 125.43 (d, $^2J_{C\text{-}F}$ = 30.5 Hz), 115.98 (d, $^2J_{C\text{-}F}$ = 7.6 Hz), 113.89, 113.84, 110.26, 108.50, 107.78, 42.15 (4C), 30.95 (2C), one low-field carbon were either not observed or is overlapping with another low-field carbon. ^{19}F NMR (376 MHz, DMSO-d_6) δ -125.86, -129.02. DART- MS: *m/z* calcd. for $C_{14}H_{17}FN_5S$ $(M+H)^+$ 306.11832, found 306.11716.

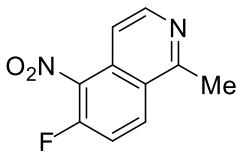

6-Fluoro-1-methyl-5-nitroisoquinoline (S18). To a solution of **S11** (0.584 g, 3.623 mmol) in sulfuric acid (0.8 mL) at 0℃ was added KNO_3 (0.366 g, 3.623 mmol) in sulfuric acid (1.2 mL). The mixture was heated at 60℃ for 2 h and then poured slowly over crushed ice. The solution was made alkaline with

NH_4OH; the resulting tan precipitate was filtered, washed with water, and dried to afford **S18** as a tan solid (0.264 g, 35%). ^{1}H NMR (500 MHz, $CDCl_3$) δ 8.58 (d, J = 6.1 Hz, 1H), 8.41 (dd, J = 9.4, 4.9 Hz, 1H), 7.70 (d, J = 6.0 Hz, 1H), 7.55 (t, J = 9.2 Hz, 1H), 3.07 (s, 3H). ^{13}C NMR (125 MHz, $CDCl_3$) δ 159.08, 155.06 (d, $^1J_{C\text{-}F}$ = 266.6 Hz), 144.50, 132.29 (d, $^3J_{C\text{-}F}$ = 10.0 Hz), 129.83 (2C), 124.19, 117.40 (d, $^2J_{C\text{-}F}$ = 23.5 Hz), 113.60, 22.41. ^{19}F NMR (376 MHz, $CDCl_3$) δ -113.01. DART-MS: *m/z* calcd. for $C_{10}H_8FN_2O_2$ $(M+H)^+$ 207.05643, found 207.05690.

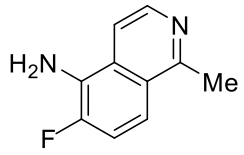

6-Fluoro-1-methylisoquinolin-5-amine (S19). To a solution of **S18** (0.264 g, 1.28 mmol) in MeOH (60 mL) iron powder (0.214 g, 3.83 mmol) and HCl (1 mL, 12 M in H_2O). The mixture was refluxed for 2 h and then a solution of sodium hydroxide (2 mL, 6 M in H_2O) was added. The mixture was filtered and extracted with diethyl ether (200 mL). The organic layer was dried over Na_2SO_4, filtered, and then concentrated *in vacuo*. The crude residue was purified by flash column chromatography (gradient, 10–30% EtOAc:hexanes). The isoquinoline **S19** was obtained as a brown solid (145.8 mg, 82%). ^{1}H NMR (500 MHz, $CDCl_3$) δ 8.36 (d, J = 6.2 Hz, 1H), 7.62 (dd, J = 9.1, 4.8 Hz, 2H), 7.44 (d, J = 9.9 Hz, 1H), 4.27 (br s, 2H), 3.06 (s, 3H). ^{13}C NMR (125 MHz, $CDCl_3$) δ 164.80, 159.77 (d, $^1J_{C\text{-}F}$ = 263.7 Hz), 150.34, 139.41 (d, $^3J_{C\text{-}F}$ = 10.8 Hz), 137.94, 133.78, 128.91, 122.74 (d, $^2J_{C\text{-}F}$ = 22.7 Hz), 118.04 (d, $^4J_{C\text{-}F}$ = 5.2 Hz), 27.69. ^{19}F NMR (376 MHz, $CDCl_3$) δ -125.82. DART-MS: *m/z* calcd. for $C_{10}H_{10}FN_2$ $(M+H)^+$ 177.08225, found 177.08291.

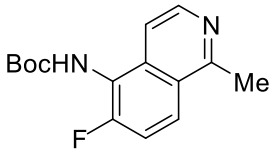

***tert*-Butyl (6-fluoro-1-methylisoquinolin-5-yl)carbamate (S20).** To a solution of **S19** (0.715 g, 4.06 mmol) in THF (15 mL) was added DMAP (49.5 mg, 0.41 mmol) then Boc_2O (2.21 g, 10.14 mmol) and the mixture was stirred at 22 °C overnight. After completion of the reaction as attested by TLC, K_2CO_3 (1.68 g, 12.17 mmol) and MeOH (10 mL) were added to the reaction mixture and was refluxed overnight. The mixture was then concentrated *in vacuo* and resuspended in EtOAc (20 mL) and water (20 mL). The organic layer was separated and the aqueous layer was extracted with EtOAc (3 × 20 mL). The organic layers were combined and dried over Na_2SO_4, filtered, and then concentrated *in vacuo*. The crude residue was purified by flash column chromatography (gradient, 5–20% EtOAc:hexanes). The isoquinoline **S20** was obtained as a brown oil (0.303 g, 27%). ^{1}H NMR (500 MHz, $CDCl_3$) δ 8.40 (d, J = 6.0 Hz, 1H), 8.06 (dd, J = 9.3, 5.0 Hz, 1H), 7.65 (d, J = 6.0 Hz, 1H), 7.39 (t, J = 9.3 Hz, 1H), 6.59 (br s, 1H), 2.95 (s, 3H), 1.50 (s, 9H). ^{13}C NMR (125 MHz, $CDCl_3$) δ 160.58 (d, $^1J_{C\text{-}F}$ = 260.2 Hz), 157.19, 153.19, 137.68, 131.09 (d, $^4J_{C\text{-}F}$ = 4.9 Hz), 128.23 (d, $^3J_{C\text{-}F}$ = 10.7 Hz), 124.83, 124.45, 121.14 (d, $^2J_{C\text{-}F}$ = 22.1 Hz), 119.60, 82.72, 28.15 (3C), 17.84. ^{19}F NMR (376 MHz, $CDCl_3$) δ -112.86. DART-MS: *m/z* calcd. for $C_{15}H_{18}FN_2O_2$ $(M+H)^+$ 277.13468, found 277.13425.

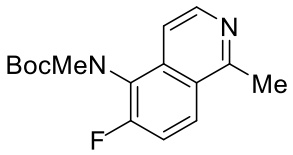

***tert*-Butyl methyl(6-fluoro-1-methylisoquinolin-5-yl)carbamate (S21).** To a solution of **S20** (0.150 g, 0.543 mmol) in THF (4 mL) was added NaH 60% in mineral oil (28.0 mg, 0.706 mmol). After effervescence ceased, the resulting solution was refluxed for 30 min. To the reaction mixture was added the MeI (0.10 g, 0.706 mmol) in THF (0.5 mL) and the solution refluxed overnight. The mixture was concentrated and passed through a silica plug (1:10-2:1 EtOAc:hexanes). The mixture was concentrated *in vacuo* and the crude residue was purified by flash column chromatography (gradient, 10–30% EtOAc:hexanes). The isoquinoline **S21** was obtained as a mixture of rotational isomers as an amber oil (0.120 g, 76%). ^{1}H NMR (500 MHz, $CDCl_3$) δ 8.44 (d, J = 5.8 Hz, 1.27H), 8.16–8.02 (m, 1.27H), 7.51 (d, J = 6.0 Hz, 1H), 7.49 (d, J = 6.3 Hz, 0.27H), 7.39 (t, J = 9.3 Hz, 1.27H), 3.26 (s, 0.81H), 3.25 (s, 3H), 2.98 (s, 3H), 2.96 (s, 0.81H), 1.56 (s, 2.43H), 1.26 (s, 9H). ^{13}C NMR (125 MHz, $CDCl_3$) δ 158.89, 158.88, 158.09 (d, $^{1}J_{C\text{-}F}$ = 254.3 Hz), 154.97, 154.78, 143.18 (2C), 135.55, 135.36 (d, $^{4}J_{C\text{-}F}$ = 3.7 Hz), 127.66 (d, $^{3}J_{C\text{-}F}$ = 9.7 Hz), 127.38 (d, $^{3}J_{C\text{-}F}$ = 9.6 Hz), 125.25, 125.06 (2C), 124.88, 124.78, 117.42 (d, $^{2}J_{C\text{-}F}$ = 24.0 Hz), 117.12 (d, $^{2}J_{C\text{-}F}$ = 24.1 Hz), 114.35 (d, $^{3}J_{C\text{-}F}$ = 5.8 Hz), 81.18, 80.61, 37.43, 36.39, 28.35 (3C), 27.99 (3C), 22.62, 22.56, one low-field carbon were either not observed or is overlapping with another low-field carbon. ^{19}F NMR (376 MHz, $CDCl_3$) δ -114.54, -115.33. DART-MS: *m/z* calcd. for $C_{16}H_{20}FN_2O_2$ $(M+H)^+$ 291.15033, found 291.15011.

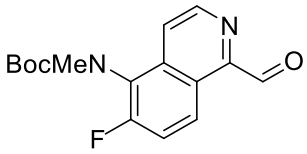

***tert*-Butyl methyl(6-fluoro-1-formylisoquinolin-5-yl)carbamate (S22).** To a solution of **S21** (0.1000 g, 0.344 mmol) in 1,4-dioxane (2 mL) was added SeO_2 (38.2 mg, 0.344 mmol). The mixture was stirred at 60 °C overnight then cooled to 22 °C. The mixture was concentrated *in vacuo* and the crude residue was purified by flash column chromatography (gradient, 5–25% EtOAc:hexanes). The isoquinoline **S22** was obtained as an off-white solid containing a mixture of rotamers (45.3 mg, 43%). ^{1}H NMR (500 MHz, $CDCl_3$) δ 10.37 (s, 1H), 10.35 (s, 0.3H), 9.35 (dd, J = 9.4, 5.1 Hz, 1.3H), 8.82 (d, J = 5.8 Hz, 1.3H), 7.92 (d, J = 5.7 Hz, 1H), 7.88 (d, J = 5.8 Hz, 0.3H), 7.56 (t, J = 9.4 Hz, 1.3H), 3.29 (s, 0.9H), 3.28 (s, 3H), 1.57 (s, 2.7H), 1.25 (s, 9H). ^{13}C NMR (125 MHz, $CDCl_3$) δ 195.40 (2C), 158.41 (d, $^{1}J_{C\text{-}F}$ = 257.6 Hz), 154.77 (2C), 149.92, 143.81, 143.72 (2C), 136.73 (d, $^{4}J_{C\text{-}F}$ = 4.6 Hz), 136.59 (d, $^{4}J_{C\text{-}F}$ = 3.8 Hz), 128.17 (d, $^{3}J_{C\text{-}F}$ = 10.7 Hz), 127.91 (d, $^{3}J_{C\text{-}F}$ = 9.3 Hz), 124.72 (d, $^{3}J_{C\text{-}F}$ = 13.3 Hz), 124.00, 123.80, 120.68 (d, $^{2}J_{C\text{-}F}$ = 24.7 Hz), 120.44 (d, $^{2}J_{C\text{-}F}$ = 24.1 Hz), 120.31, 120.22 (d, $^{3}J_{C\text{-}F}$ = 6.3 Hz), 81.55, 81.00, 37.58, 36.53, 28.32 (3C), 27.97 (3C), two low-field carbon were either not observed or is overlapping with another low-field carbon. ^{19}F NMR (376 MHz, $CDCl_3$) δ -112.18, -112.95. DART-MS: *m/z* calcd. for $C_{16}H_{18}FN_2O_3$ $(M+H)^+$ 305.1296, found 305.12819.

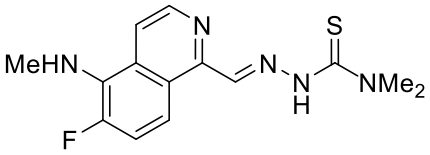

and
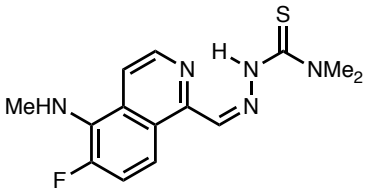

(*E*)-2-((6-Fluoro-5-(methylamino)isoquinolin-1-yl)methylene)-*N*,*N*-dimethylhydrazine-1-carbothioamide and (*Z*)-2-((6-Fluoro-5-(methylamino)isoquinolin-1-yl)methylene)-*N*,*N*-dimethylhydrazine-1-carbothioamide (HCT14). To a solution of **S22** (10.0 mg, 0.033 mmol) in EtOH (0.5 mL) was added 4,4-dimethyl-3-thiosemicarbazide (3.9 mg, 0.033 mmol) and HCl (33 µL, 0.197 mmol, 6 M in H_2O). The mixture was stirred and refluxed for 1.5 h then cooled to 22 °C. The hydrochloride salt that formed was then neutralized with saturated aqueous $NaHCO_3$ solution (0.5 mL). the precipitate of the desired compound was collected by filtration, washed with water, EtOH and then dried to yield the isoquinoline **HCT14** as a pale-yellow solid (6.7 mg, 67%). ^{1}H NMR (500 MHz, DMSO-d_6) δ 15.96 (s, 0.17H), 11.22 (Br s, 1H), 9.20 (s, 1H), 8.62–8.54 (m, 1.17H), 8.52 (s, 0.17H), 8.34 (d, J = 5.5 Hz, 1H), 8.20 (d, J = 6.2 Hz, 0.17H), 8.07 (dd, J = 9.3, 4.2 Hz, 0.17H), 7.87 (br s, 1H), 7.56 (dd, J = 13.6, 9.2 Hz, 0.17H), 7.33 (dd, J = 13.4, 9.5 Hz, 1H), 6.10 (br s, 0.17H), 5.69 (br s, 1H), 3.41 (s, 1.02H), 3.27 (s, 6H), 3.10 (t, J = 5.5 Hz, 0.51H), 3.05 (t, J = 5.2 Hz, 3H). A ^{13}C NMR was not obtained. ^{19}F NMR (376 MHz, $CDCl_3$) δ - 129.05, -129.53. DART-MS: *m/z* calcd. for $C_{14}H_{17}FN_5S$ $(M+H)^+$ 305.11832, found 305.11719.

[1]HNMR and [13]CNMR of compounds **S1-S22** and **HCT1-15**

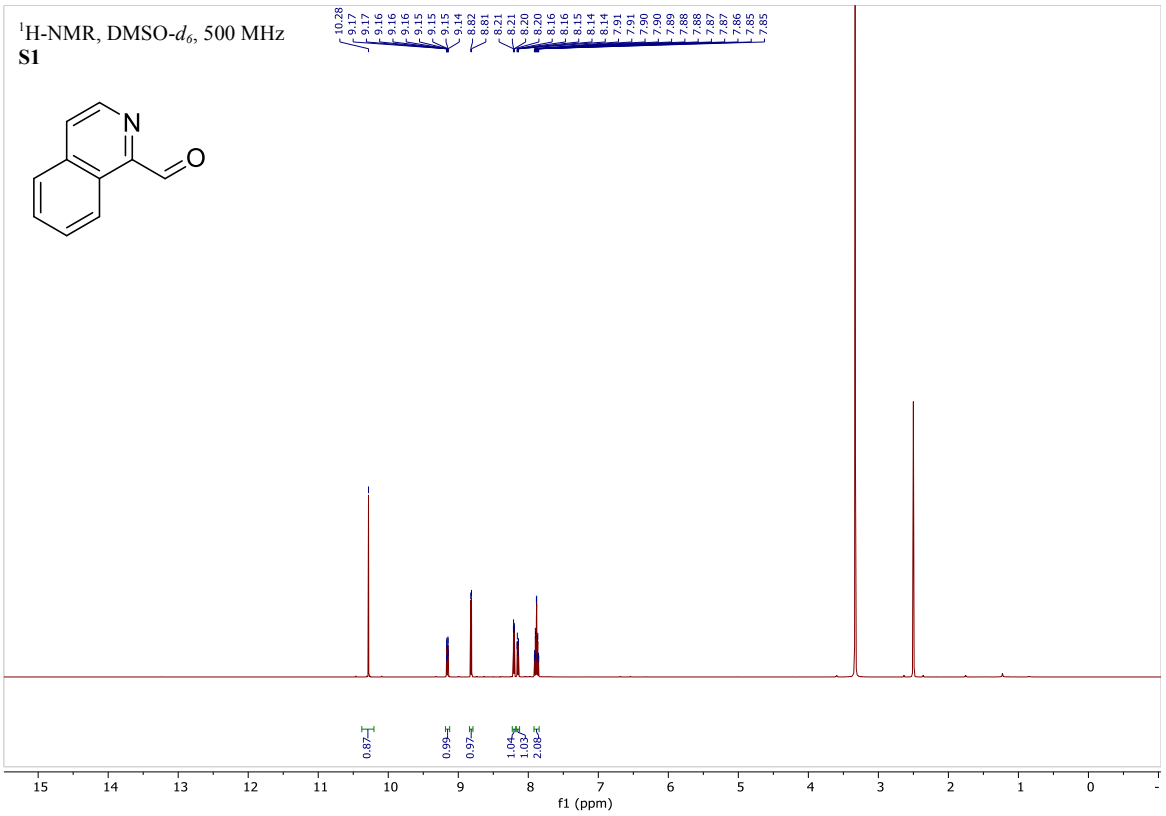

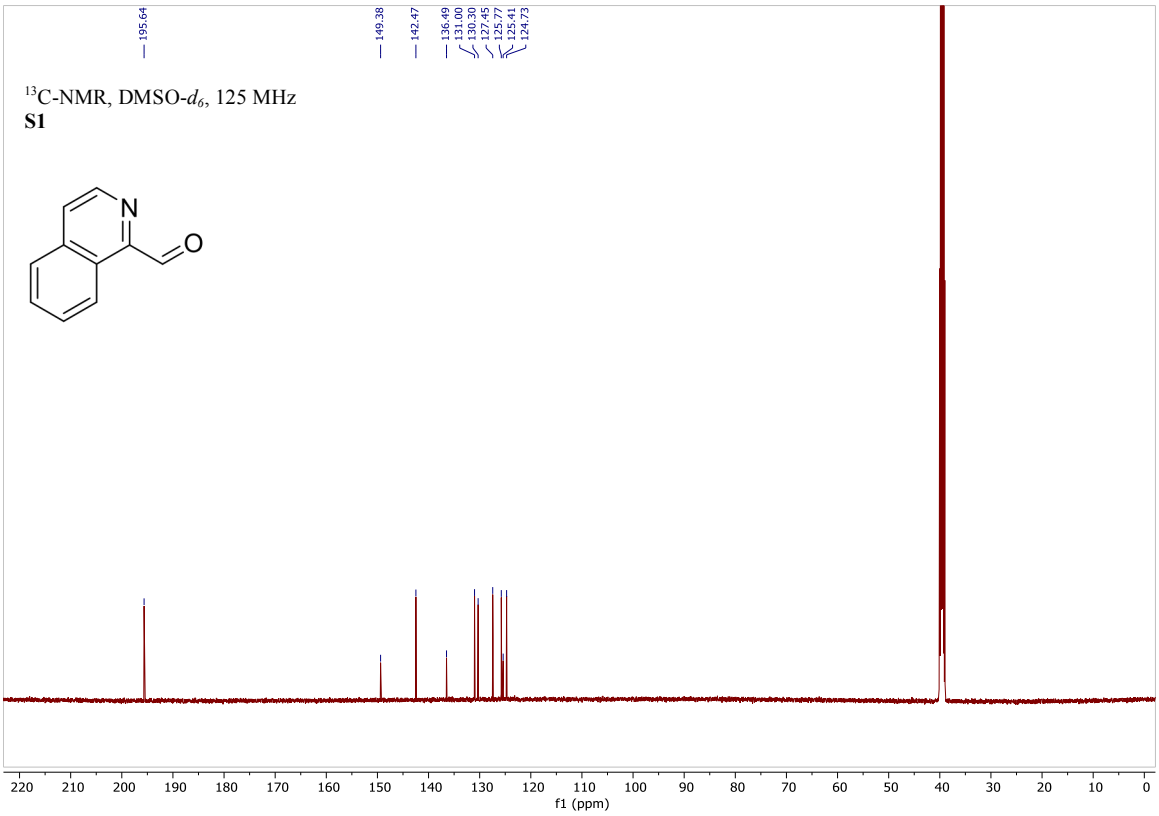

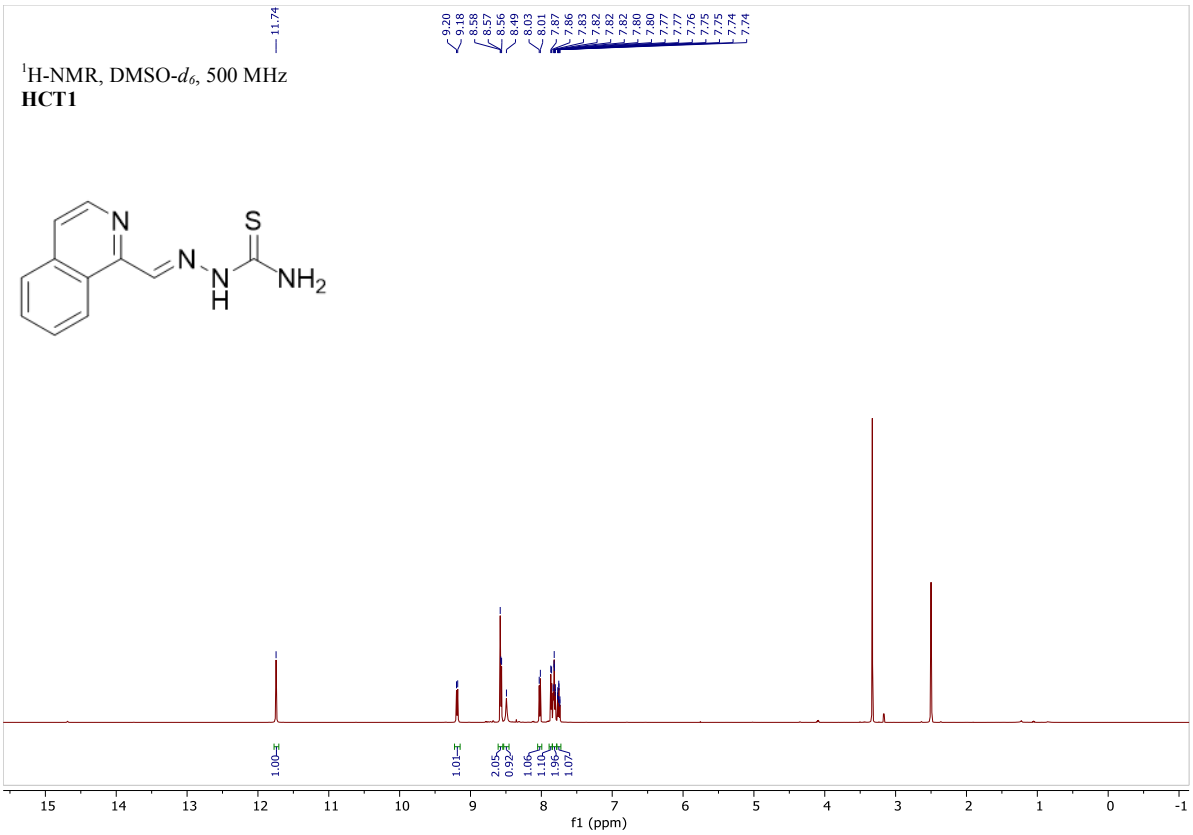

^{1}H-NMR, DMSO-d_6, 500 MHz
HCT1

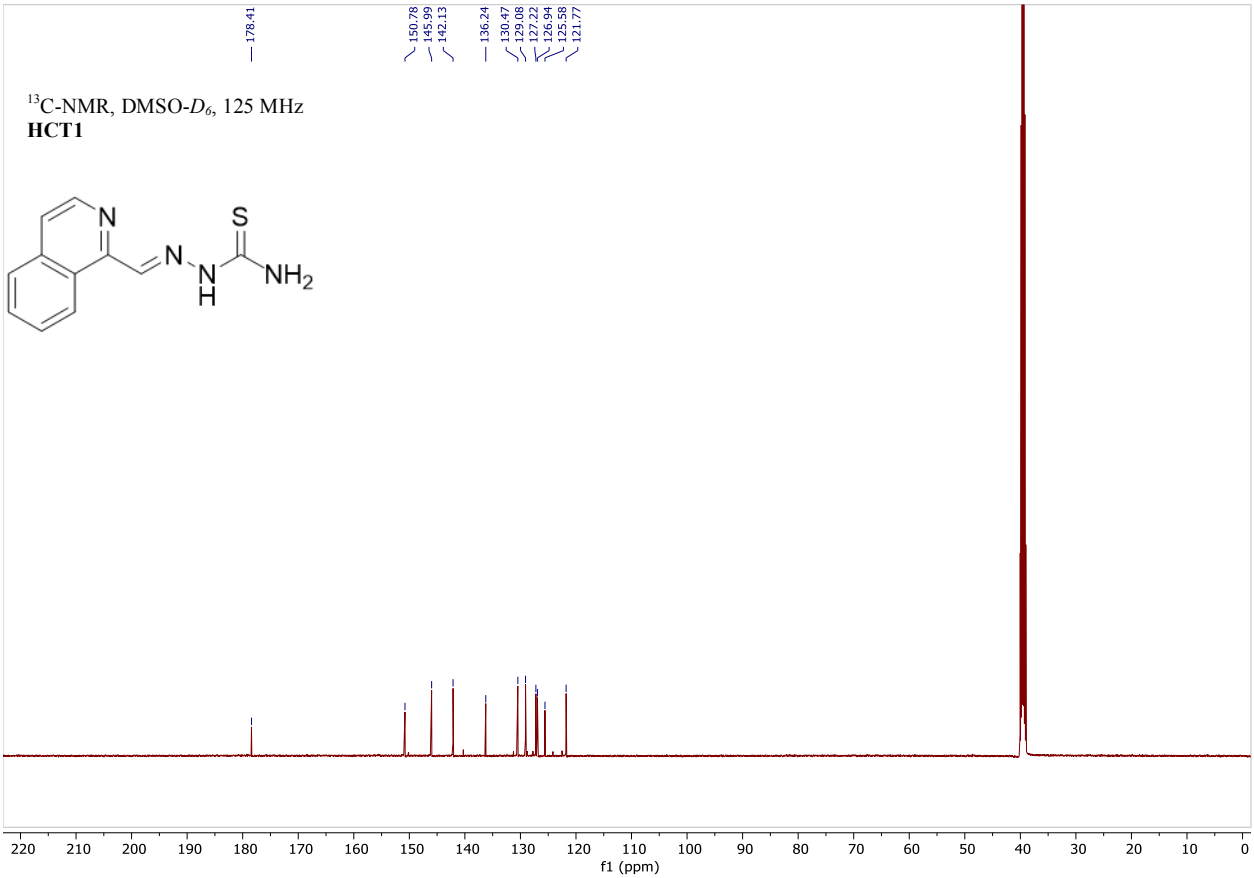

^{13}C-NMR, DMSO-D_6, 125 MHz
HCT1

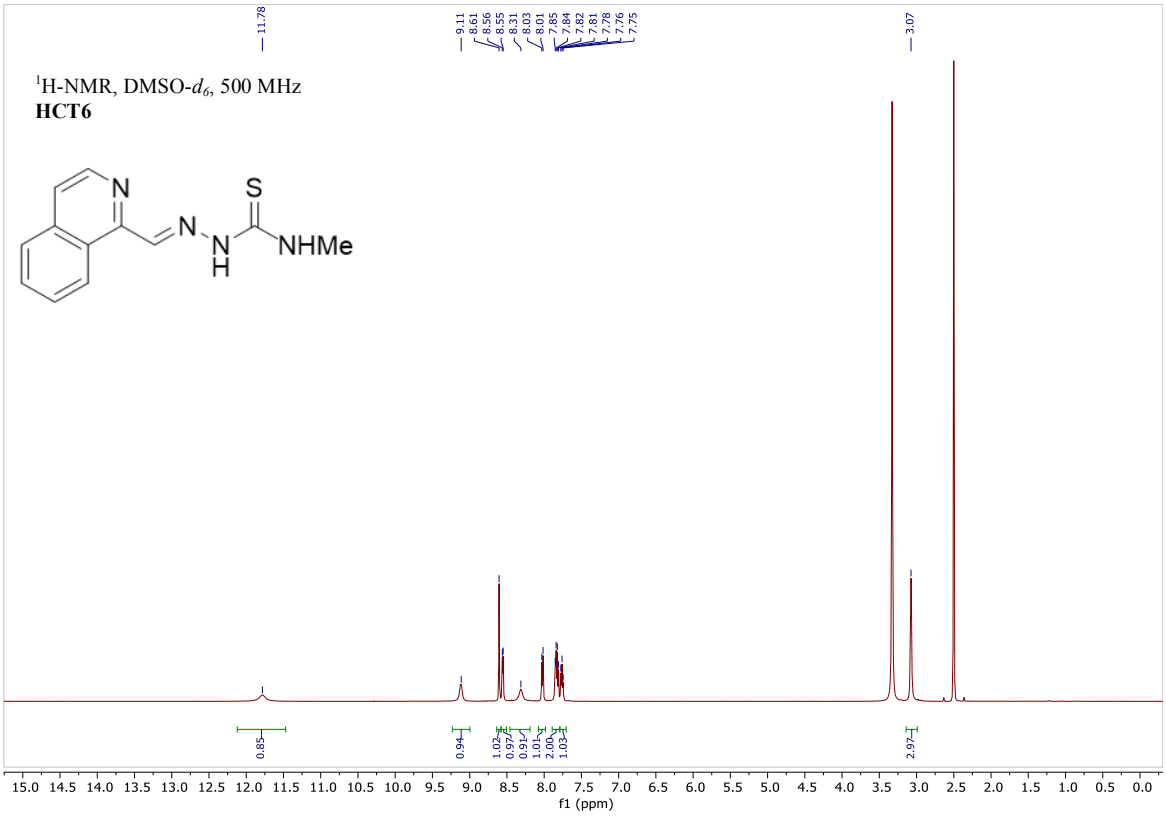

^{1}H-NMR, DMSO-d_6, 500 MHz
HCT6

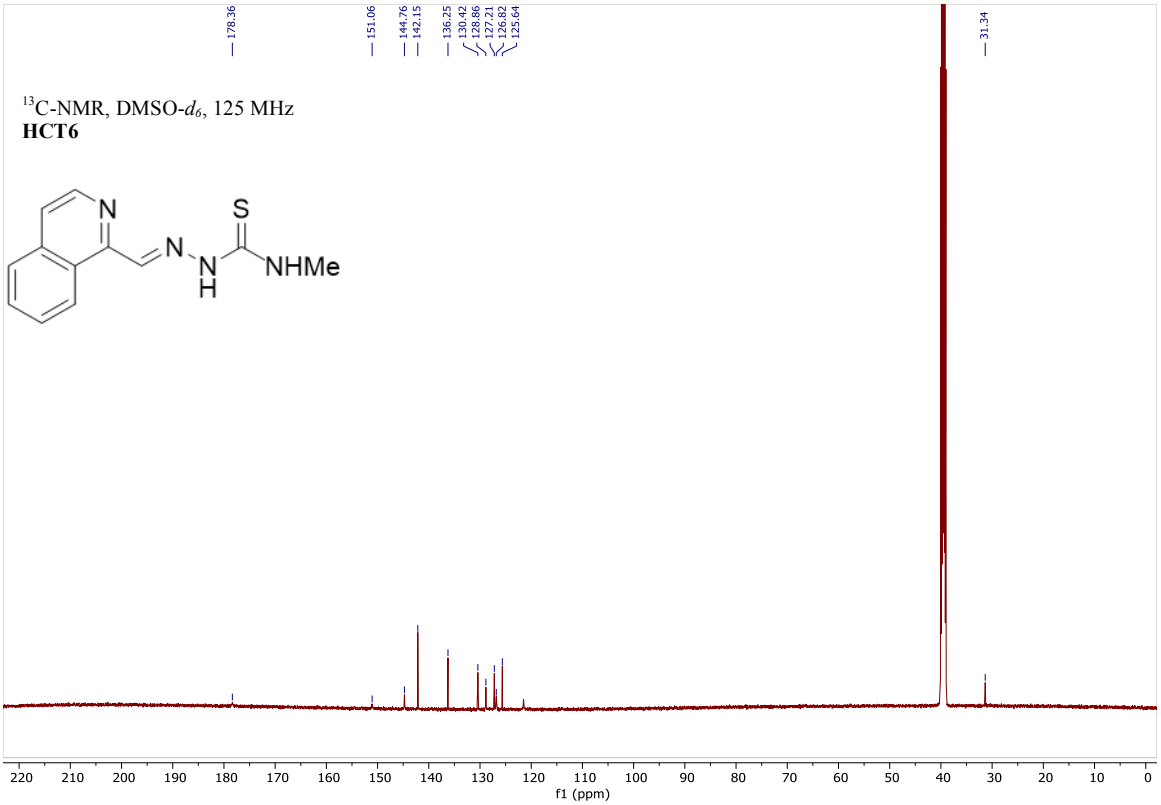

^{13}C-NMR, DMSO-d_6, 125 MHz
HCT6

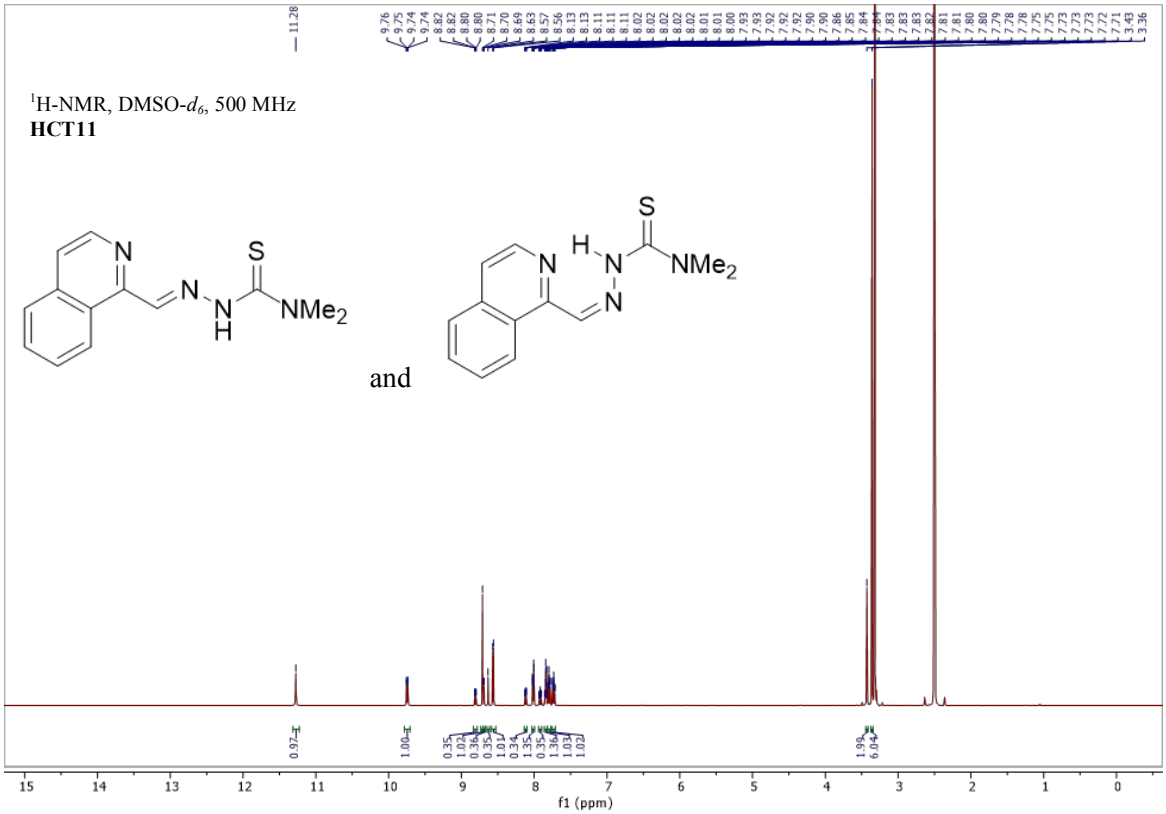
[1]H-NMR, DMSO-d6, 500 MHz
HCT11
and
f1 (ppm)

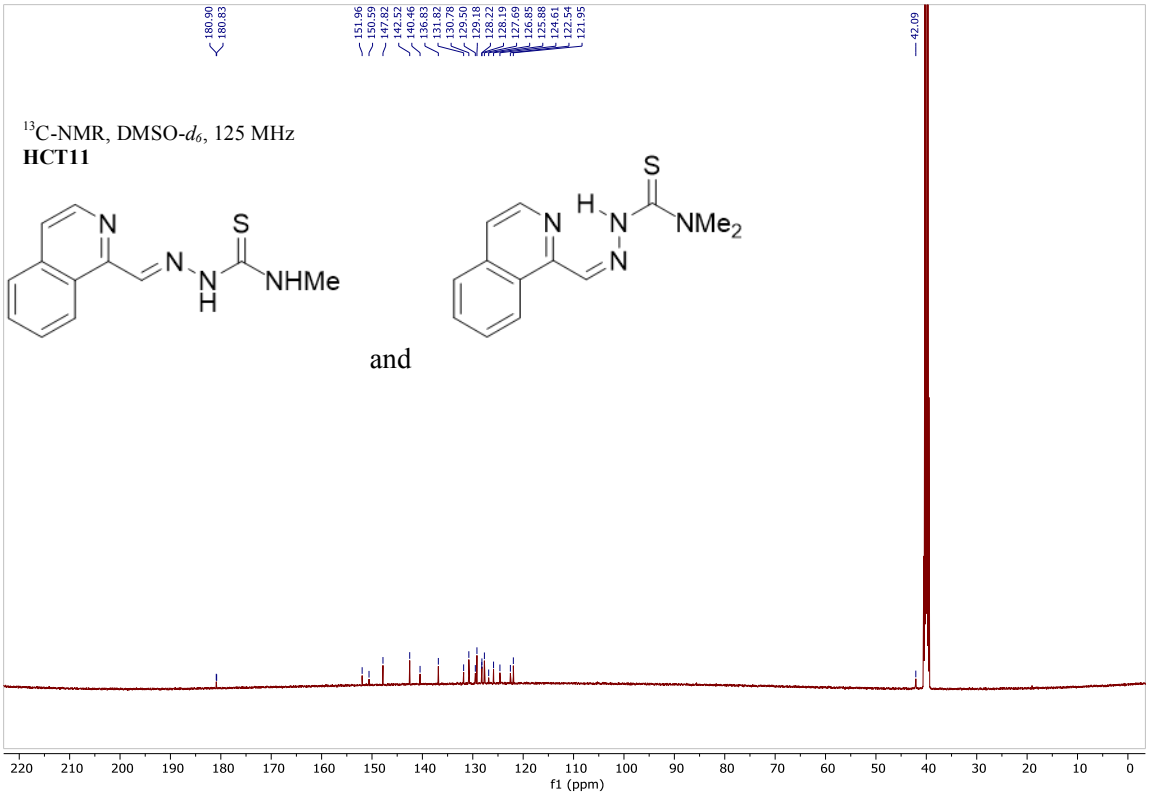
[13]C-NMR, DMSO-d6, 125 MHz
HCT11
and
f1 (ppm)

^{1}H-NMR, $CDCl_3$, 500 MHz
S2

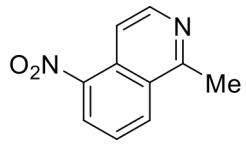

^{13}C-NMR, $CDCl_3$, 125 MHz
S2

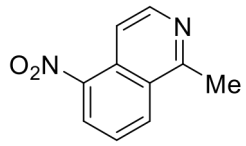

^{1}H-NMR, $CDCl_3$, 500 MHz
S3

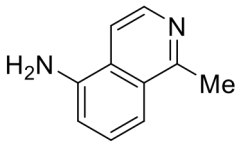

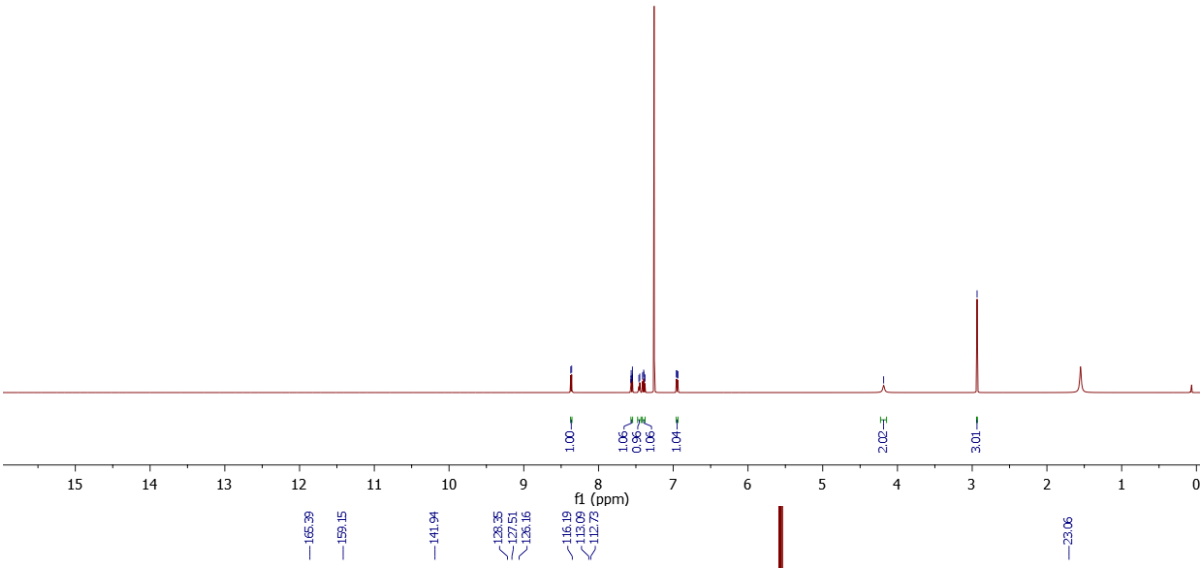

^{13}C-NMR, $CDCl_3$, 125 MHz
S3

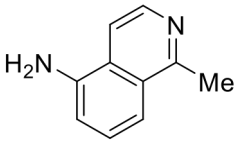

^{1}H-NMR, $CDCl_3$, 500 MHz
S4

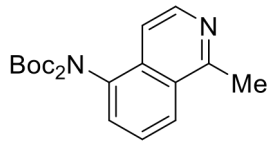

^{13}C-NMR, $CDCl_3$, 125 MHz
S4

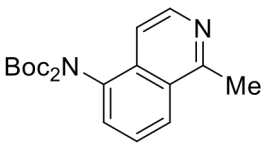

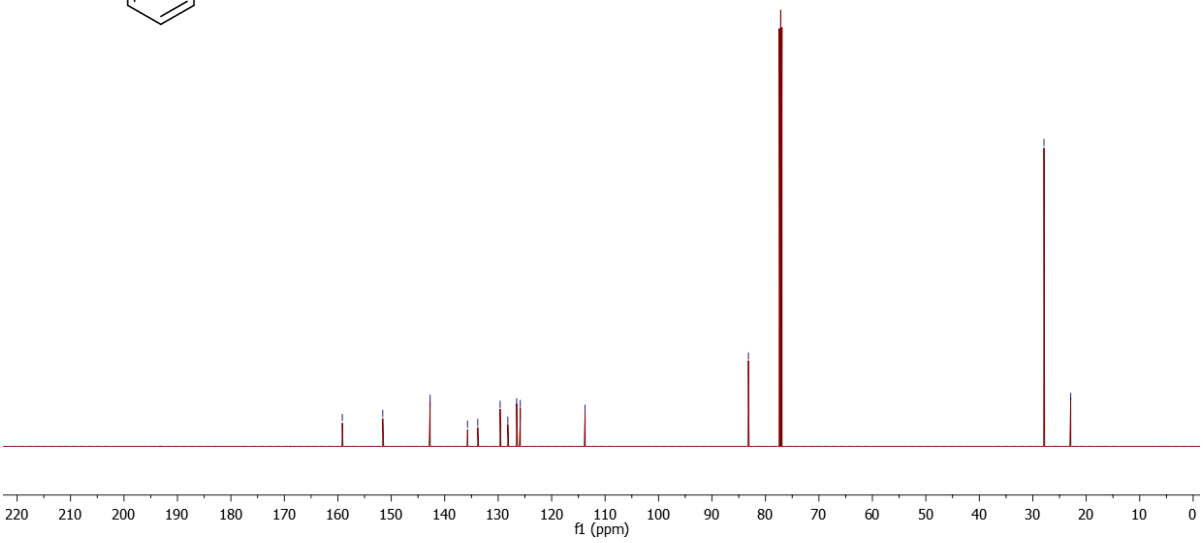

^{1}H-NMR, $CDCl_3$, 500 MHz
S5

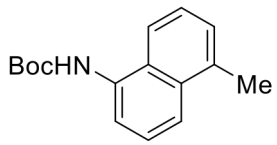

^{13}C-NMR, $CDCl_3$, 125 MHz
S5

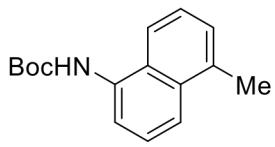

^{1}H-NMR, $CDCl_3$, 500 MHz
S6

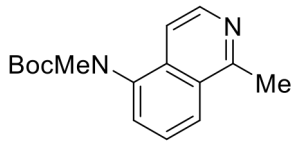

^{1}3C-NMR, $CDCl_3$, 125 MHz
S6

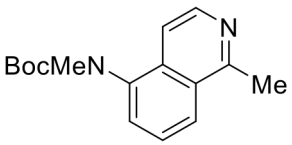

^{1}H-NMR, $CDCl_3$, 500 MHz
S7

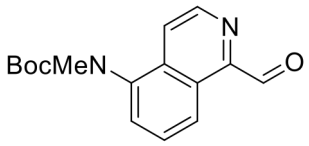

^{13}C-NMR, $CDCl_3$, 125 MHz
S7

^{1}H-NMR, $CDCl_3$, 500 MHz
S8

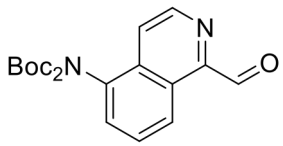

^{13}C-NMR, $CDCl_3$, 125 MHz
S8

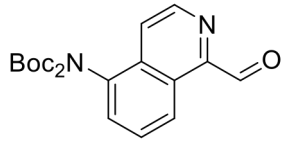

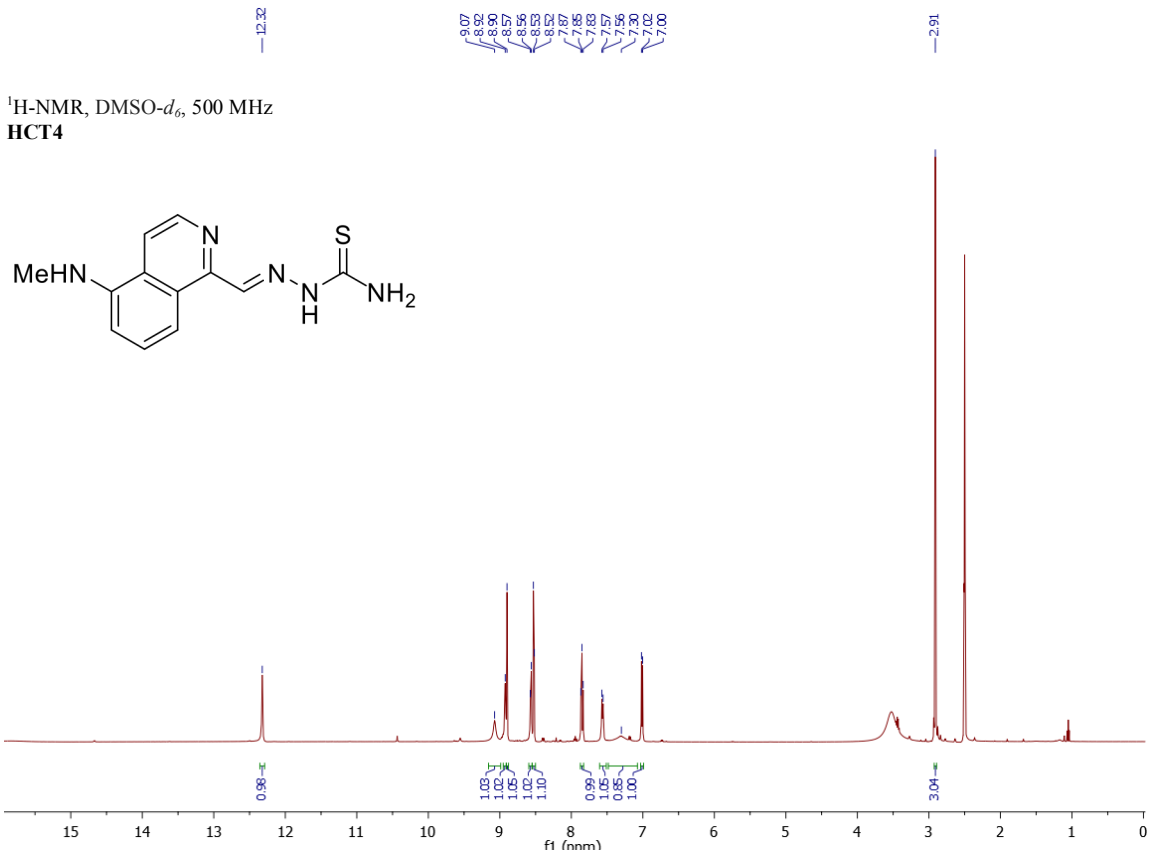

[1]H-NMR, DMSO-d_6, 500 MHz
HCT4

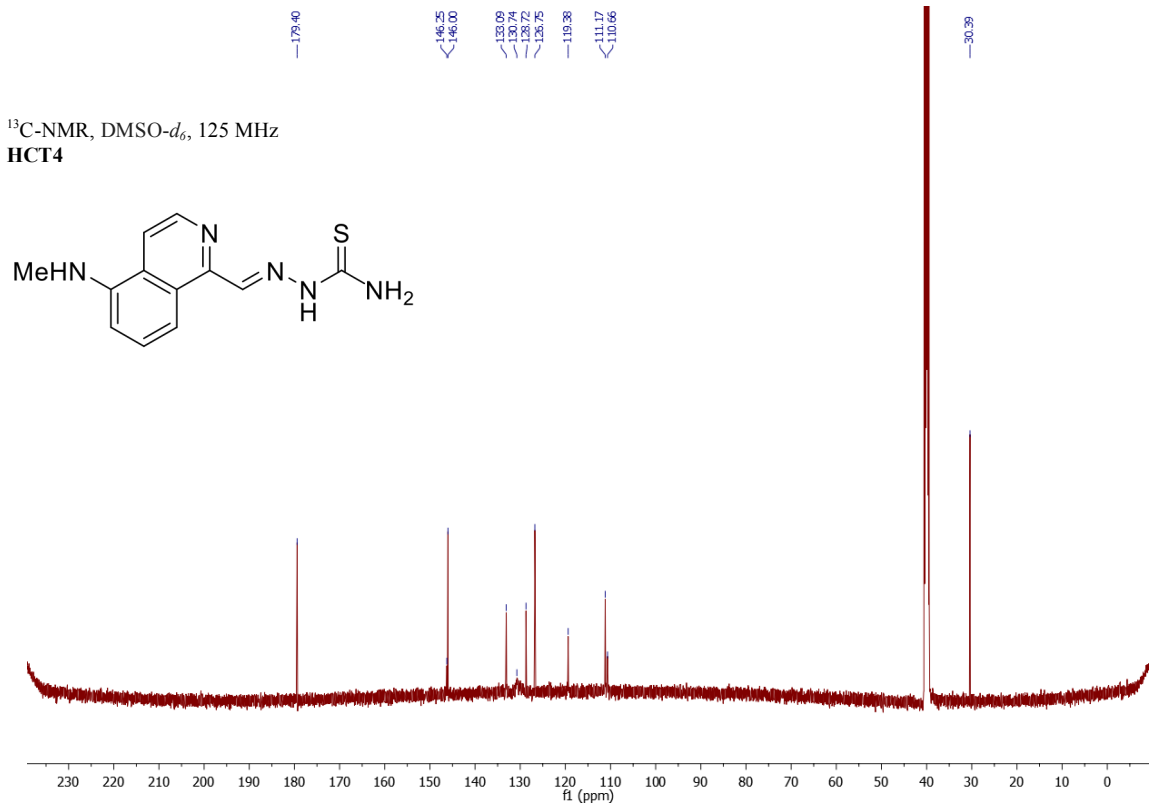

[13]C-NMR, DMSO-d_6, 125 MHz
HCT4

^{1}H-NMR, DMSO-d_6, 500 MHz
HCT9

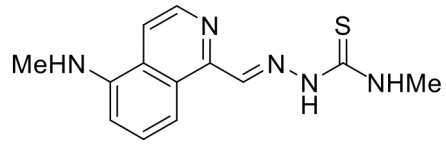

and

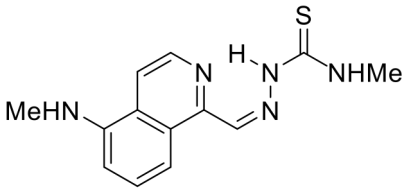

^{13}C-NMR, DMSO-d_6, 125 MHz
HCT9

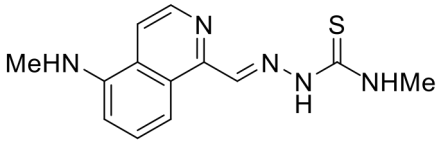

and

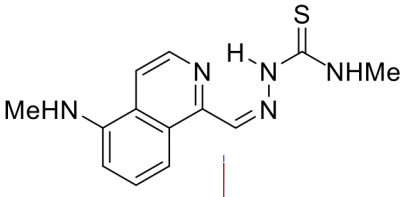

^{1}H-NMR, DMSO-d_6, 500 MHz
HCT5

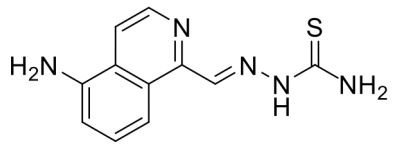

^{13}C-NMR, DMSO-d_6, 125 MHz
HCT5

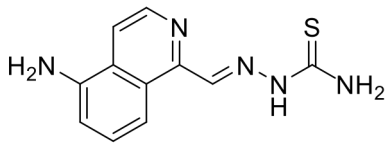

[1]H-NMR, DMSO-d_6, 500 MHz
HCT10

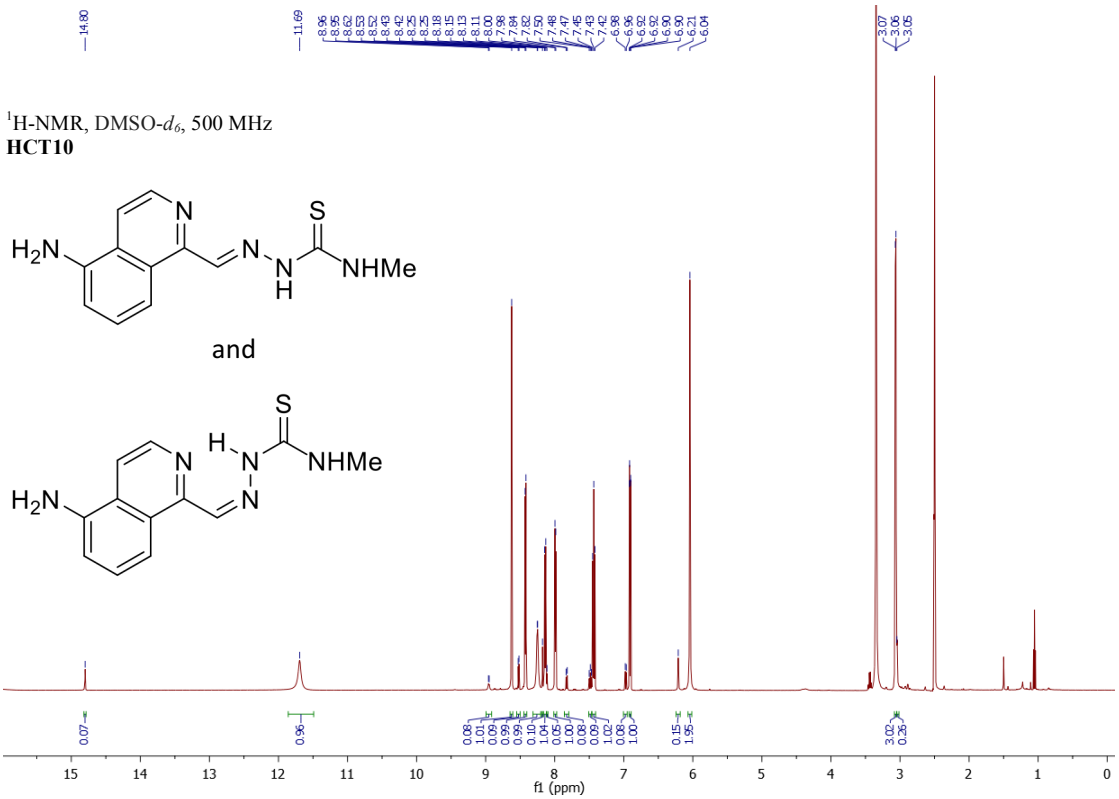

and

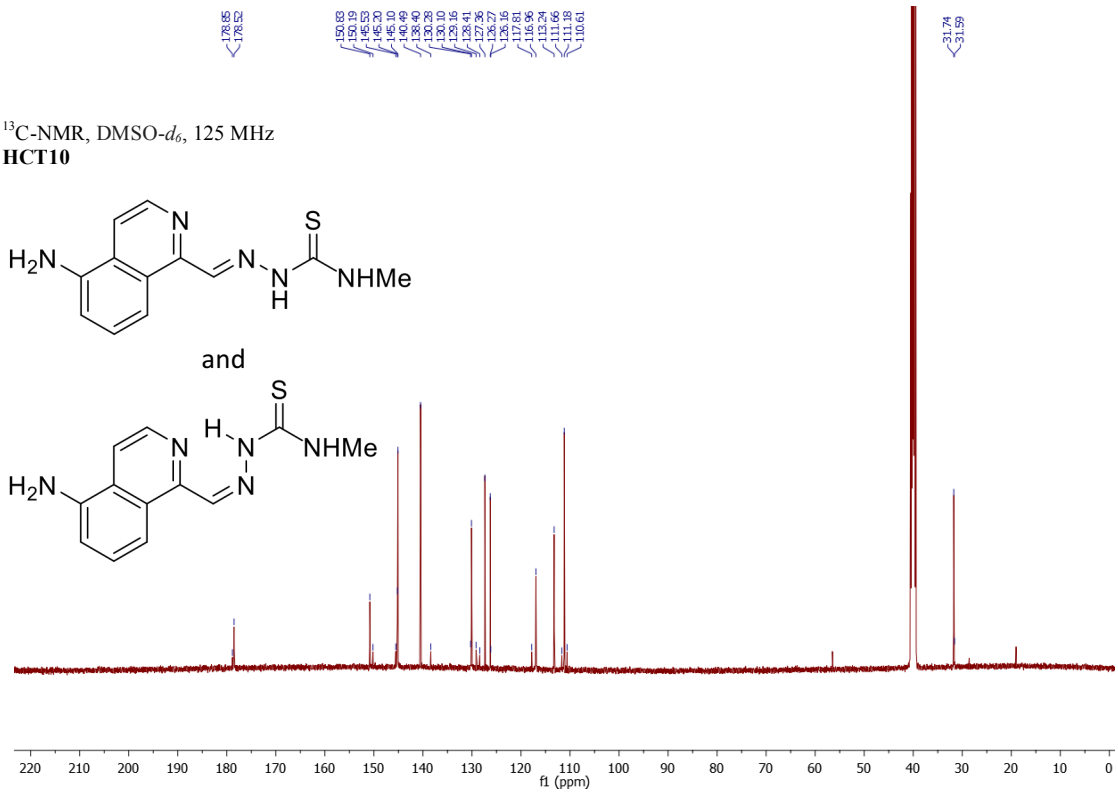

[13]C-NMR, DMSO-d_6, 125 MHz
HCT10

and

^{1}H-NMR, DMSO-d_6, 500 MHz
S9

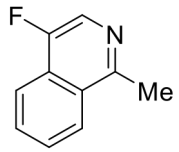

^{13}C-NMR, DMSO-d_6, 125 MHz
S9

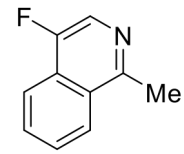

^{1}H-NMR, DMSO-d_6, 500 MHz
S10

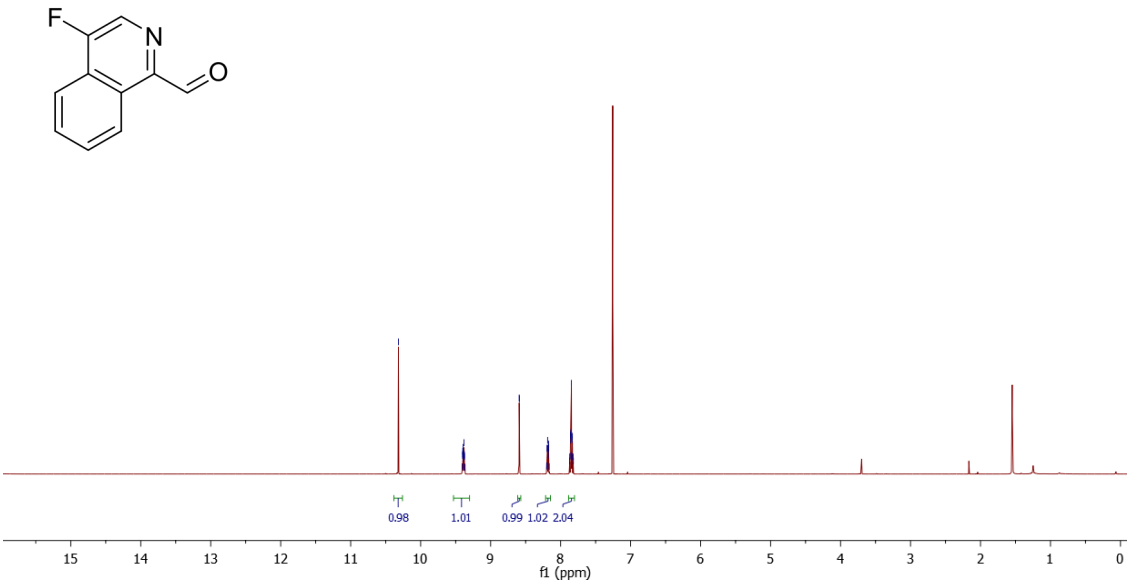

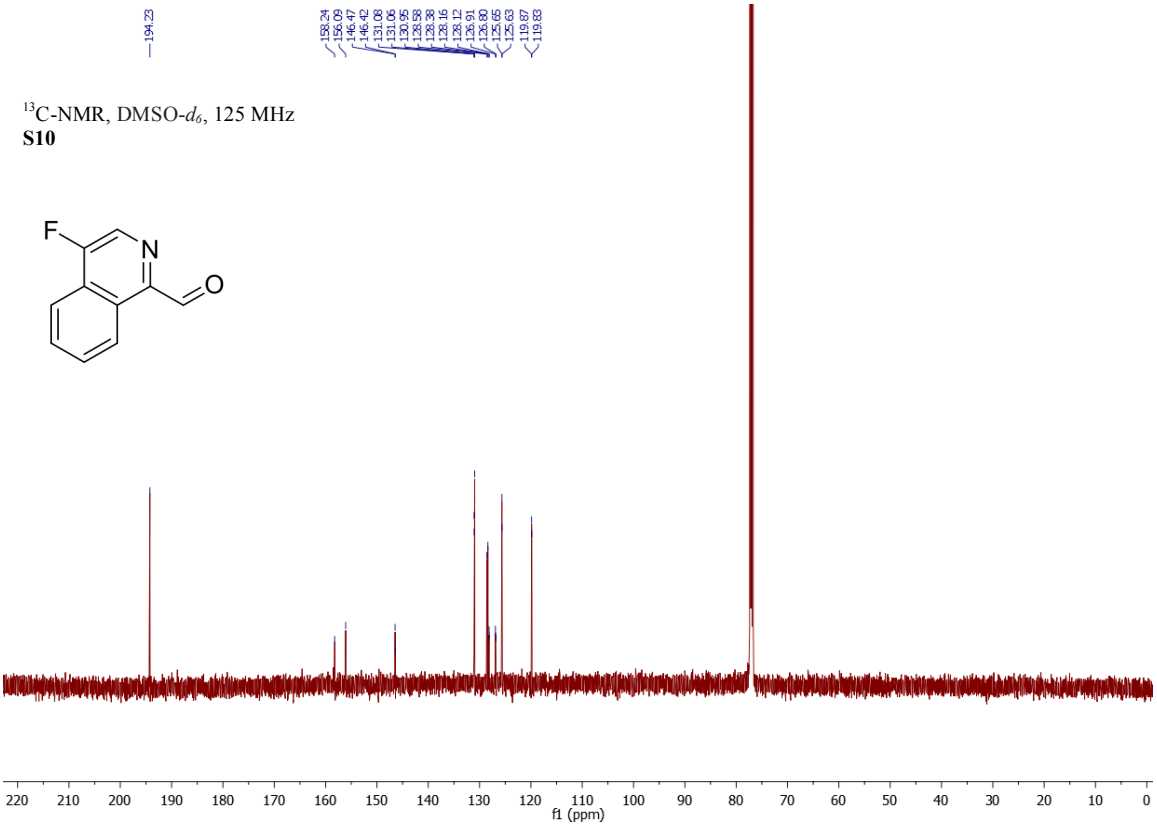

^{13}C-NMR, DMSO-d_6, 125 MHz
S10

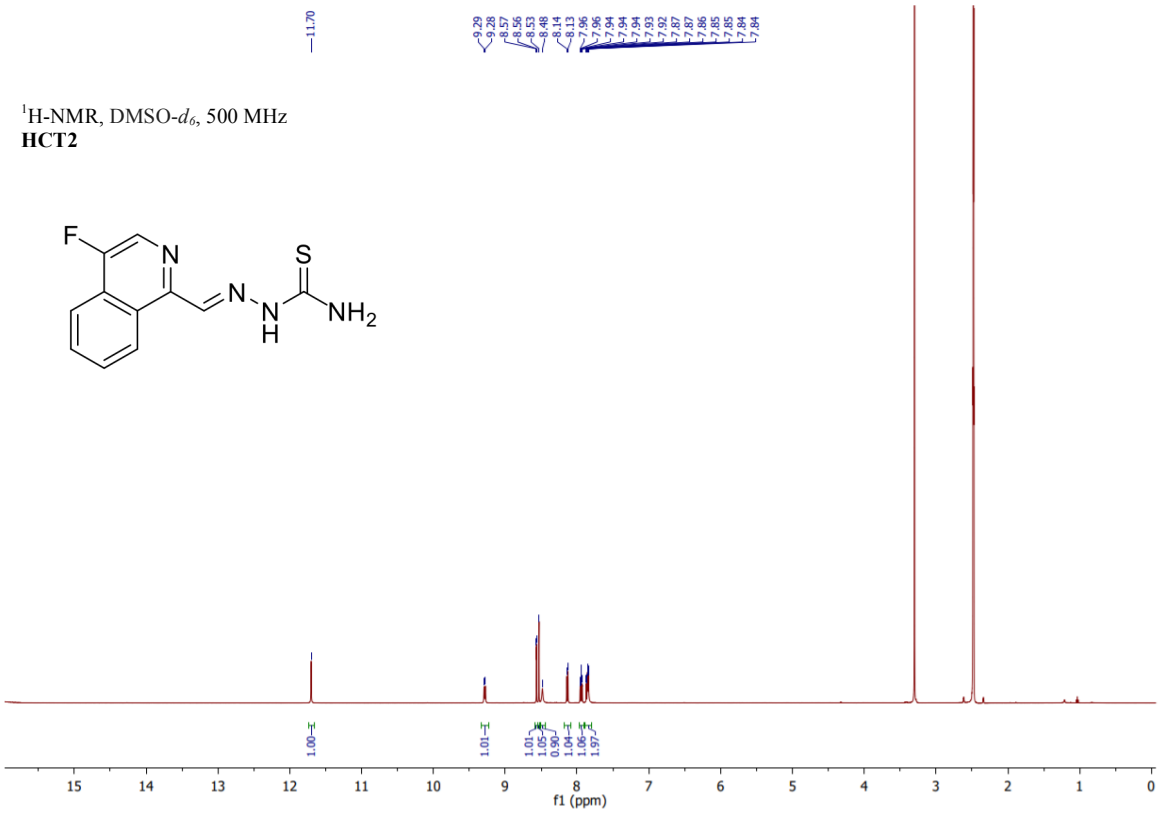

^{1}H-NMR, DMSO-d_6, 500 MHz
HCT2

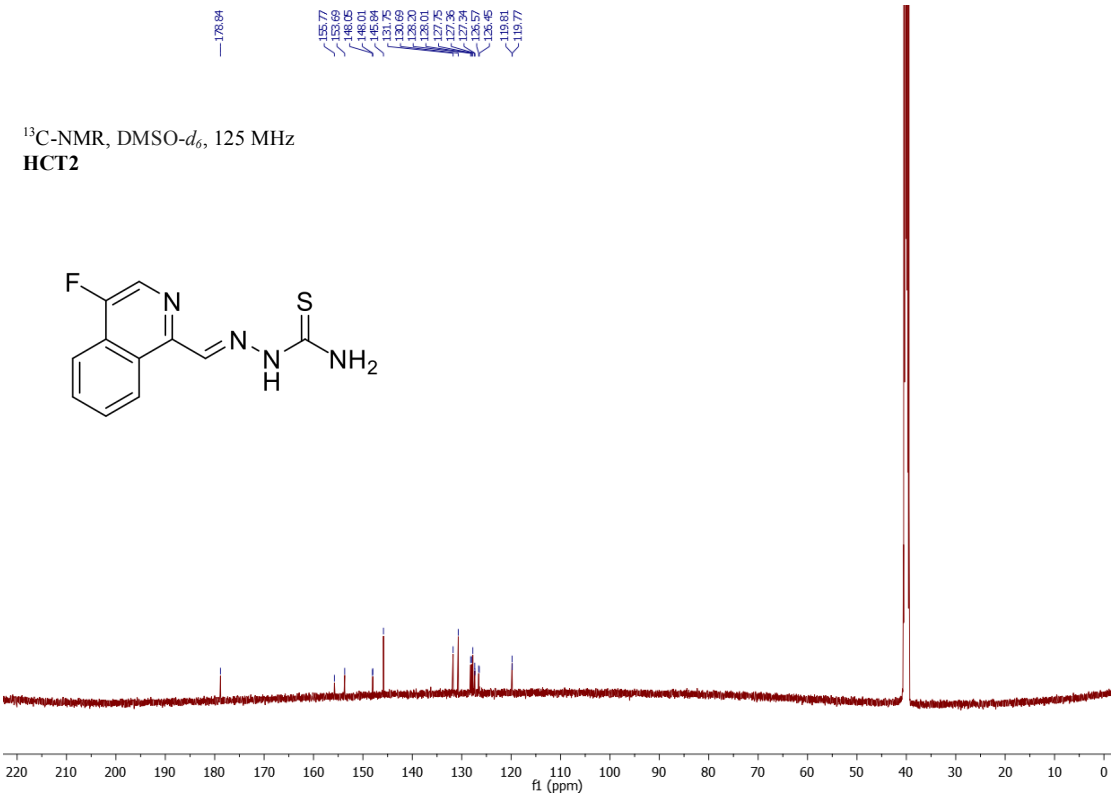

^{13}C-NMR, DMSO-d_6, 125 MHz
HCT2

^{1}H-NMR, DMSO-d_6, 500 MHz
HCT7

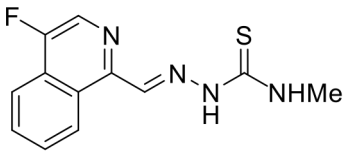

^{13}C-NMR, DMSO-d_6, 125 MHz
HCT7

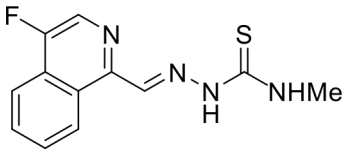

^{1}H-NMR, DMSO-d_6, 500 MHz
HCT12

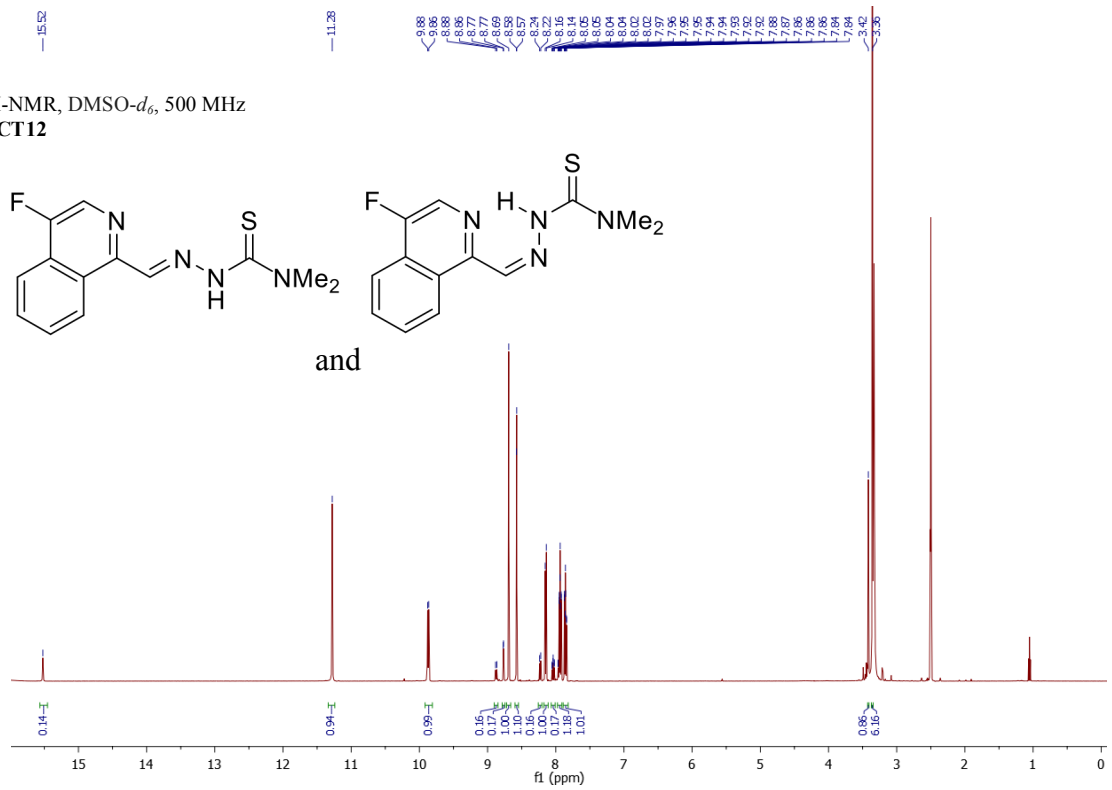

and

r

^{13}C-NMR, DMSO-d_6, 125 MHz
HCT12

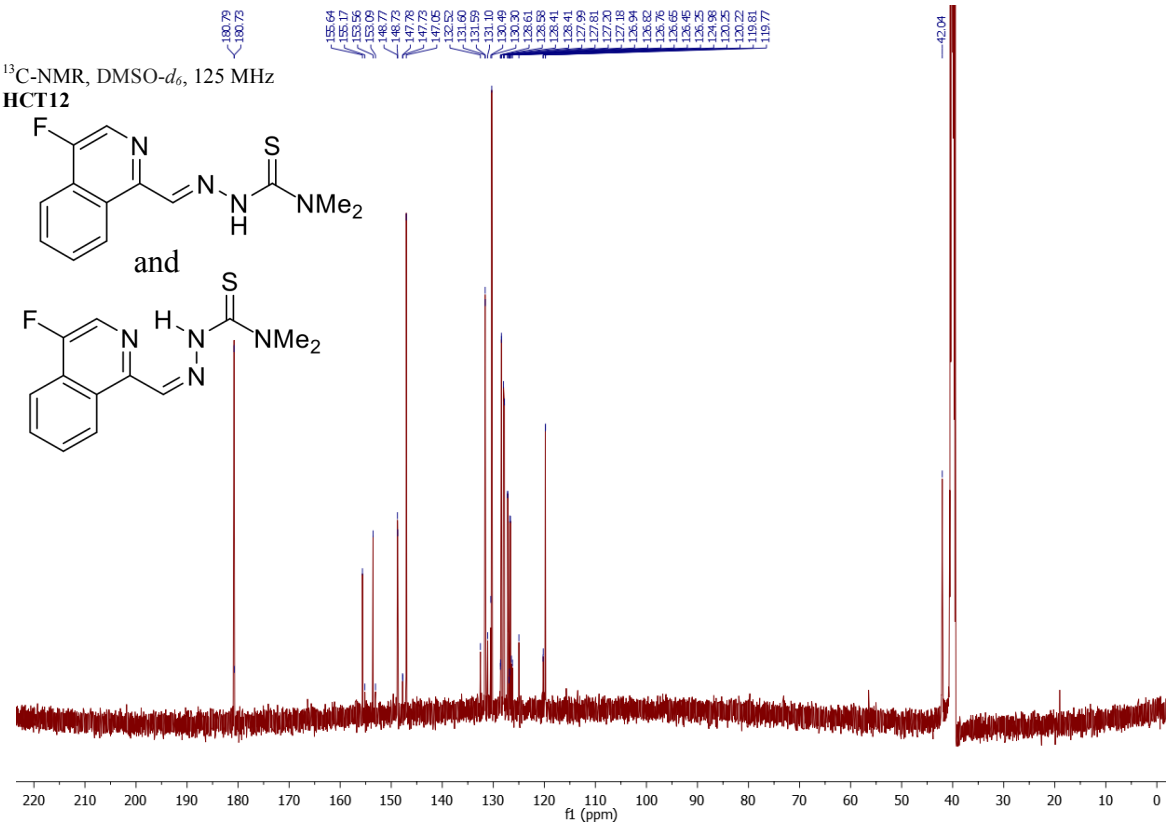

and

^{1}H-NMR, DMSO-d_6, 500 MHz
S11

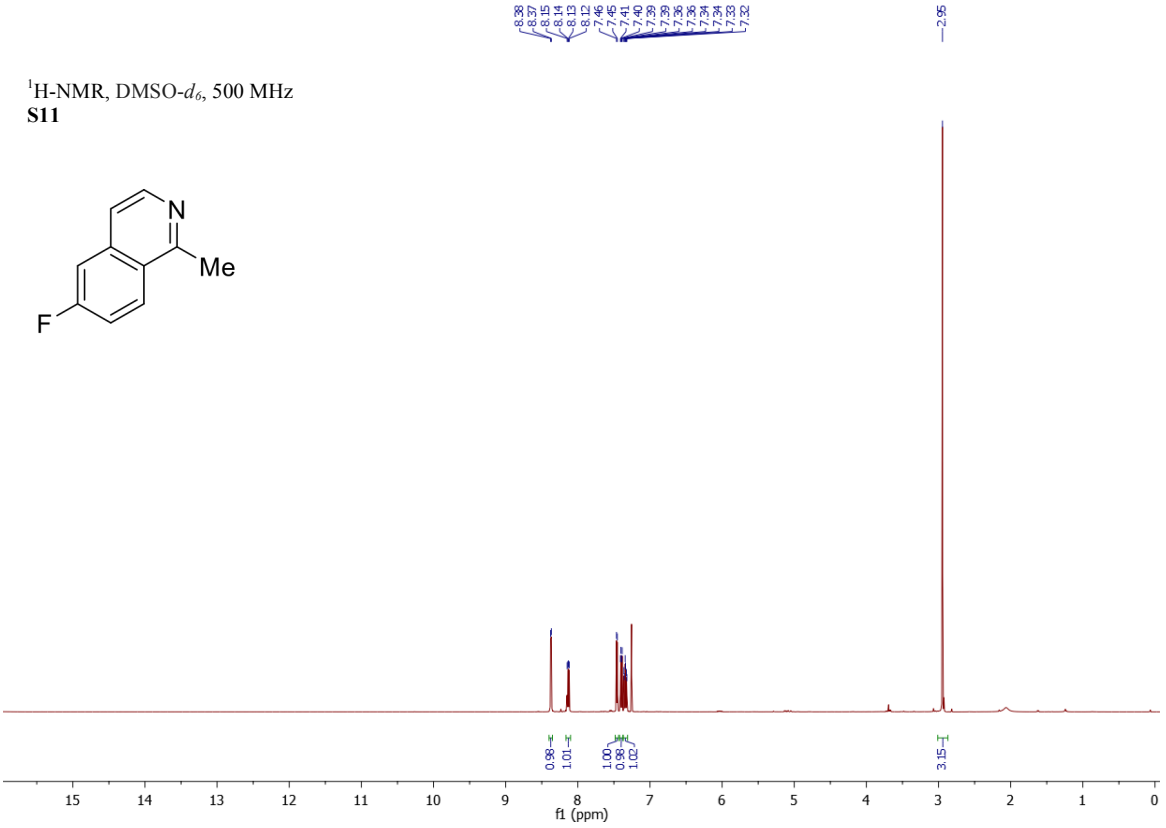

^{13}C-NMR, DMSO-d_6, 125 MHz
S11

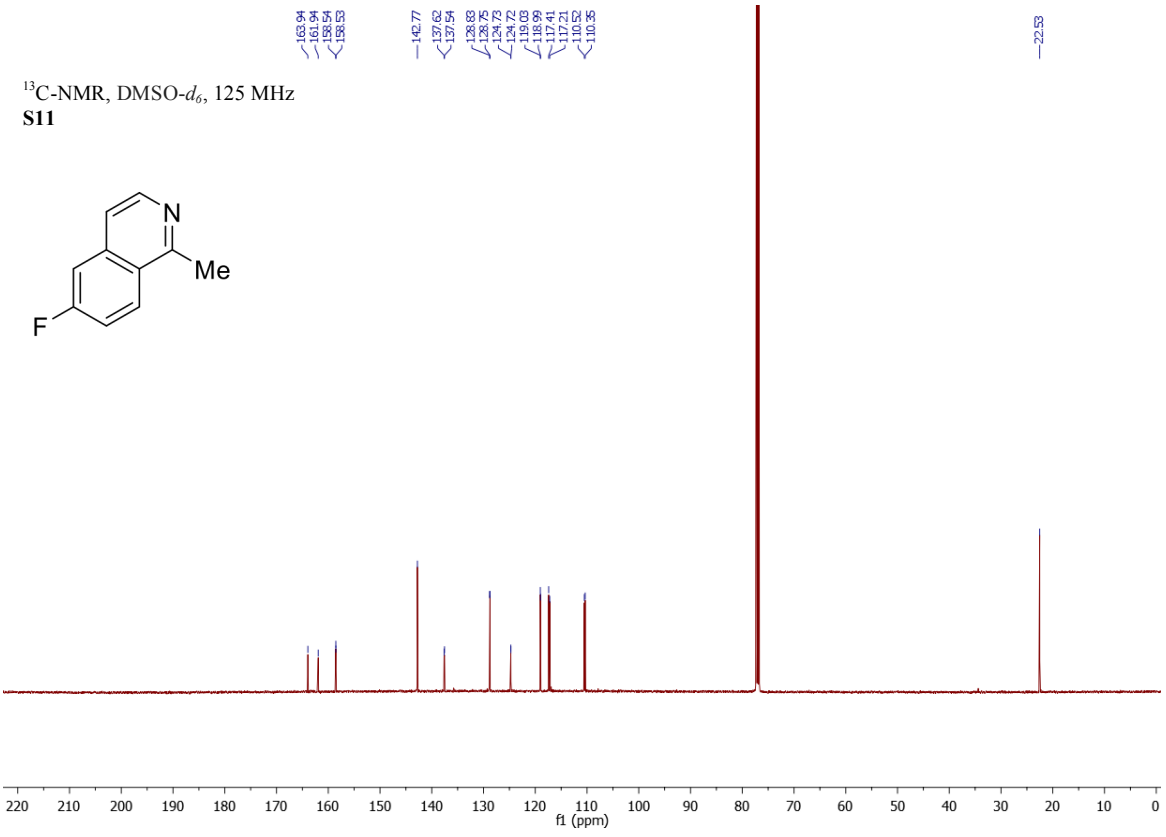

^{1}H-NMR, DMSO-d_6, 500 MHz
S12

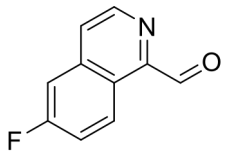

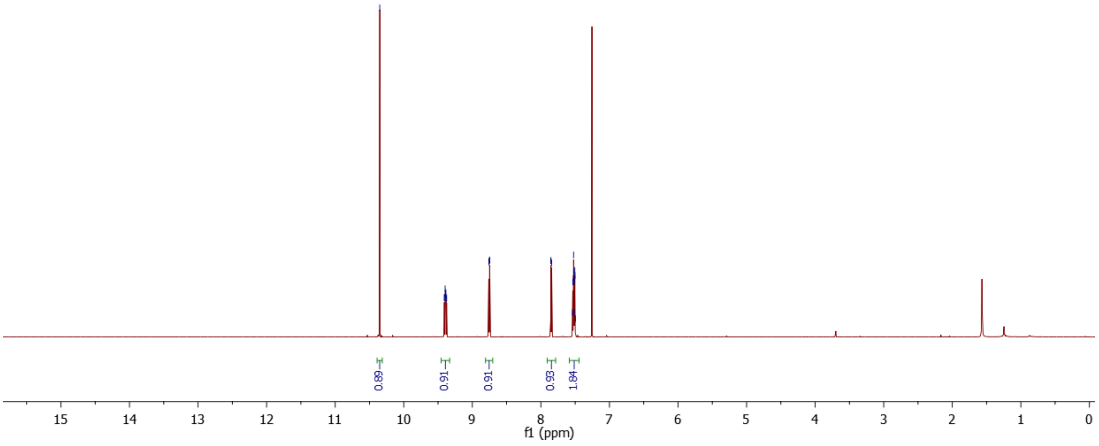

^{13}C-NMR, DMSO-d_6, 125 MHz
S12

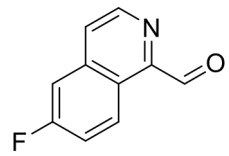

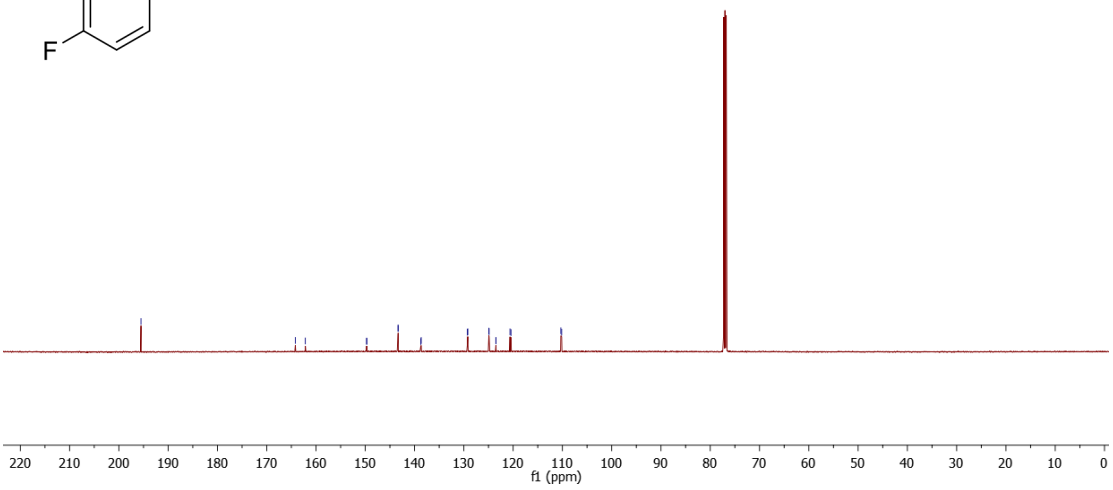

^{1}H-NMR, DMSO-d_6, 500 MHz
HCT3

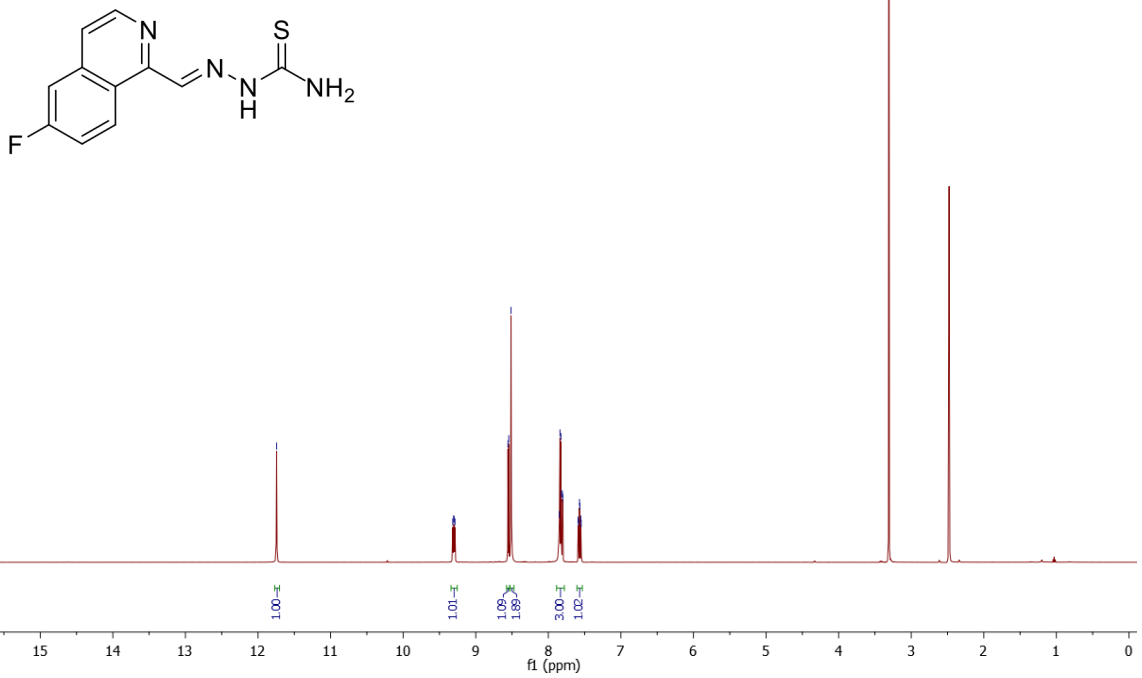

^{13}C-NMR, DMSO-d_6, 125 MHz
HCT3

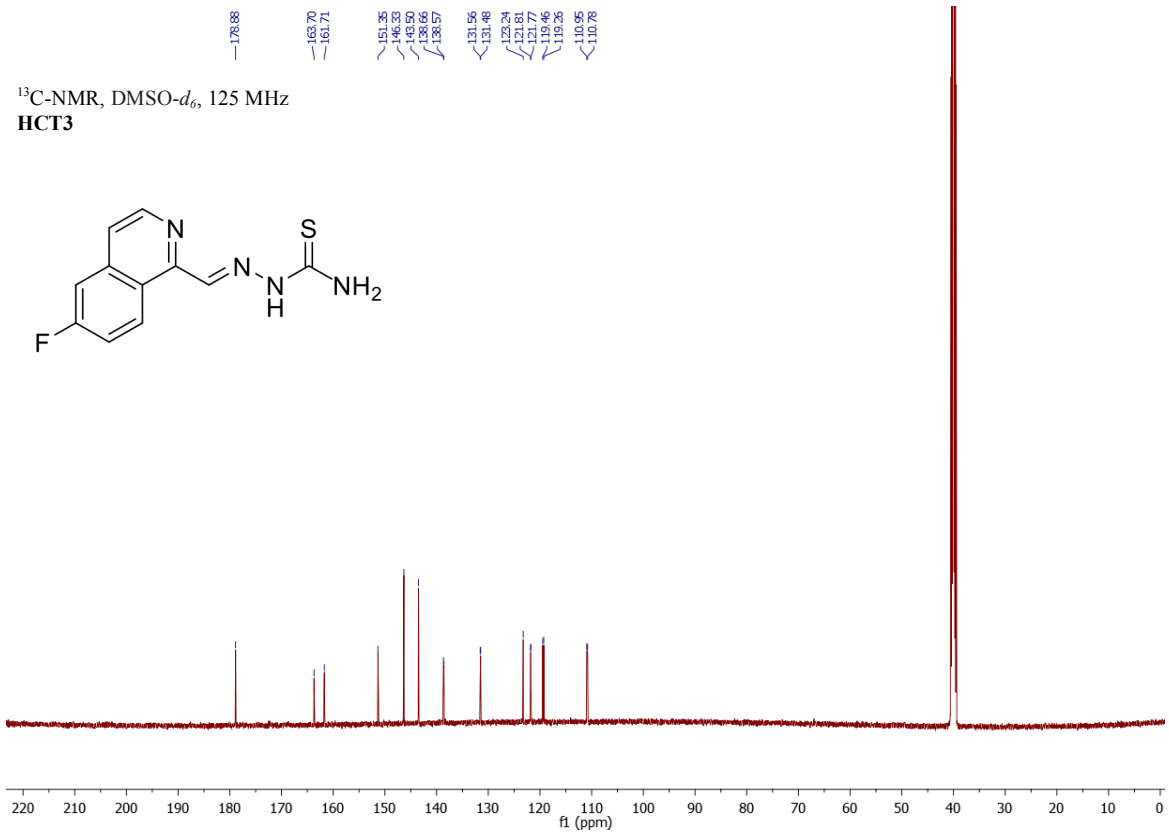

[1]H-NMR, DMSO-d_6, 500 MHz
HCT8

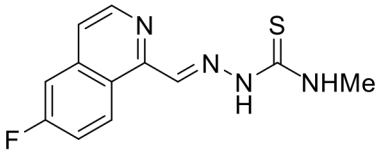

[13]C-NMR, DMSO-d_6, 125 MHz
HCT8

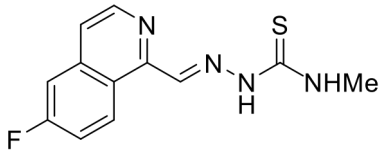

^{1}H-NMR, DMSO-d_6, 500 MHz
HCT13

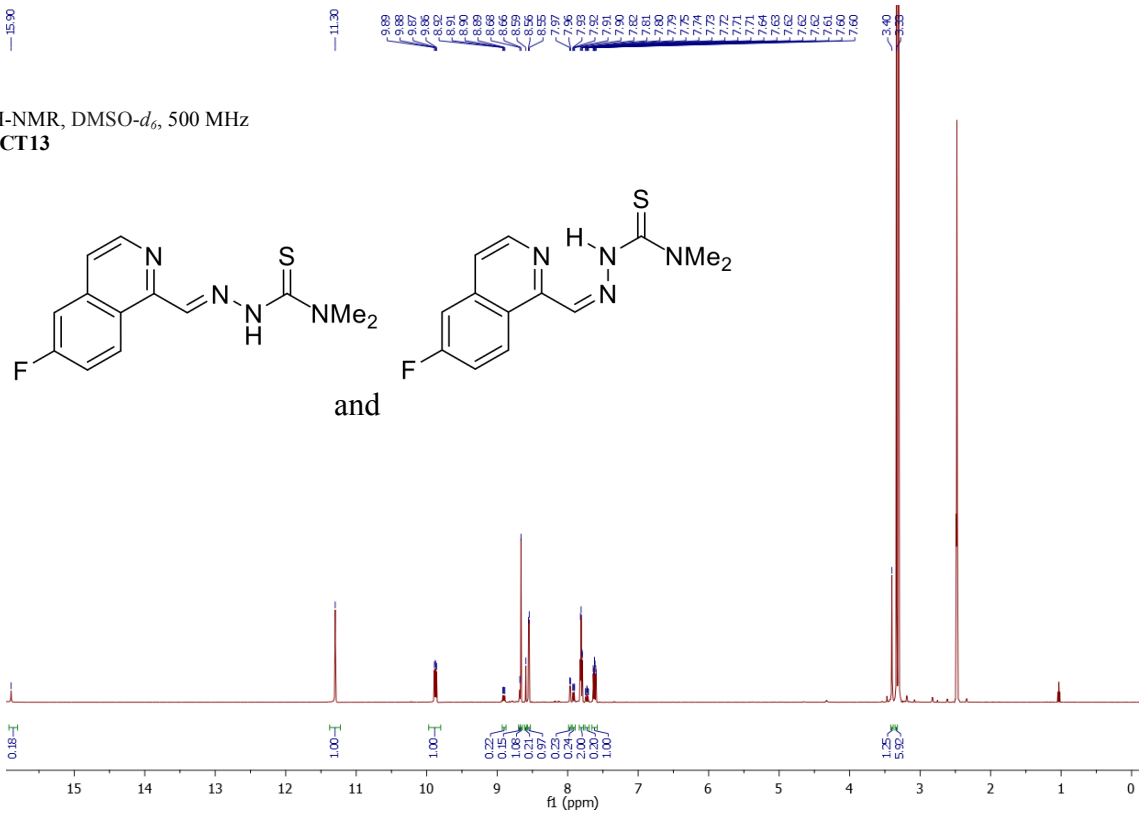

and

^{13}C-NMR, DMSO-d_6, 125 MHz
HCT13

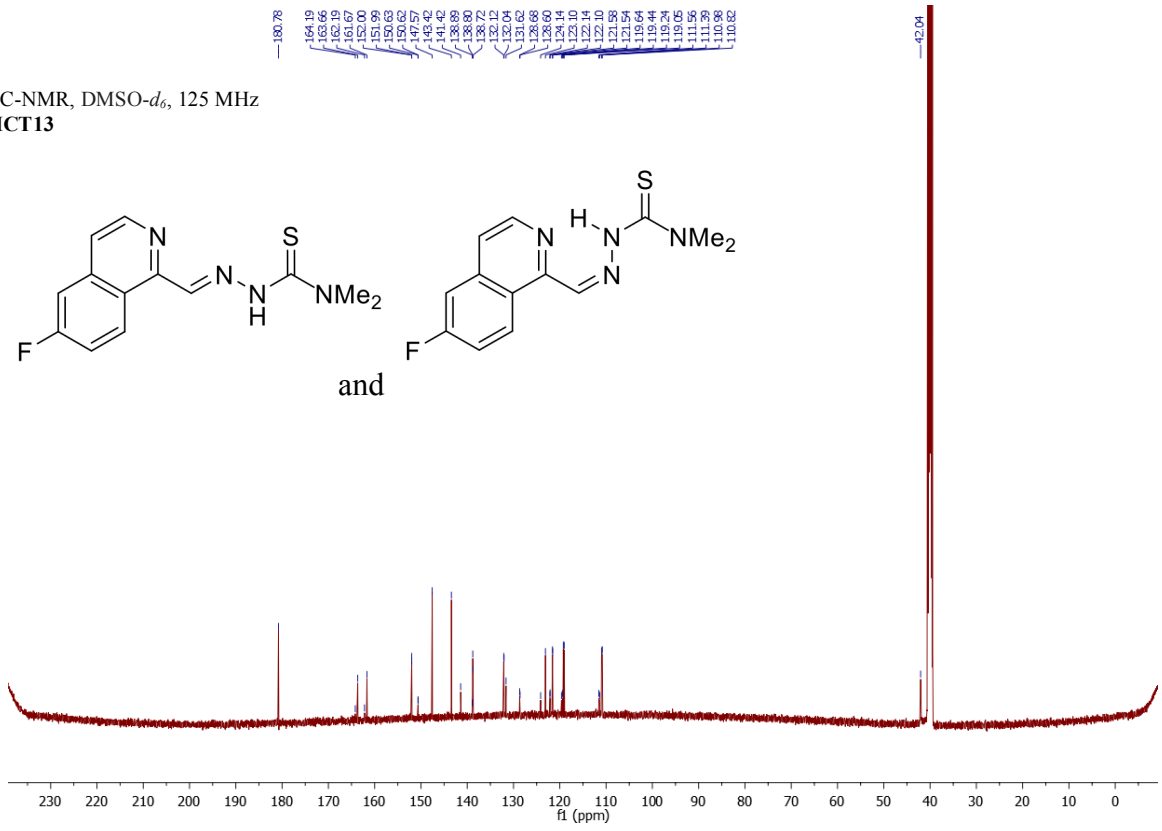

and

^{1}H-NMR, $CDCl_3$, 500 MHz
S13

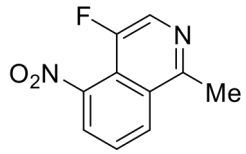

^{1}3C-NMR, $CDCl_3$, 500 MHz
S13

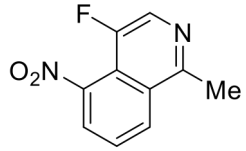

^{1}H-NMR, $CDCl_3$, 400 MHz
S14

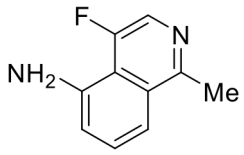

^{13}C-NMR, $CDCl_3$, 125 MHz
S14

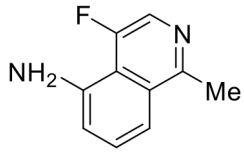

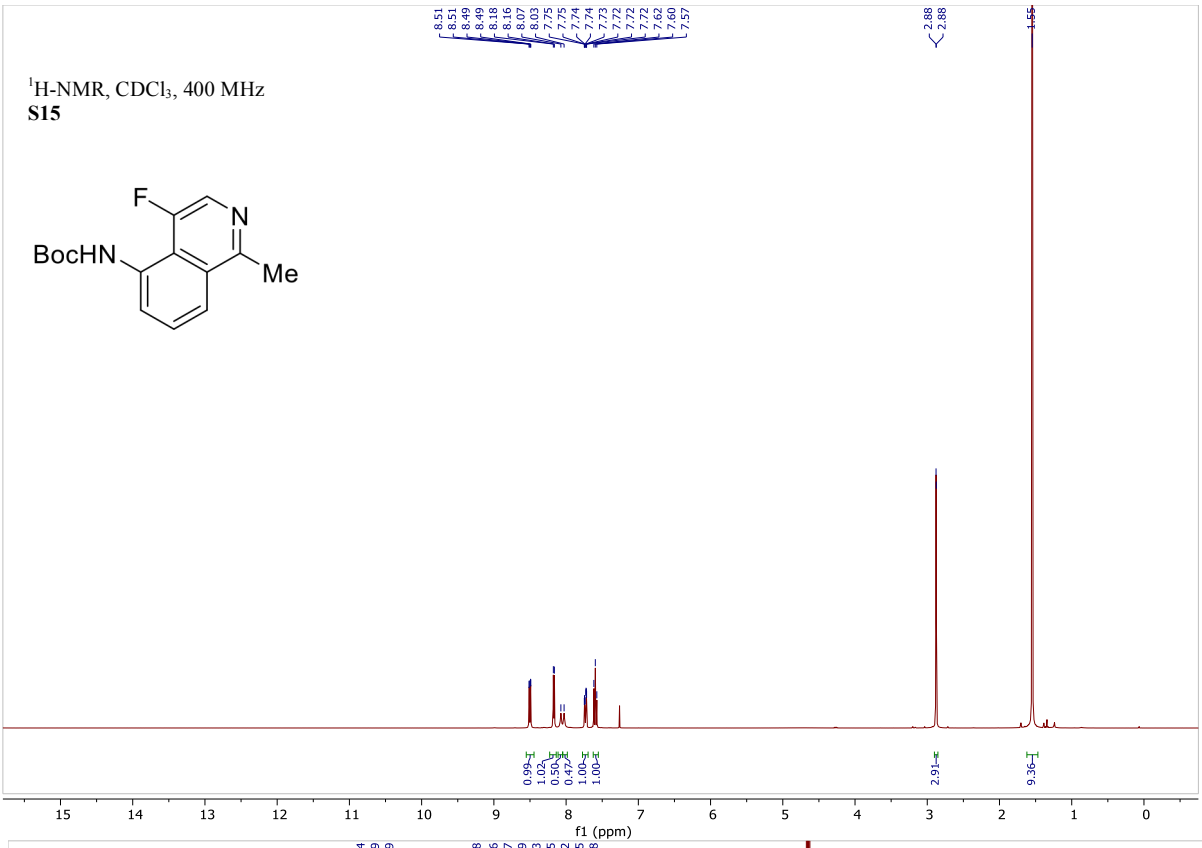

^{1}H-NMR, $CDCl_3$, 400 MHz
S15

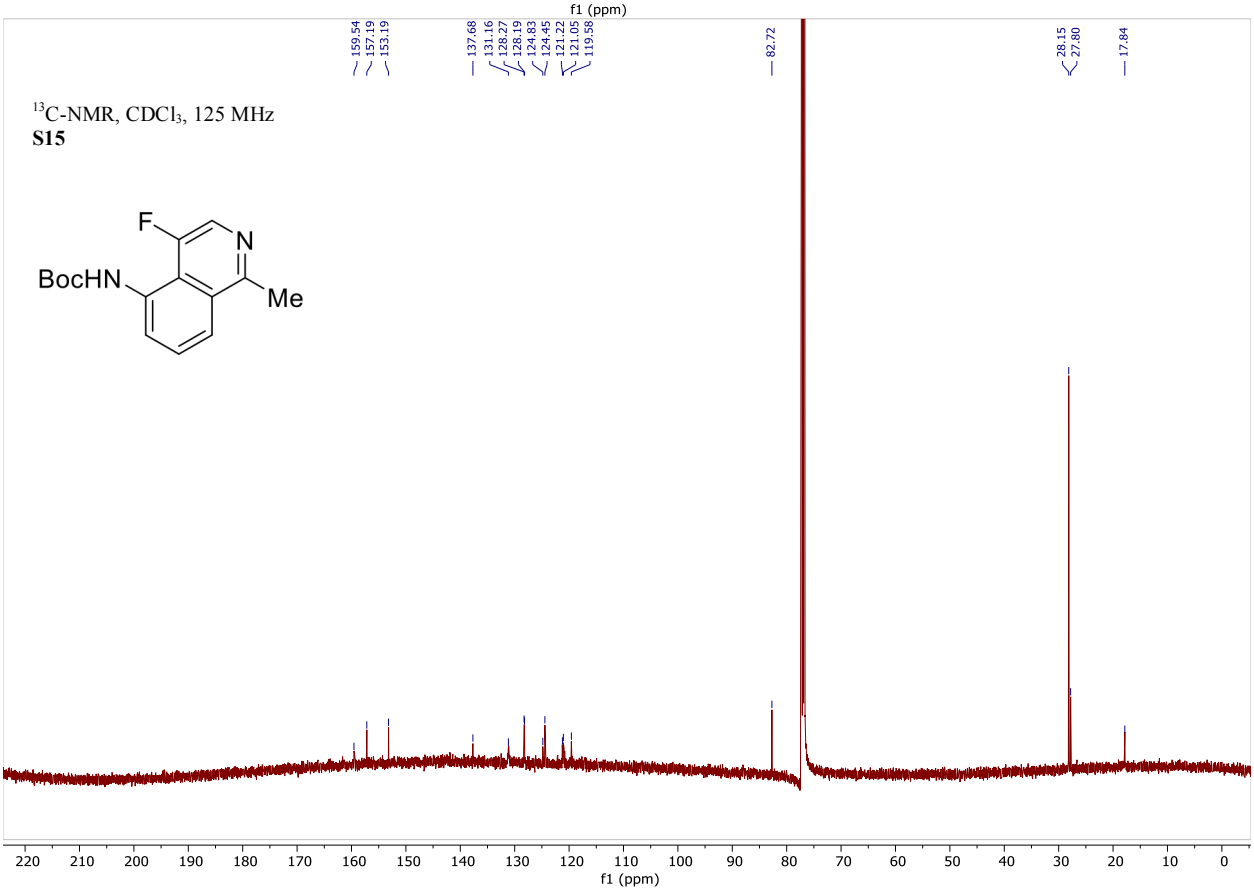

^{13}C-NMR, $CDCl_3$, 125 MHz
S15

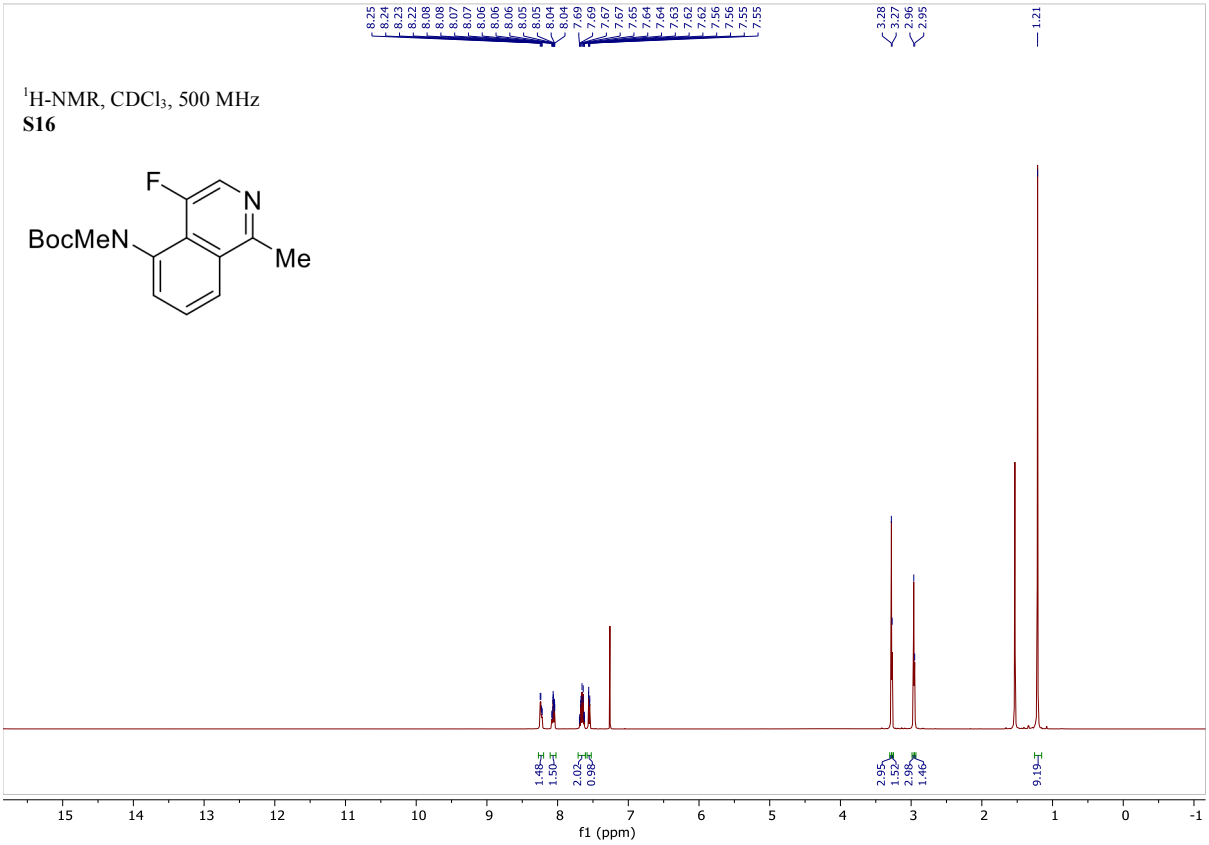

^{1}H-NMR, $CDCl_3$, 500 MHz
S16

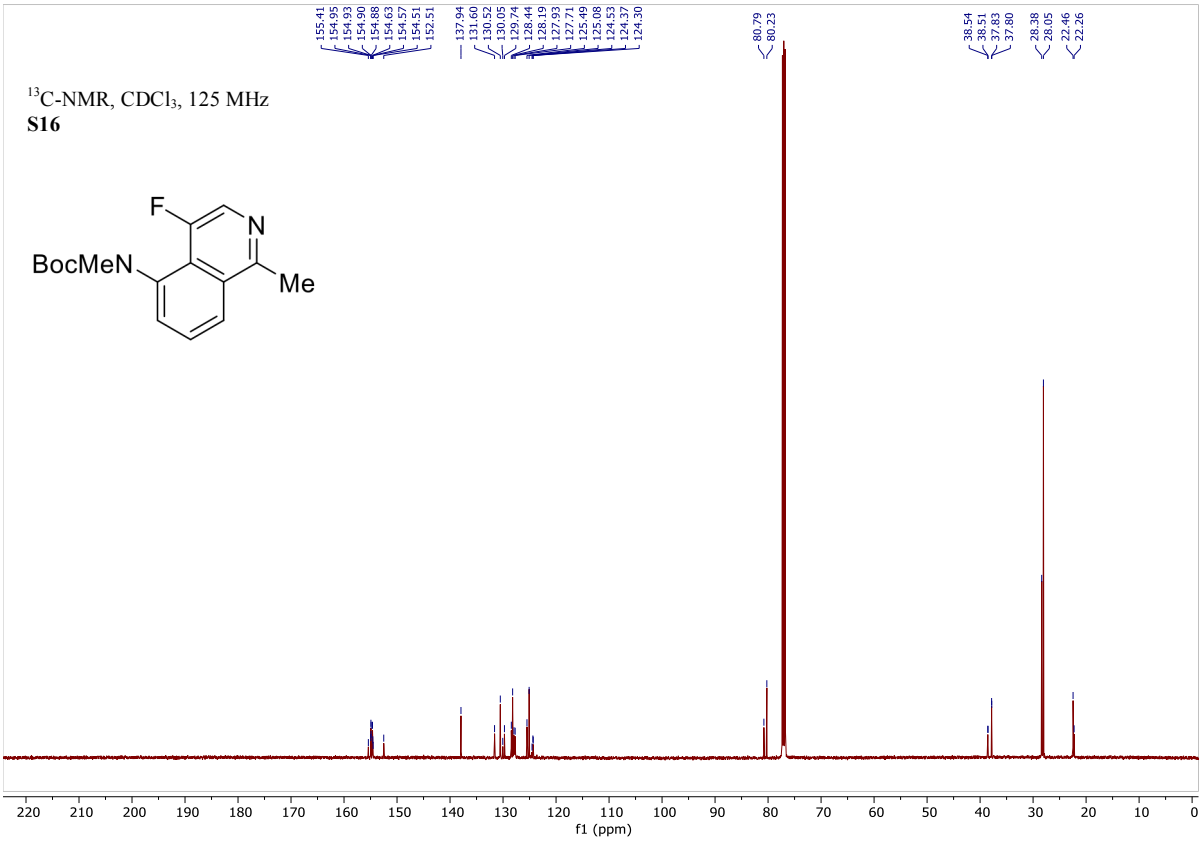

^{13}C-NMR, $CDCl_3$, 125 MHz
S16

^{1}H-NMR, $CDCl_3$, 500 MHz
S17

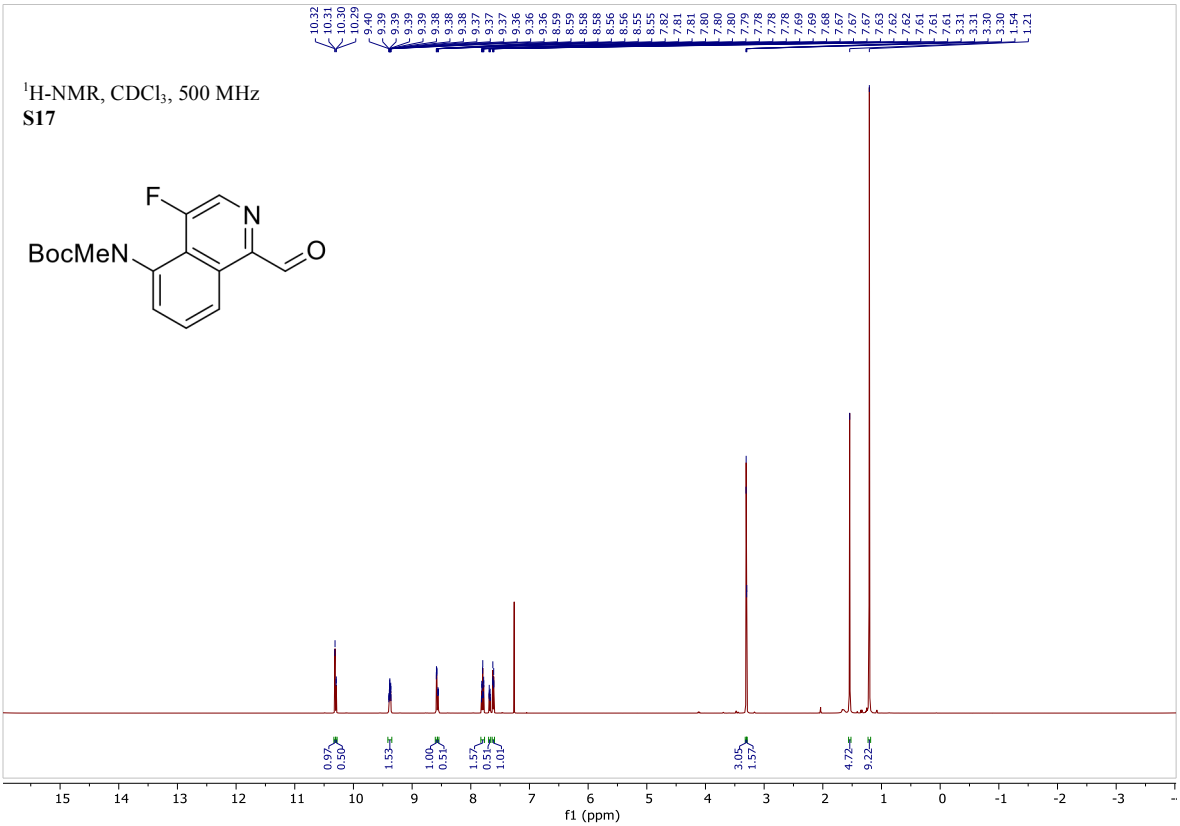

^{13}C-NMR, $CDCl_3$, 125 MHz
S17

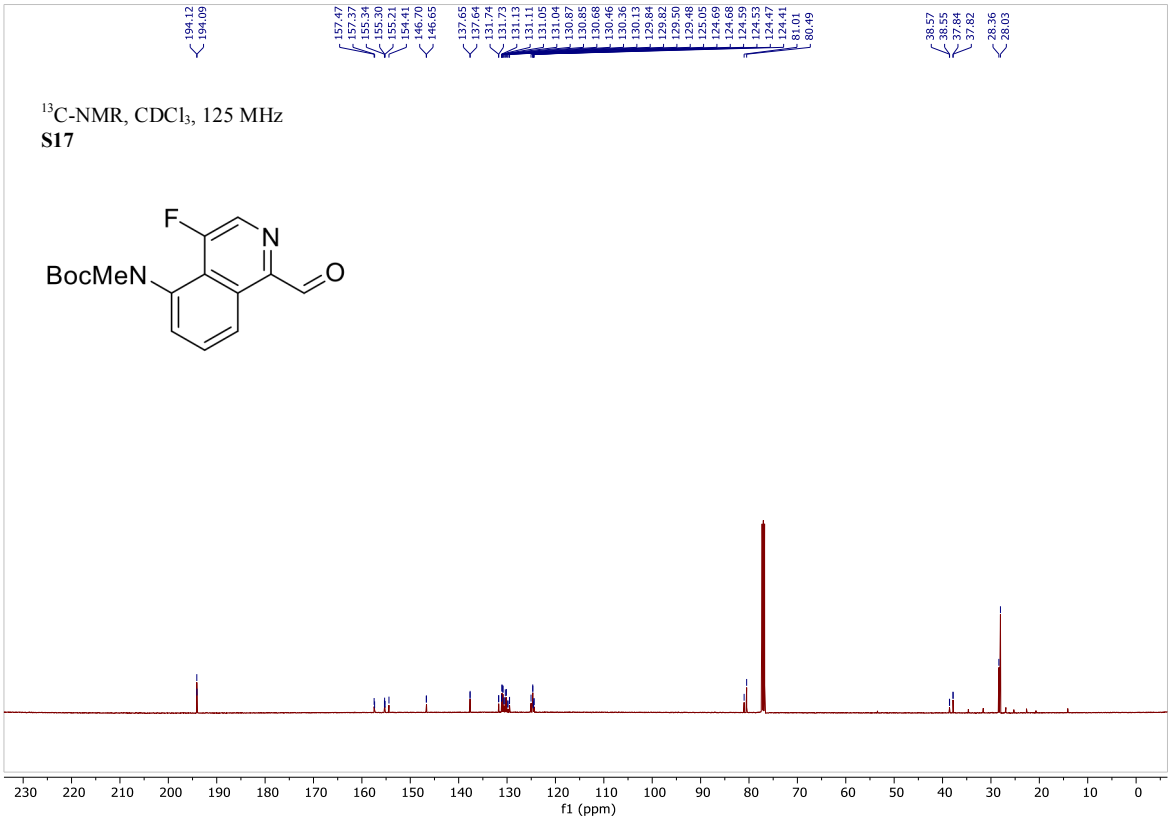

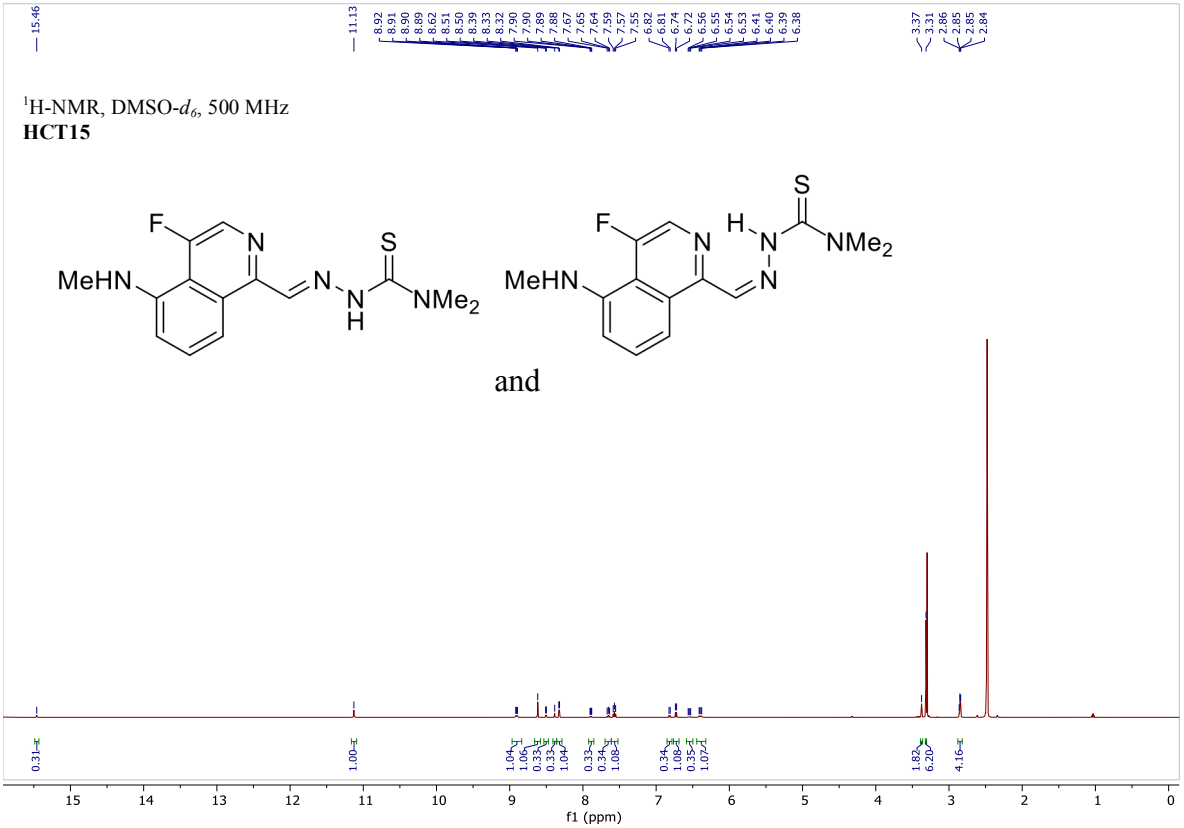

^{1}H-NMR, DMSO-d_6, 500 MHz
HCT15

and

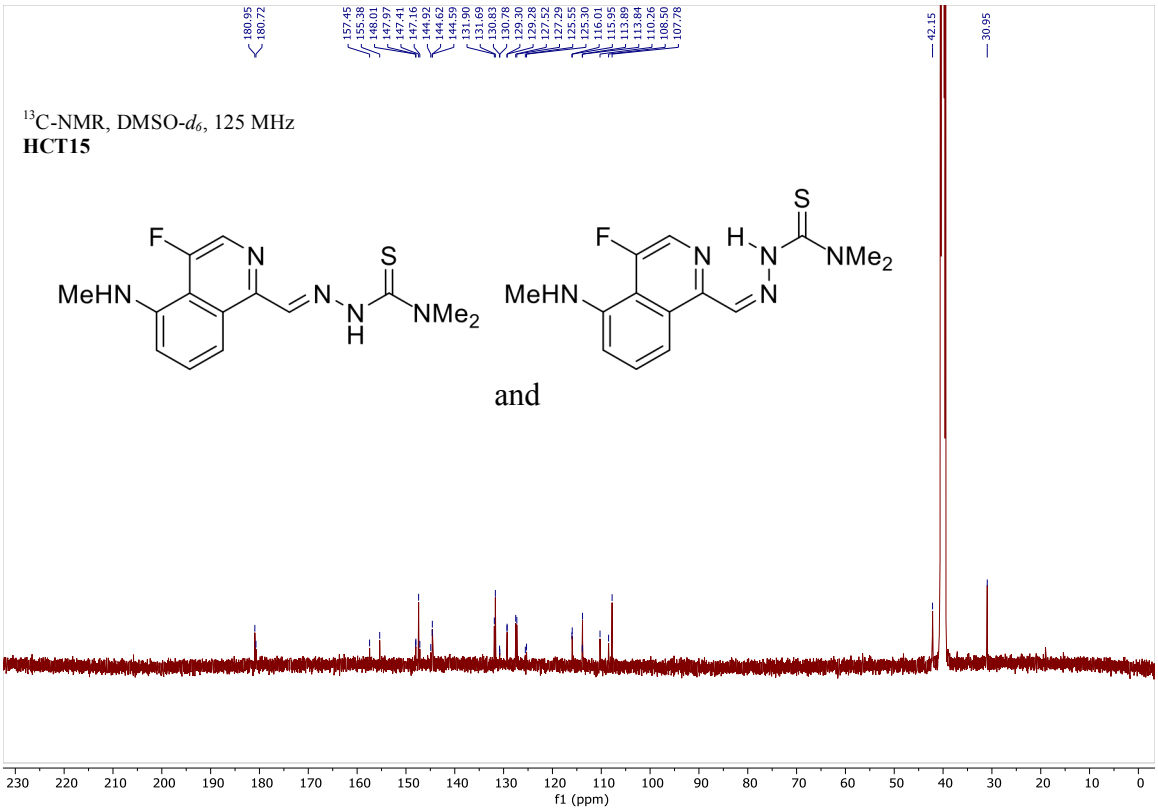

^{13}C-NMR, DMSO-d_6, 125 MHz
HCT15

and

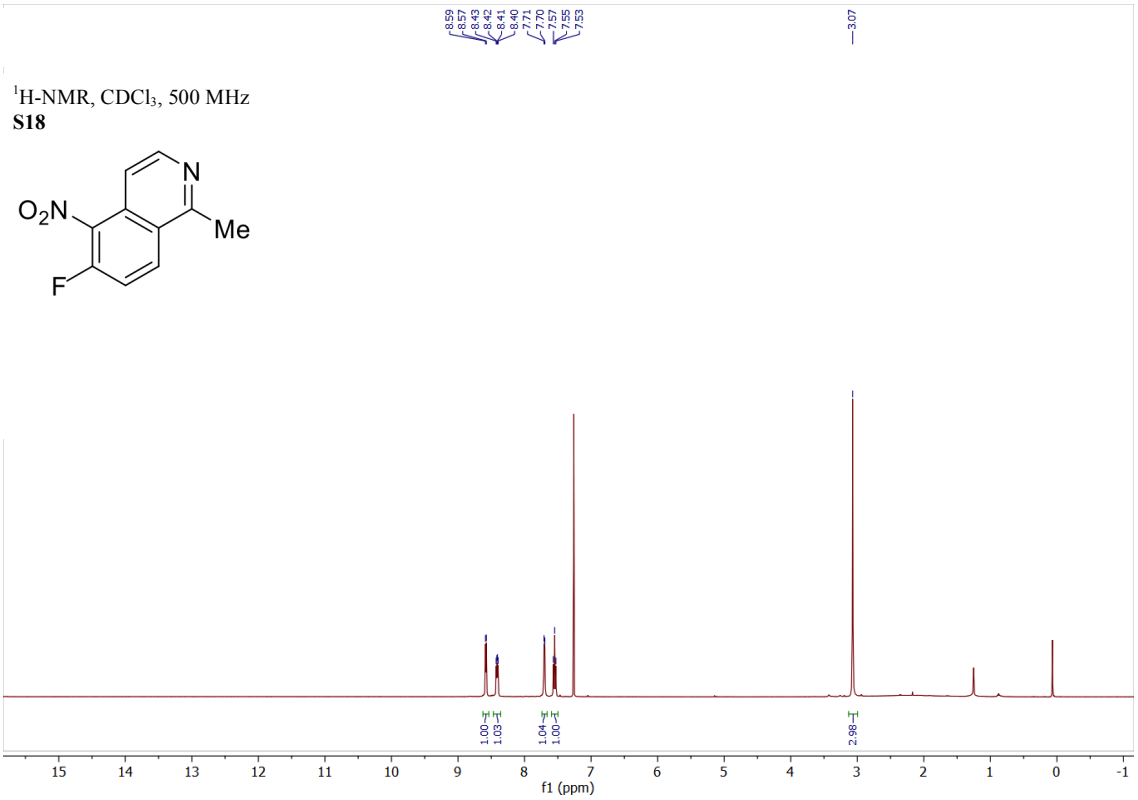

^{1}H-NMR, $CDCl_3$, 500 MHz
S18

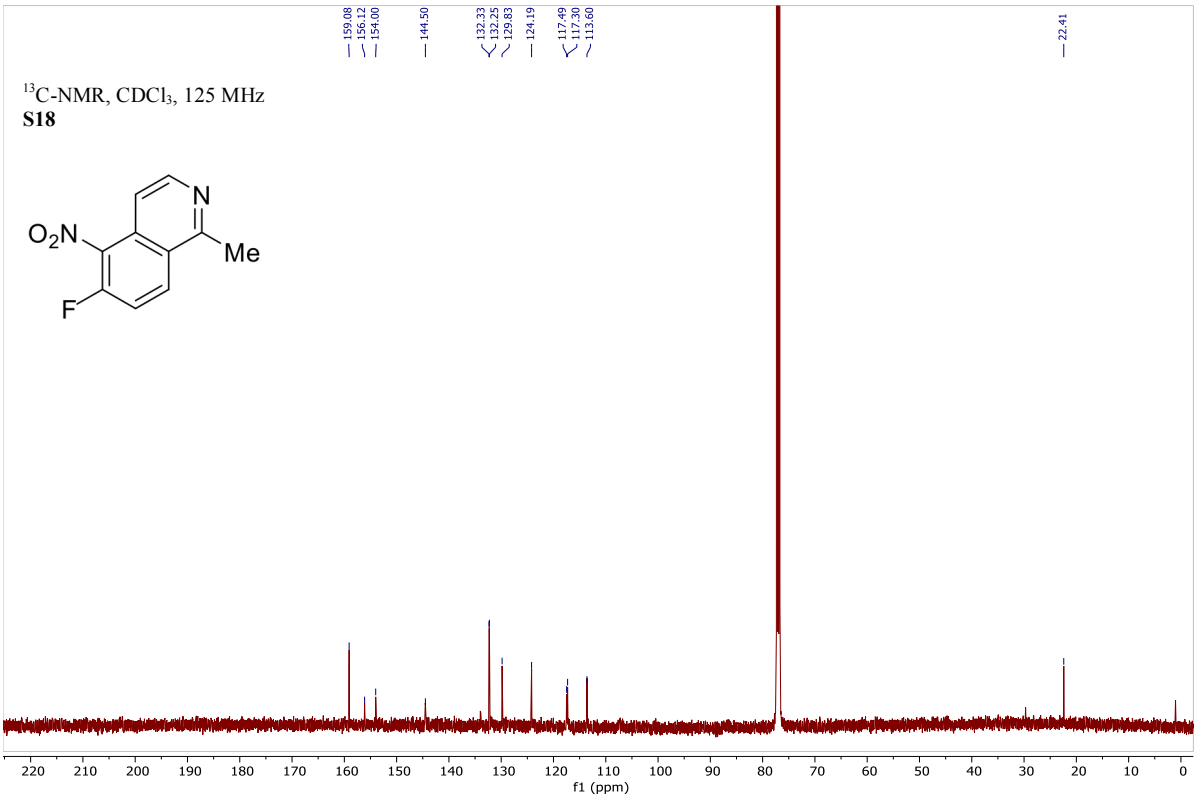

^{13}C-NMR, $CDCl_3$, 125 MHz
S18

^{1}H-NMR, $CDCl_3$, 500 MHz
S19

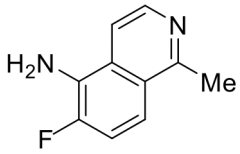

^{13}C-NMR, $CDCl_3$, 125 MHz
S19

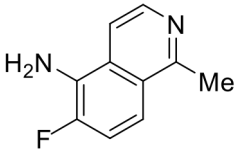

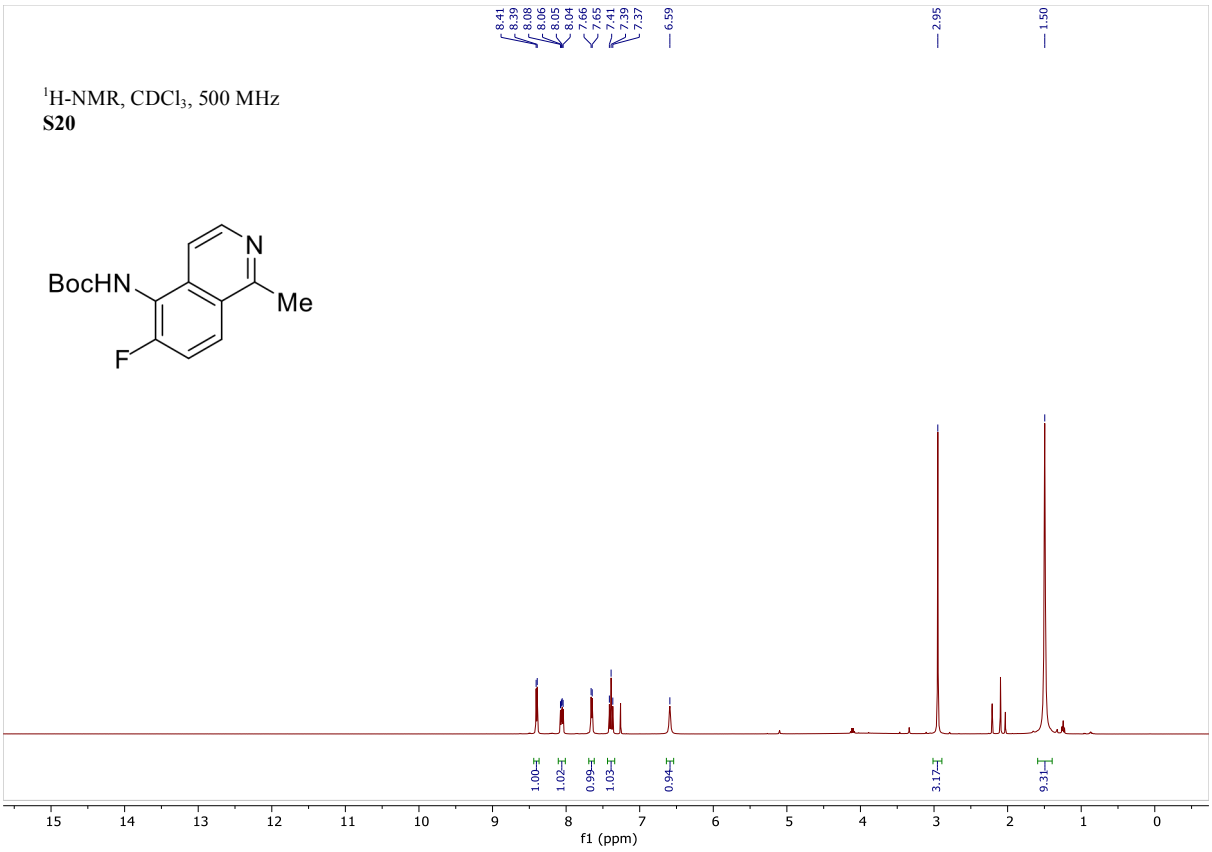

^{1}H-NMR, $CDCl_3$, 500 MHz
S20

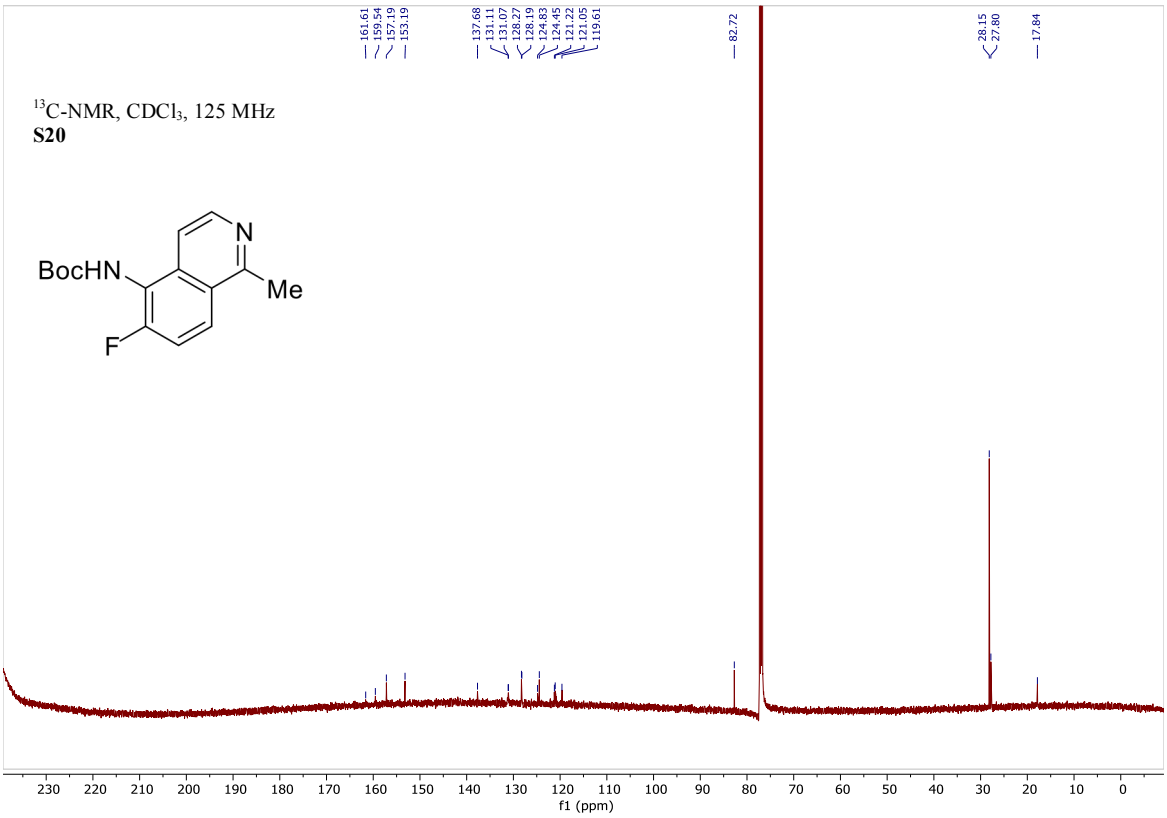

^{13}C-NMR, $CDCl_3$, 125 MHz
S20

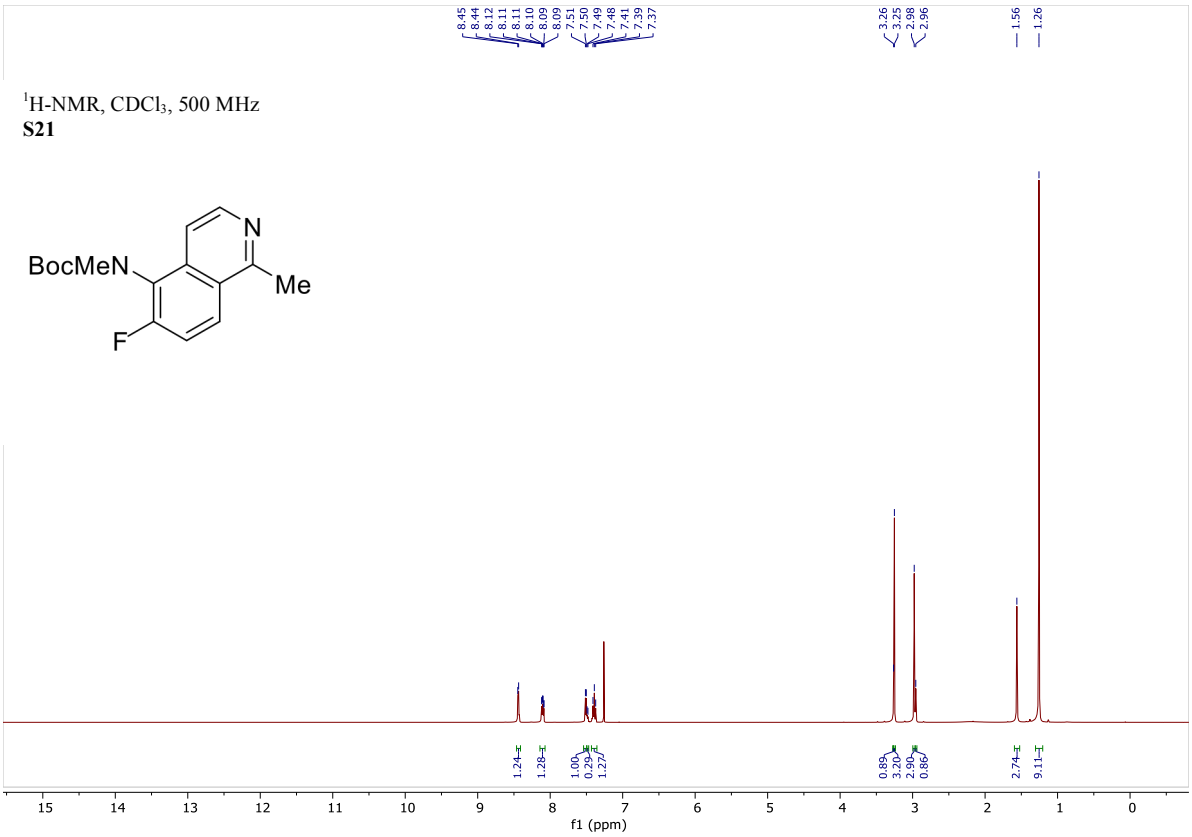

^{1}H-NMR, $CDCl_3$, 500 MHz
S21

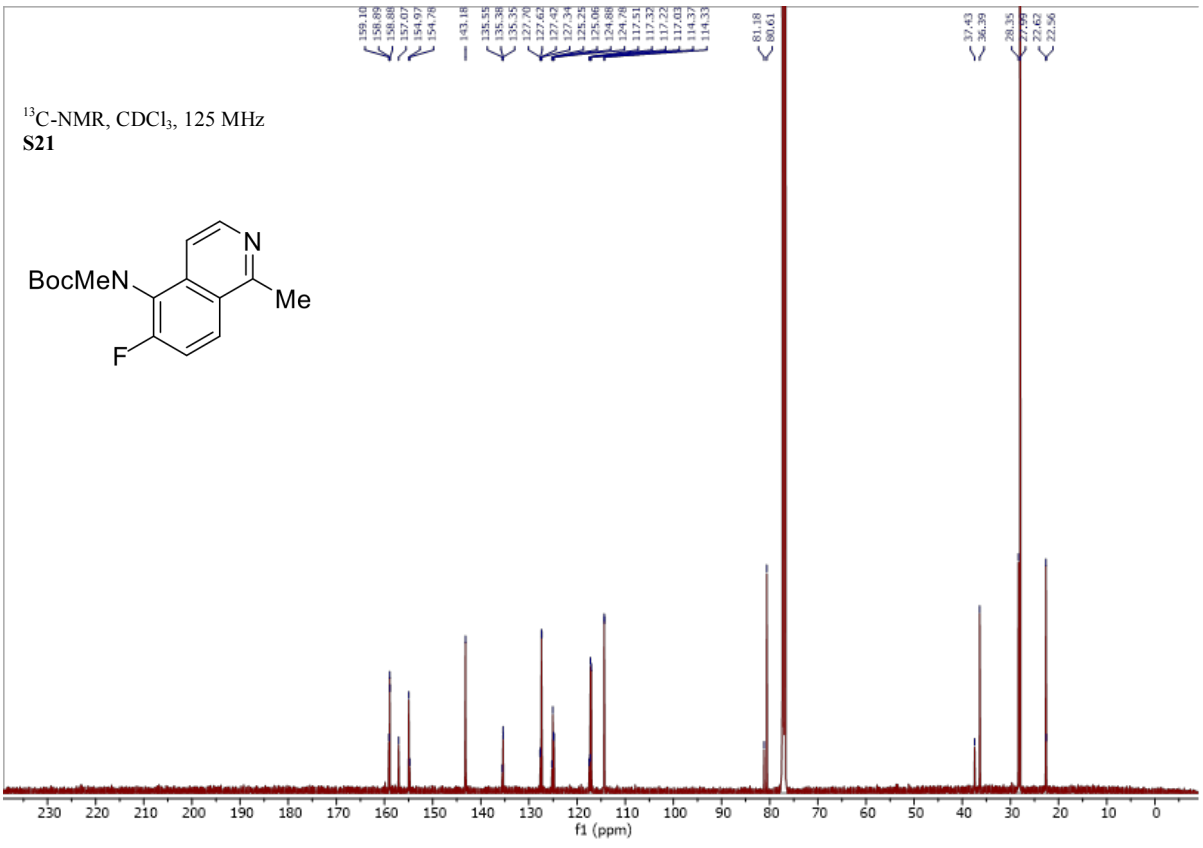

^{13}C-NMR, $CDCl_3$, 125 MHz
S21

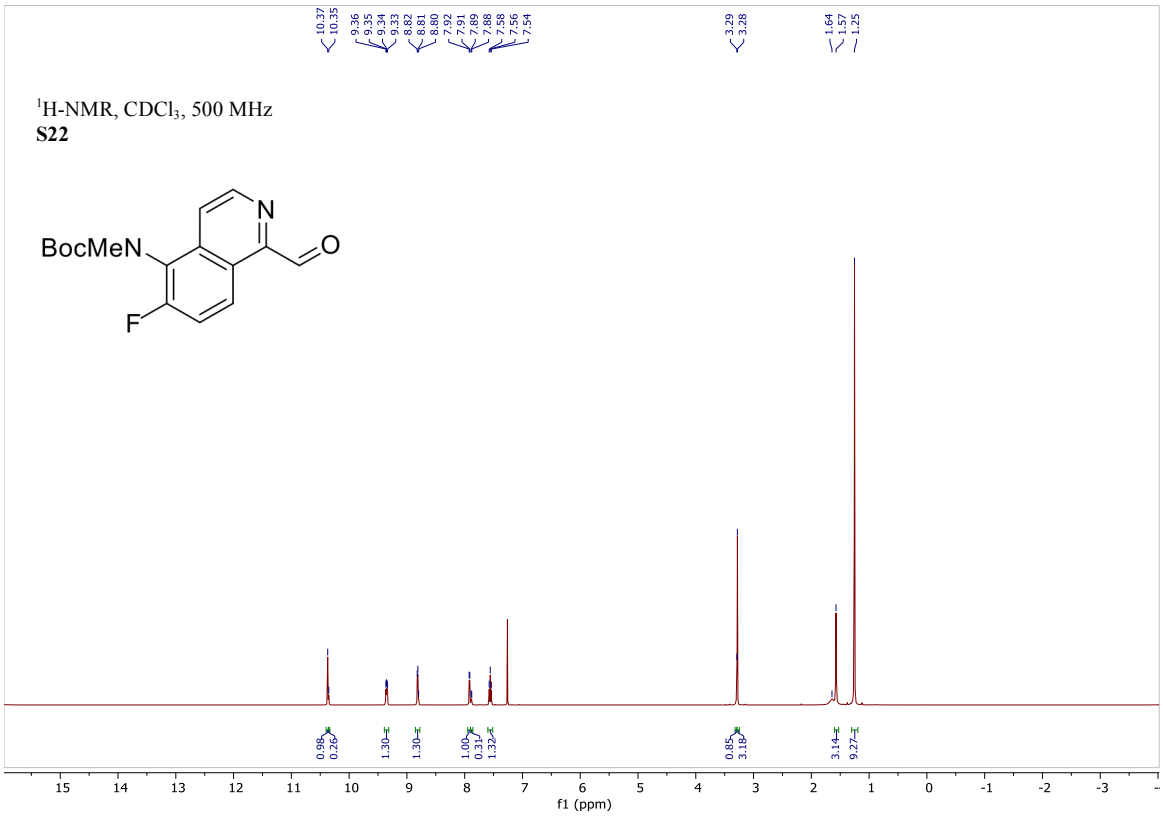

^{1}H-NMR, $CDCl_3$, 500 MHz
S22

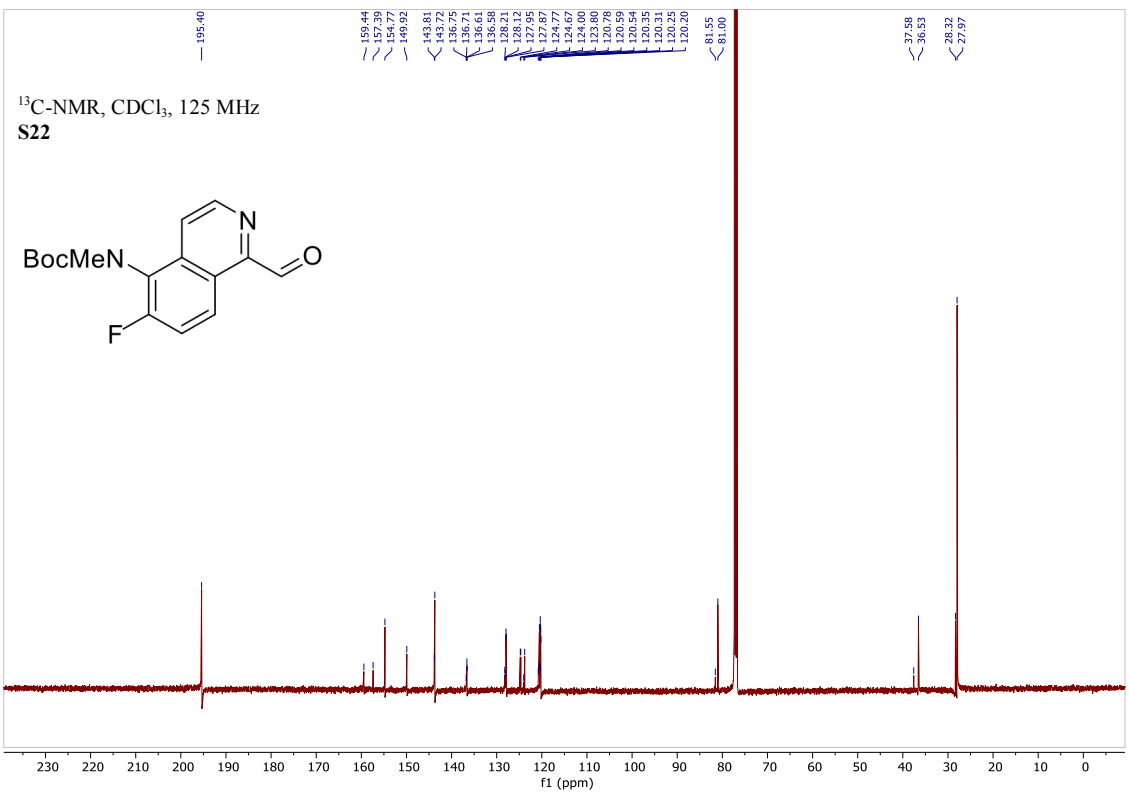

^{13}C-NMR, $CDCl_3$, 125 MHz
S22

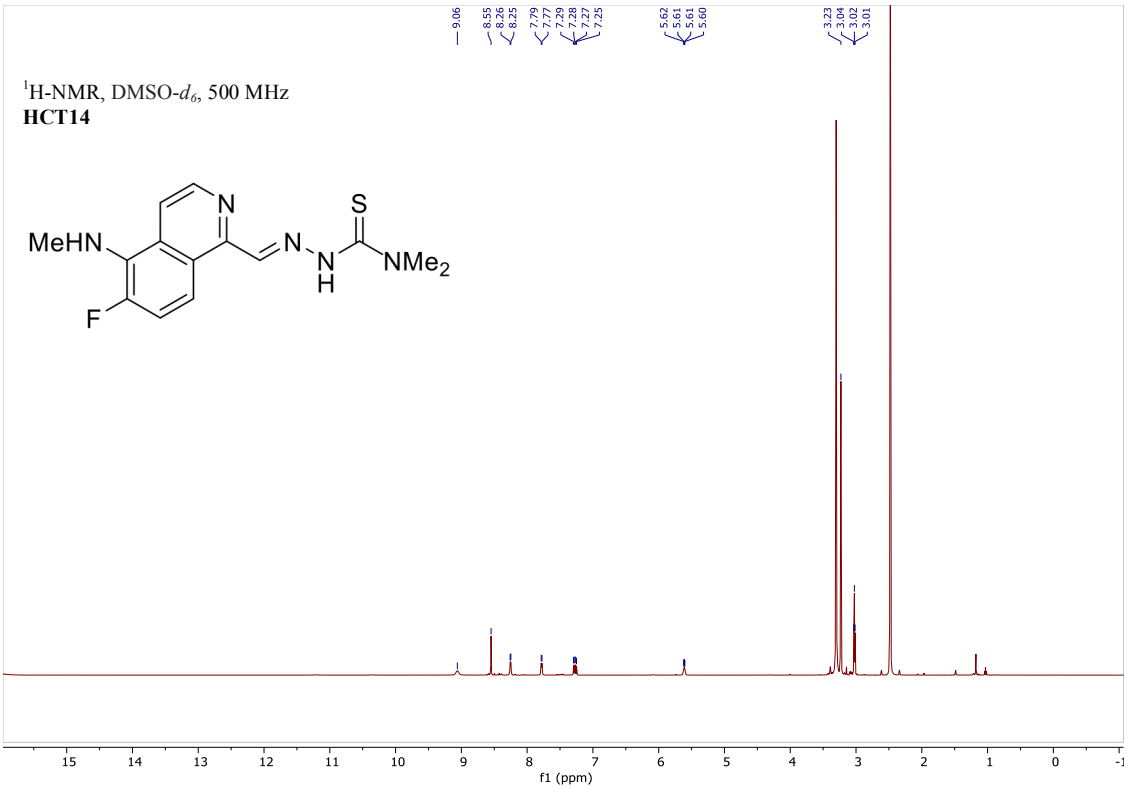
9.06
8.55
8.26
8.25
7.79
7.77
7.29
7.28
7.27
7.25
5.62
5.61
5.61
5.60
3.23
3.04
3.02
3.01
1H-NMR, DMSO-d6, 500 MHz
HCT14
MeHN
N
S
N
N
H
NMe2
F
f1 (ppm)

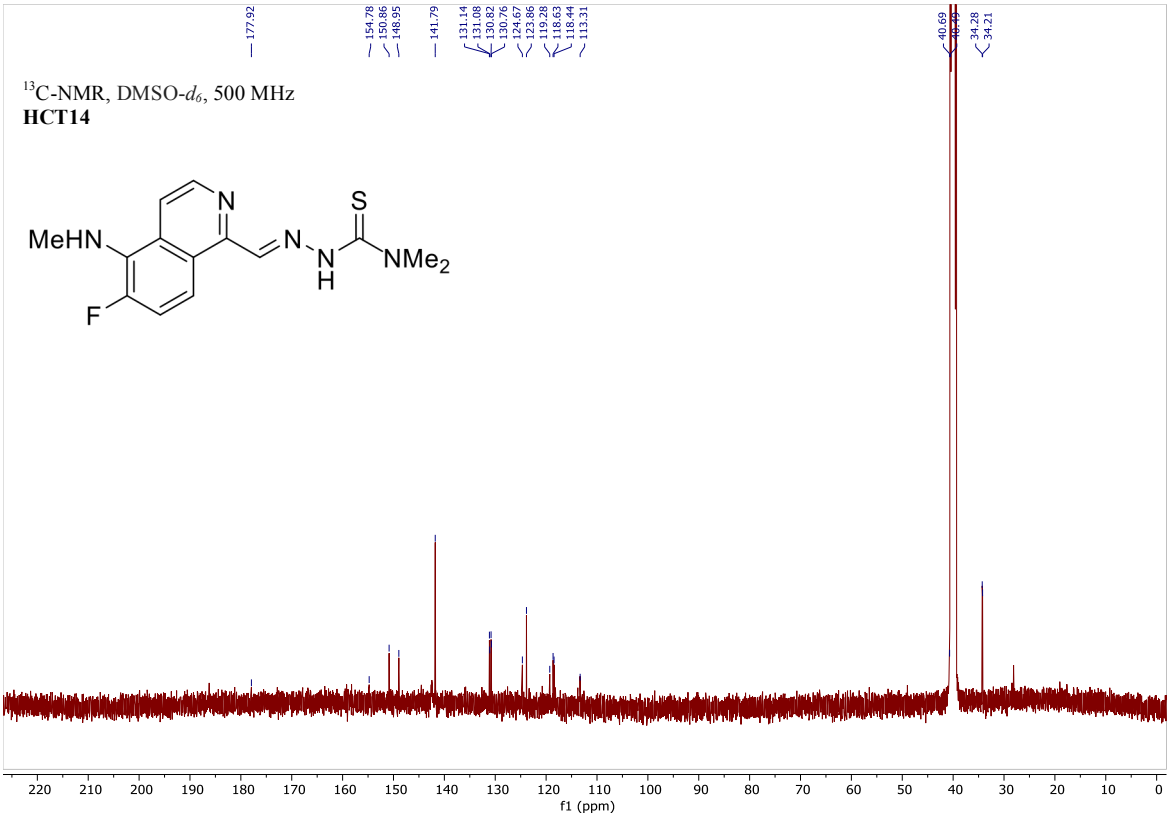
177.92
154.78
150.86
148.95
141.79
131.14
131.08
130.82
130.76
124.67
123.86
119.28
118.63
118.44
113.31
40.69
40.28
34.28
34.21
13C-NMR, DMSO-d6, 500 MHz
HCT14
MeHN
N
S
N
N
H
NMe2
F
f1 (ppm)

Supplementary Figure 3: ^{19}FNMR of compounds **S9-S22** and **HCT2, 3, 7, 8, and 12 – 15**

^{19}F-NMR, $CDCl_3$, 376 MHz
S9

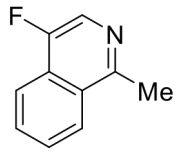

^{19}F-NMR, $CDCl_3$, 376 MHz
S10

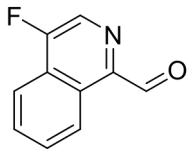

^{19}F-NMR, $CDCl_3$, 376 MHz
HCT2

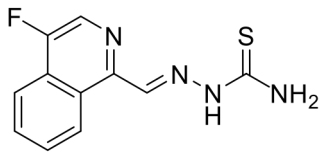

^{19}F-NMR, $CDCl_3$, 376 MHz
HCT7

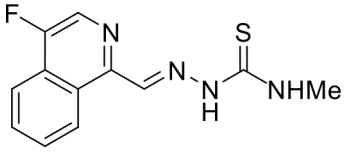

^{19}F-NMR, $CDCl_3$, 376 MHz
HCT12

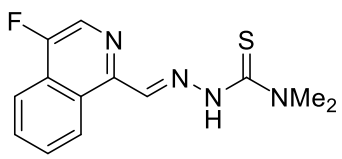

and

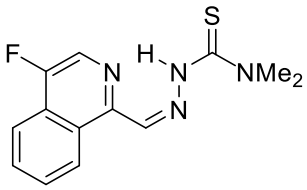

^{19}F-NMR, $CDCl_3$, 376 MHz
S11

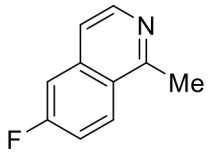

^{19}F-NMR, $CDCl_3$, 376 MHz
S12

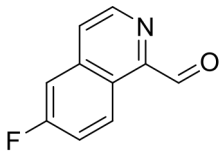

^{19}F-NMR, $CDCl_3$, 376 MHz
HCT3

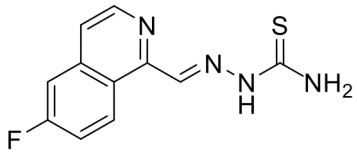

^{19}F-NMR, $CDCl_3$, 376 MHz

HCT8

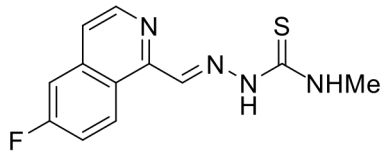

^{19}F-NMR, $CDCl_3$, 376 MHz

HCT13

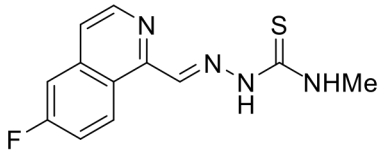

and

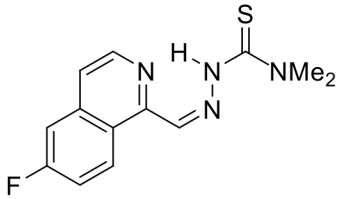

^{19}F-NMR, $CDCl_3$, 376 MHz

S13

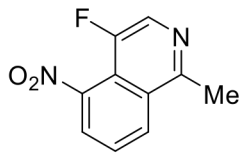

^{19}F-NMR, $CDCl_3$, 376 MHz

S14

^{19}F-NMR, $CDCl_3$, 376 MHz
S15

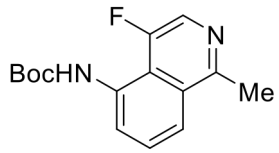

^{19}F-NMR, $CDCl_3$, 376 MHz
S16

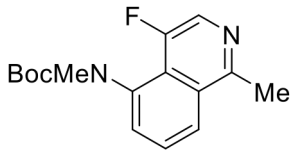

^{19}F-NMR, $CDCl_3$, 376 MHz
S17

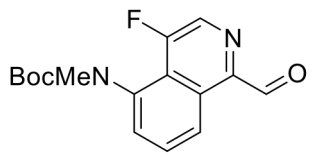

^{19}F-NMR, DMSO-d_6, 376 MHz
HCT15

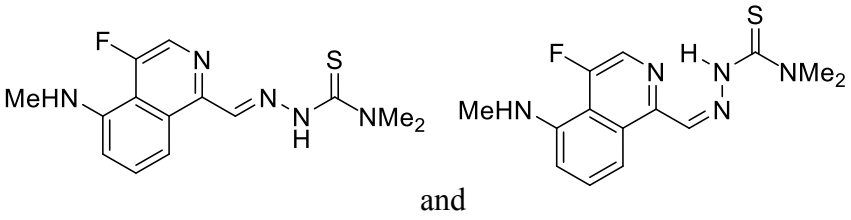

and

^{19}F-NMR, $CDCl_3$, 376 MHz
S18

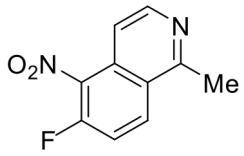

^{19}F-NMR, $CDCl_3$, 376 MHz
S19

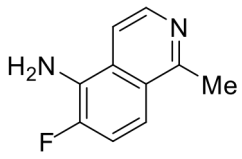

^{19}F-NMR, $CDCl_3$, 376 MHz
S20

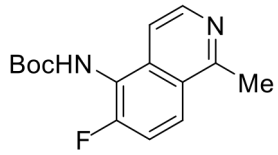

^{19}F-NMR, $CDCl_3$, 376 MHz
S21

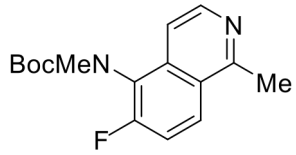

^{19}F-NMR, $CDCl_3$, 376 MHz
S22

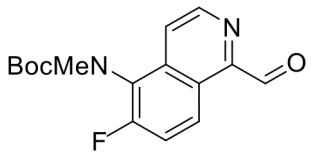

^{19}F-NMR, DMSO-d_6, 376 MHz
HCT14

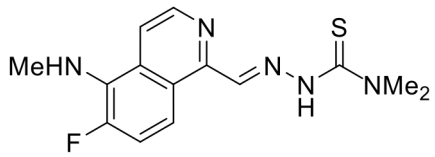

Supplementary Figure 4: HPLC analysis of **HCT1-15**

HPLC analysis of HCT1

Data File C:\HPCHEM\1\DATA\2018\052218\HCT-2.D Sample Name: HCT-2

```
======================================================================
Injection Date  : 5/22/2018 5:23:56 PM          Seq. Line :   3
Sample Name     : HCT-2                          Location : Vial 2
Acq. Operator   : JC                                 Inj :   1
                                                 Inj Volume : 10 µl
Acq. Method     : C:\HPCHEM\1\METHODS\JC-RP1.M
Last changed    : 5/22/2018 3:51:27 PM by JC
Analysis Method : C:\HPCHEM\1\METHODS\JV095.M
Last changed    : 12/12/2018 12:25:44 PM by Juno
                  (modified after loading)
```

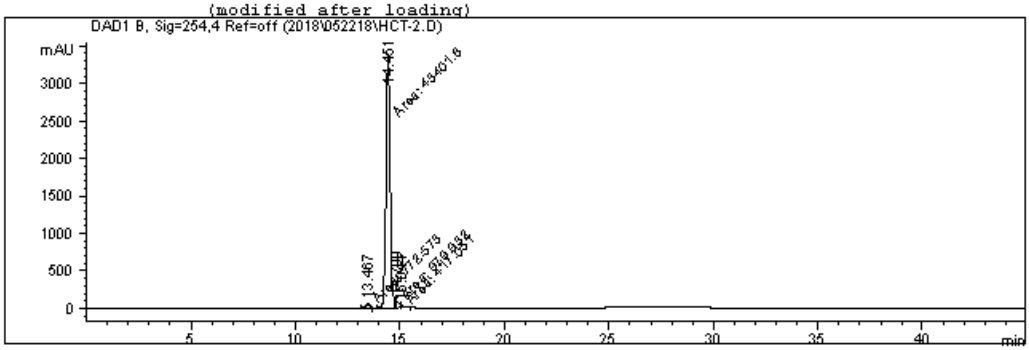


```
======================================================================
                        Area Percent Report
======================================================================

Sorted By             :      Signal
Multiplier            :      1.0000
Dilution              :      1.0000
Use Multiplier & Dilution Factor with ISTDs


Signal 1: DAD1 B, Sig=254,4 Ref=off

Peak RetTime Type  Width     Area      Height     Area
  #   [min]        [min]   [mAU*s]     [mAU]       %
----|-------|----|-------|----------|----------|--------|
   1  13.467 MM    0.2548  772.57324   50.52861   1.6953
   2  14.451 MM    0.2133 4.34016e4  3390.72119  95.2392
   3  14.799 MM    0.1675  979.93152   97.52905   2.1503
   4  15.044 MM    0.1827  417.05139   32.53645   0.9152

Totals :                  4.5571le4  3571.31531
```

\\Pmsl-analysis2\HP LaserJet P3015 on Ne00:
Letter 8 1/2 x 11 in/Portrait

Close | normal | Page 1 of 1

HPLC analysis of HCT2

Data File C:\HPCHEM\1\DATA\2018\052418\--HCT-20.D Sample Name: HCT-20

```
======================================================================
Injection Date  : 5/24/2018 8:41:49 PM          Seq. Line :   4
Sample Name     : HCT-20                         Location : Vial 3
Acq. Operator   : JC                                 Inj :   1
                                                 Inj Volume : 10 µl
Acq. Method     : C:\HPCHEM\1\METHODS\JC-RP1.M
Last changed    : 5/23/2018 1:25:21 PM by JC
Analysis Method : C:\HPCHEM\1\METHODS\JV095.M
Last changed    : 12/12/2018 12:25:44 PM by Juno
                  (modified after loading)
```

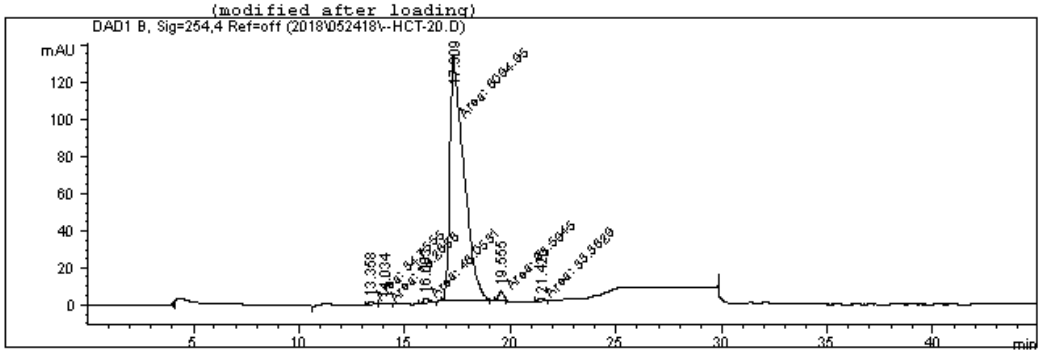


```
======================================================================
                        Area Percent Report
======================================================================

Sorted By             :      Signal
Multiplier            :      1.0000
Dilution              :      1.0000
Use Multiplier & Dilution Factor with ISTDs


Signal 1: DAD1 B, Sig=254,4 Ref=off

Peak RetTime Type  Width     Area      Height     Area
  #   [min]        [min]   [mAU*s]     [mAU]       %
----|-------|----|-------|----------|----------|--------|
   1  13.358 MM    0.2960   34.75550    1.95683   0.5498
   2  14.034 MM    0.4160   18.26581 7.31878e-1   0.2890
   3  16.003 MM    0.3672   46.05307    2.09044   0.7286
   4  17.309 MM    0.7684 6094.95312  132.20535  96.4241
   5  19.555 MM    0.2949   93.59449    5.28906   1.4807
   6  21.426 MM    0.3386   33.36292    1.64216   0.5278
```

\\Pmsl-analysis2\HP LaserJet P3015 on Ne00:
Letter 8 1/2 x 11 in/Portrait

Close | normal | Page 1 of 1

HPLC analysis of HCT3

Data File C:\HPCHEM\1\DATA\2018\070218\HCT25(B1.D Sample Name: HCT25(B1)

```
    ======================================================================
    Injection Date  : 7/2/2018 1:46:02 PM            Seq. Line :   1
    Sample Name     : HCT25(B1)                       Location : Vial 61
    Acq. Operator   : JC                                  Inj :   1
                                                     Inj Volume : 250 µl
    Different Inj Volume from Sequence !     Actual Inj Volume : 10 µl
    Acq. Method     : C:\HPCHEM\1\METHODS\JC-ISOQS.M
    Last changed    : 7/2/2018 1:35:45 PM by JC
    Analysis Method : C:\HPCHEM\1\METHODS\JV095.M
    Last changed    : 12/12/2018 12:25:44 PM by Juno
                      (modified after loading)
```

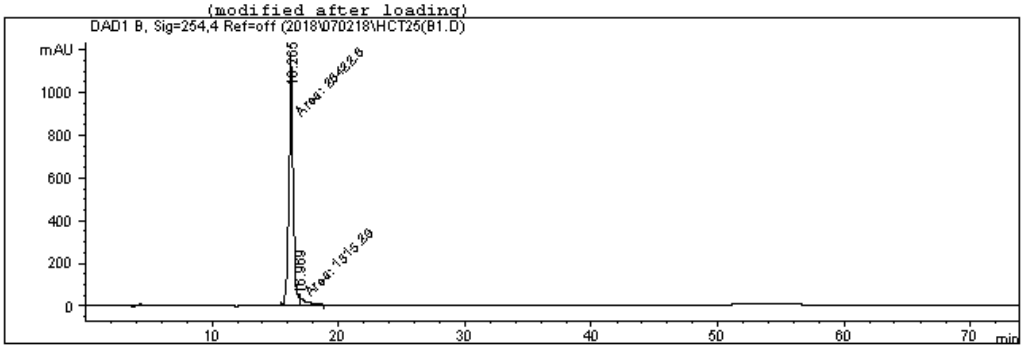


```
    ======================================================================
                              Area Percent Report
    ======================================================================

    Sorted By             :      Signal
    Multiplier            :      1.0000
    Dilution              :      1.0000
    Use Multiplier & Dilution Factor with ISTDs


    Signal 1: DAD1 B, Sig=254,4 Ref=off

    Peak RetTime Type  Width     Area      Height     Area
      #   [min]        [min]   [mAU*s]     [mAU]       %
    ----|-------|----|-------|----------|----------|--------|
       1  16.265 MM    0.3742 2.64226e4  1176.90479  95.2581
       2  16.969 MM    0.4744 1315.29187   33.62722   4.7419

    Totals :                  2.77379e4  1210.53201

     Results obtained with enhanced integrator!
```

\\Pmsl-analysis2\HP LaserJet P3015 on Ne00:
Letter 8 1/2 x 11 in/Portrait

Close | normal | Page 1 of 1

HPLC analysis of HCT4

Data File C:\HPCHEM\1\DATA\2018\052318\-HCT-13.D Sample Name: HCT-13

```
==================================================================
Injection Date  : 5/23/2018 3:43:29 PM          Seq. Line :   4
Sample Name     : HCT-13                         Location : Vial 3
Acq. Operator   : JC                                 Inj :   1
                                                Inj Volume : 10 µl
Acq. Method     : C:\HPCHEM\1\METHODS\JC-RP1.M
Last changed    : 5/23/2018 1:25:21 PM by JC
Analysis Method : C:\HPCHEM\1\METHODS\JV095.M
Last changed    : 12/12/2018 12:25:44 PM by Juno
                  (modified after loading)
```

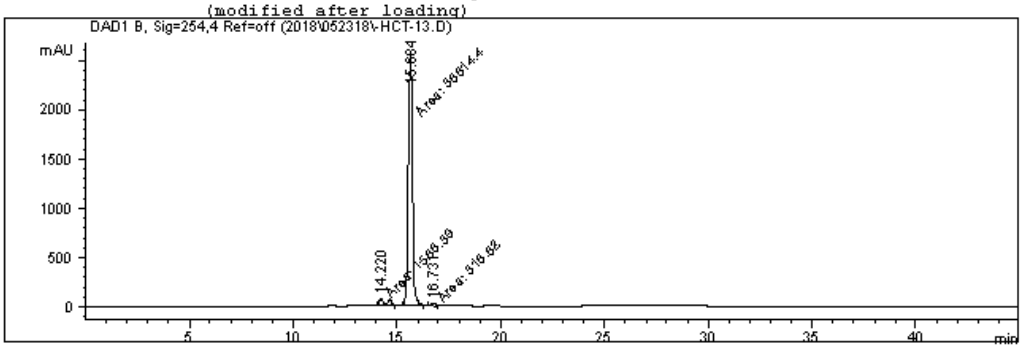


```
==================================================================
                        Area Percent Report
==================================================================

Sorted By             :      Signal
Multiplier            :      1.0000
Dilution              :      1.0000
Use Multiplier & Dilution Factor with ISTDs


Signal 1: DAD1 B, Sig=254,4 Ref=off

Peak RetTime Type  Width     Area      Height     Area
  #   [min]        [min]   [mAU*s]     [mAU]       %
----|-------|----|-------|----------|----------|--------|
   1  14.220 MM    0.4198 1566.38757   62.18721   4.0478
   2  15.684 MM    0.2410 3.68144e4  2545.99316  95.1335
   3  16.731 MM    0.2644  316.82050   19.97300   0.8187

Totals :                  3.86976e4  2628.15338

 Results obtained with enhanced integrator!
```

\\Pmsl-analysis2\HP LaserJet P3015 on Ne00:
Letter 8 1/2 x 11 in/Portrait

Close | normal | Page 1 of 1

HPLC analysis of HCT5

Data File C:\HPCHEM\1\DATA\2018\052318\-HCT-15.D Sample Name: HCT-15

```
==================================================================
Injection Date  : 5/23/2018 5:14:51 PM          Seq. Line :   6
Sample Name     : HCT-15                         Location : Vial 5
Acq. Operator   : JC                                 Inj :   1
                                                Inj Volume : 10 µl
Acq. Method     : C:\HPCHEM\1\METHODS\JC-RP1.M
Last changed    : 5/23/2018 1:25:21 PM by JC
Analysis Method : C:\HPCHEM\1\METHODS\JV095.M
Last changed    : 12/12/2018 12:25:44 PM by Juno
                  (modified after loading)
```

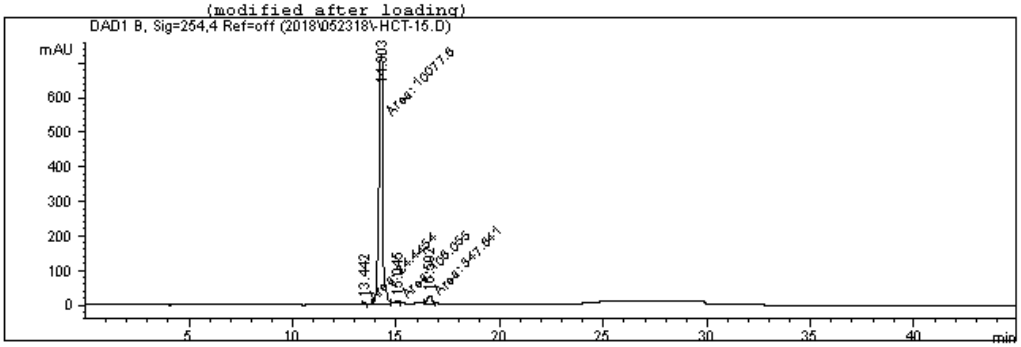


```
==================================================================
                        Area Percent Report
==================================================================

Sorted By             :      Signal
Multiplier            :      1.0000
Dilution              :      1.0000
Use Multiplier & Dilution Factor with ISTDs


Signal 1: DAD1 B, Sig=254,4 Ref=off

Peak RetTime Type  Width     Area      Height     Area
  #   [min]        [min]   [mAU*s]     [mAU]       %
----|-------|----|-------|----------|----------|--------|
   1  13.442 MM    0.1510   24.44536    2.69893   0.2316
   2  14.303 MM    0.2321 1.00778e4   723.61749  95.4686
   3  15.045 MM    0.2343  106.05492    7.54276   1.0047
   4  16.592 MM    0.2723  347.84100   21.28913   3.2951

Totals :                  1.05562e4   755.14832
```

\\Pmsl-analysis2\HP LaserJet P3015 on Ne00:
Letter 8 1/2 x 11 in/Portrait

Close | normal | Page 1 of 1

HPLC analysis of HCT6

Data File C:\HPCHEM\1\DATA\2018\062718\IQ1'.D Sample Name: IQ1'

```
==================================================================
Injection Date  : 6/27/2018 5:51:21 PM          Seq. Line :   8
Sample Name     : IQ1'                           Location : Vial 51
Acq. Operator   : JC                                 Inj :   1
                                                Inj Volume : 10 µl
Acq. Method     : C:\HPCHEM\1\METHODS\JC-RP2.M
Last changed    : 6/27/2018 4:51:44 PM by JC
                  (modified after loading)
Analysis Method : C:\HPCHEM\1\METHODS\JV095.M
Last changed    : 12/12/2018 12:25:44 PM by Juno
                  (modified after loading)
```

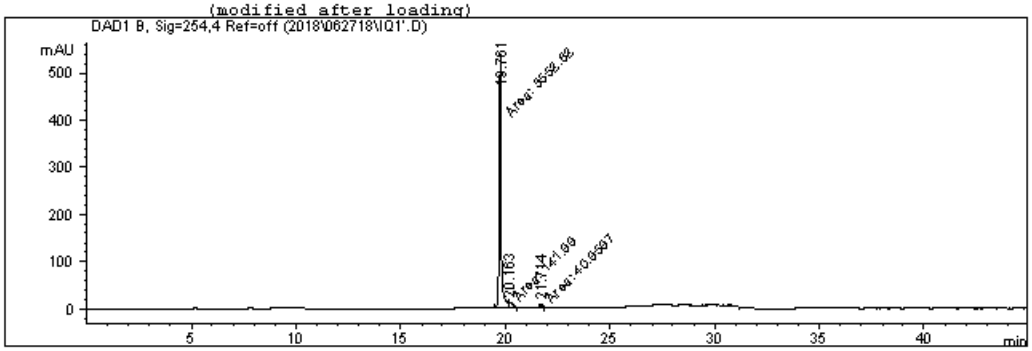


```
==================================================================
                      Area Percent Report
==================================================================

Sorted By             :      Signal
Multiplier            :      1.0000
Dilution              :      1.0000
Use Multiplier & Dilution Factor with ISTDs


Signal 1: DAD1 B, Sig=254,4 Ref=off

Peak RetTime Type  Width     Area      Height     Area
  #   [min]        [min]   [mAU*s]     [mAU]       %
----|-------|----|-------|----------|----------|--------|
   1  19.761 MM    0.1097 3552.81543  539.77997  95.1028
   2  20.163 MM    0.1535  141.98978   10.95285   3.8008
   3  21.714 MM    0.1266   40.95975    5.39103   1.0964

Totals :                  3735.76495  556.12385
```

\\Pmsl-analysis2\HP LaserJet P3015 on Ne00:
Letter 8 1/2 x 11 in/Portrait

Close | normal | Page 1 of 1

HPLC analysis of HCT7

Data File C:\HPCHEM\1\DATA\2018\052418\--HCT-21.D Sample Name: HCT-21

```
==========================================================================
Injection Date  : 5/24/2018 9:27:30 PM          Seq. Line :   5
Sample Name     : HCT-21                        Location : Vial 4
Acq. Operator   : JC                               Inj :   1
                                                Inj Volume : 10 µl
Acq. Method     : C:\HPCHEM\1\METHODS\JC-RP1.M
Last changed    : 5/23/2018 1:25:21 PM by JC
Analysis Method : C:\HPCHEM\1\METHODS\JV095.M
Last changed    : 12/12/2018 12:25:44 PM by Juno
                  (modified after loading)
```

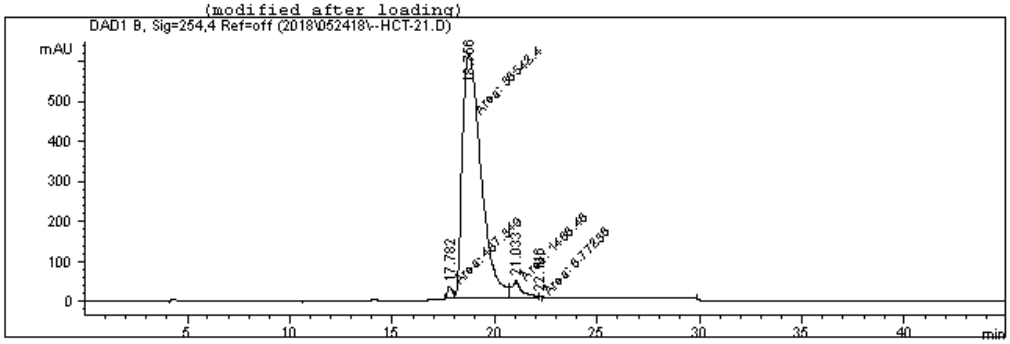


```
==========================================================================
                          Area Percent Report
==========================================================================

Sorted By             :      Signal
Multiplier            :      1.0000
Dilution              :      1.0000
Use Multiplier & Dilution Factor with ISTDs


Signal 1: DAD1 B, Sig=254,4 Ref=off

Peak RetTime Type  Width     Area      Height     Area
  #   [min]        [min]   [mAU*s]     [mAU]       %
----|-------|----|-------|----------|----------|--------|
   1  17.782 MF    0.2595  467.34909   30.01972   1.1543
   2  18.756 MF    1.0520 3.85424e4   610.60626  95.1970
   3  21.033 FM    0.6042 1468.46191   40.50690   3.6270
   4  22.116 MM    0.0907    8.77236    1.61284   0.0217

Totals :                  4.04870e4   682.74572
```

\\Pmsl-analysis2\HP LaserJet P3015 on Ne00:
Letter 8 1/2 x 11 in/Portrait

Close | normal | Page 1 of 1

HPLC analysis of HCT8

Data File C:\HPCHEM\1\DATA\2018\071618\HCT27.D Sample Name: HCT27

```
    ======================================================================
    Injection Date  : 7/16/2018 6:43:05 PM          Seq. Line :   3
    Sample Name     : HCT27                          Location : Vial 62
    Acq. Operator   : JC                                 Inj :   1
                                                    Inj Volume : 10 µl
    Acq. Method     : C:\HPCHEM\1\METHODS\JC-RP2.M
    Last changed    : 7/16/2018 5:08:35 PM by JC
    Analysis Method : C:\HPCHEM\1\METHODS\JV095.M
    Last changed    : 12/12/2018 12:25:44 PM by Juno
                      (modified after loading)
```

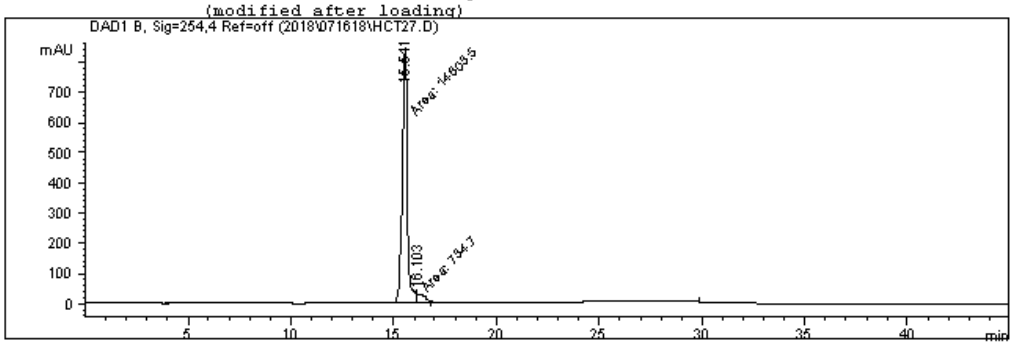


```
    ======================================================================
                              Area Percent Report
    ======================================================================

    Sorted By             :      Signal
    Multiplier            :      1.0000
    Dilution              :      1.0000
    Use Multiplier & Dilution Factor with ISTDs


    Signal 1: DAD1 B, Sig=254,4 Ref=off

    Peak RetTime Type  Width     Area      Height     Area
      #   [min]        [min]   [mAU*s]     [mAU]       %
    ----|-------|----|-------|----------|----------|--------|
       1  15.541 MM    0.2966 1.46035e4   820.66400  95.2100
       2  16.103 MM    0.3201  734.70013   29.00597   4.7900

    Totals :                  1.53382e4   849.66997

     Results obtained with enhanced integrator!
    ======================================================================
```

\\Pmsl-analysis2\HP LaserJet P3015 on Ne00:
Letter 8 1/2 x 11 in/Portrait

Close | normal | Page 1 of 1

HPLC analysis of HCT9

Data File C:\HPCHEM\1\DATA\2018\052318\-HCT-14.D Sample Name: HCT-14

```
==================================================================
Injection Date  : 5/23/2018 4:29:10 PM          Seq. Line :   5
Sample Name     : HCT-14                         Location : Vial 4
Acq. Operator   : JC                                Inj :   1
                                                Inj Volume : 10 µl
Acq. Method     : C:\HPCHEM\1\METHODS\JC-RP1.M
Last changed    : 5/23/2018 1:25:21 PM by JC
Analysis Method : C:\HPCHEM\1\METHODS\JV095.M
Last changed    : 12/12/2018 12:25:44 PM by Juno
                  (modified after loading)
```

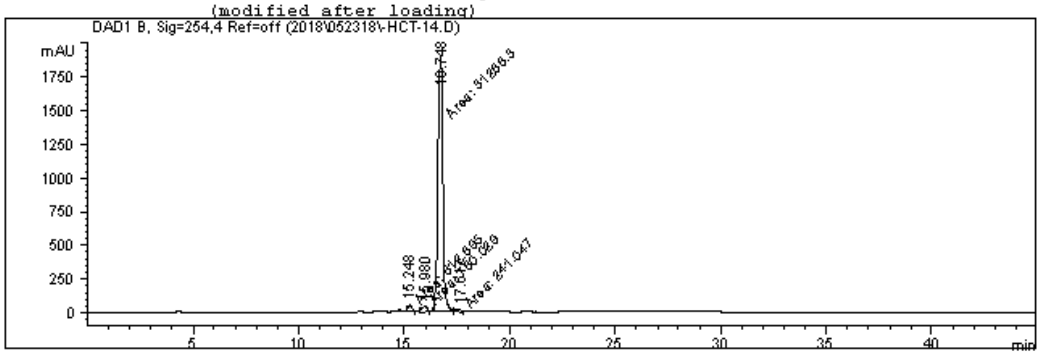


```
==================================================================
                        Area Percent Report
==================================================================

Sorted By             :      Signal
Multiplier            :      1.0000
Dilution              :      1.0000
Use Multiplier & Dilution Factor with ISTDs


Signal 1: DAD1 B, Sig=254,4 Ref=off

Peak RetTime Type  Width     Area      Height     Area
  #   [min]        [min]   [mAU*s]     [mAU]       %
----|-------|----|-------|----------|----------|--------|
   1  15.248 MM    0.2206  612.69458   46.28159   1.8633
   2  15.980 MM    0.3007  760.02936   42.12210   2.3114
   3  16.748 MM    0.2747 3.12683e4  1897.07532  95.0923
   4  17.617 MM    0.2869  241.04727   14.00450   0.7331

Totals :                  3.28821e4  1999.48352
```

\\Pmsl-analysis2\HP LaserJet P3015 on Ne00:
Letter 8 1/2 x 11 in/Portrait

Close | normal | Page 1 of 1

HPLC analysis of HCT10

Data File C:\HPCHEM\1\DATA\2018\052318\-HCT-16.D Sample Name: HCT-16

```
==================================================================
Injection Date  : 5/23/2018 6:00:34 PM          Seq. Line :   7
Sample Name     : HCT-16                         Location : Vial 6
Acq. Operator   : JC                                Inj :   1
                                                Inj Volume : 10 µl
Acq. Method     : C:\HPCHEM\1\METHODS\JC-RP1.M
Last changed    : 5/23/2018 1:25:21 PM by JC
Analysis Method : C:\HPCHEM\1\METHODS\JV095.M
Last changed    : 12/12/2018 12:25:44 PM by Juno
                  (modified after loading)
```

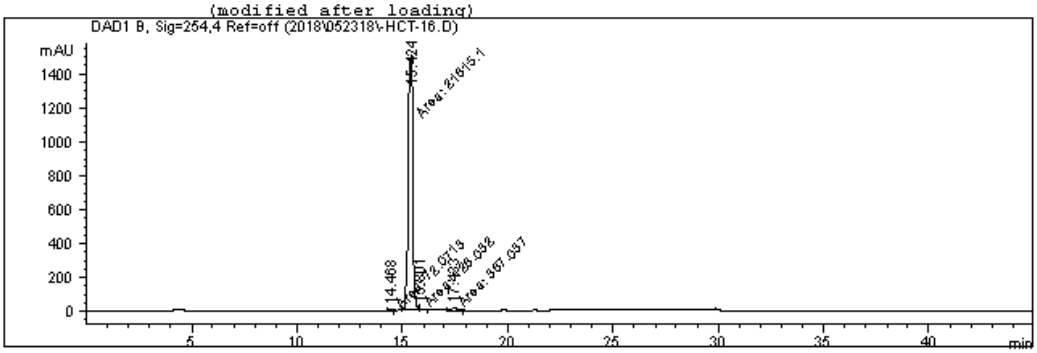


```
==================================================================
                        Area Percent Report
==================================================================

Sorted By             :      Signal
Multiplier            :      1.0000
Dilution              :      1.0000
Use Multiplier & Dilution Factor with ISTDs


Signal 1: DAD1 B, Sig=254,4 Ref=off

Peak RetTime Type  Width     Area      Height     Area
  #   [min]        [min]   [mAU*s]     [mAU]       %
----|-------|----|-------|----------|----------|--------|
   1  14.468 MM    0.2170   72.07128    5.53416   0.3217
   2  15.424 MM    0.2410 2.18151e4  1508.36548  97.3878
   3  15.801 MM    0.1281  126.03214   13.05827   0.5626
   4  17.433 MM    0.3947  387.03723   16.34200   1.7278

Totals :                  2.24003e4  1543.29991
```

\\Pmsl-analysis2\HP LaserJet P3015 on Ne00:
Letter 8 1/2 x 11 in/Portrait

Close | normal | Page 1 of 1

HPLC analysis of HCT11

Data File C:\HPCHEM\1\DATA\2018\062718\IQ1''.D Sample Name: IQ1''

```
    ======================================================================
    Injection Date  : 6/27/2018 6:37:07 PM          Seq. Line :   9
    Sample Name     : IQ1''                         Location : Vial 52
    Acq. Operator   : JC                               Inj :   1
                                                   Inj Volume : 10 µl
    Acq. Method     : C:\HPCHEM\1\METHODS\JC-RP2.M
    Last changed    : 6/27/2018 4:51:44 PM by JC
                      (modified after loading)
    Analysis Method : C:\HPCHEM\1\METHODS\JV095.M
    Last changed    : 12/12/2018 12:25:44 PM by Juno
                      (modified after loading)
```

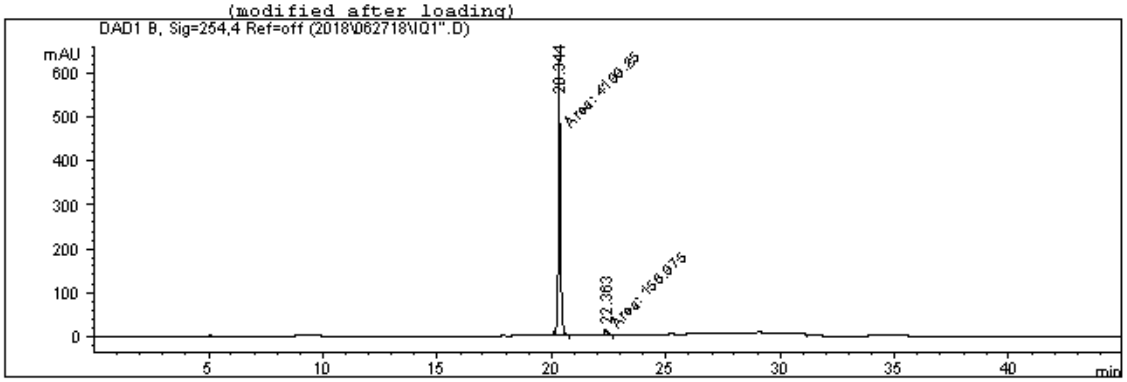


```
    ======================================================================
                              Area Percent Report
    ======================================================================

    Sorted By             :      Signal
    Multiplier            :      1.0000
    Dilution              :      1.0000
    Use Multiplier & Dilution Factor with ISTDs


    Signal 1: DAD1 B, Sig=254,4 Ref=off

    Peak RetTime Type  Width     Area      Height     Area
      #   [min]        [min]   [mAU*s]     [mAU]       %
    ----|-------|----|-------|----------|----------|--------|
       1  20.344 MM    0.1105 4199.24951  633.14288  96.3965
       2  22.363 MM    0.1682  156.97470   15.55715   3.6035

    Totals :                  4356.22421  648.70003

     Results obtained with enhanced integrator!
```

HPLC analysis of HCT12

Data File C:\HPCHEM\1\DATA\2018\071718\HCT32B12.D Sample Name: HCT32b12

```
==================================================================
Injection Date  : 7/17/2018 10:33:19 PM          Seq. Line :   2
Sample Name     : HCT32b12                        Location : Vial 61
Acq. Operator   : JC                                 Inj :   1
                                                 Inj Volume : 10 µl
Acq. Method     : C:\HPCHEM\1\METHODS\JC-RP2.M
Last changed    : 7/17/2018 9:46:20 PM by JC
Analysis Method : C:\HPCHEM\1\METHODS\JV095.M
Last changed    : 12/12/2018 12:25:44 PM by Juno
                  (modified after loading)
```

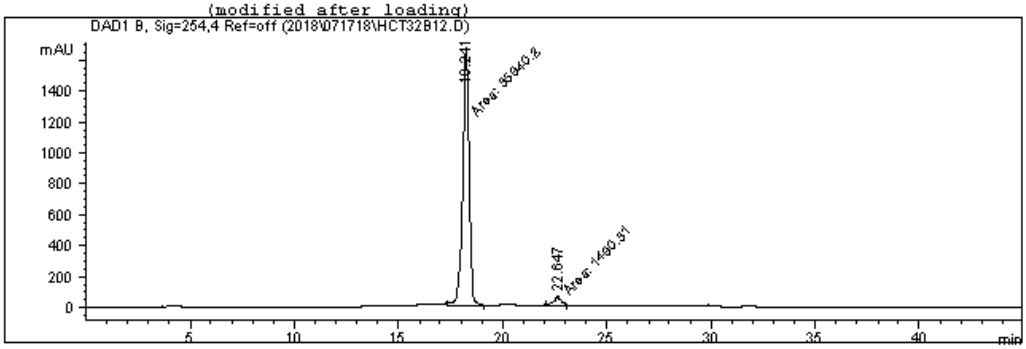


```
==================================================================
                        Area Percent Report
==================================================================

Sorted By             :      Signal
Multiplier            :      1.0000
Dilution              :      1.0000
Use Multiplier & Dilution Factor with ISTDs


Signal 1: DAD1 B, Sig=254,4 Ref=off

Peak RetTime Type  Width     Area      Height     Area
  #   [min]        [min]   [mAU*s]     [mAU]       %
----|-------|----|-------|----------|----------|--------|
   1  18.241 MM    0.3684 3.59402e4  1626.01050  96.0185
   2  22.647 MM    0.4370 1490.30554   56.83894   3.9815

Totals :                  3.74305e4  1682.84944

 Results obtained with enhanced integrator!
==================================================================
```

\\Pmsl-analysis2\HP LaserJet P3015 on Ne00:
Letter 8 1/2 x 11 in/Portrait

Close | normal | Page 1 of 1

HPLC analysis of HCT13

Data File C:\HPCHEM\1\DATA\2018\062718\HCT28.D Sample Name: HCT28

```
==================================================================
Injection Date  : 6/27/2018 2:48:17 PM          Seq. Line :   4
Sample Name     : HCT28                          Location : Vial 55
Acq. Operator   : JC                                 Inj :   1
                                                Inj Volume : 10 µl
Acq. Method     : C:\HPCHEM\1\METHODS\JC-RP2.M
Last changed    : 6/27/2018 12:29:49 PM by JC
Analysis Method : C:\HPCHEM\1\METHODS\JV095.M
Last changed    : 12/12/2018 12:25:44 PM by Juno
                  (modified after loading)
```

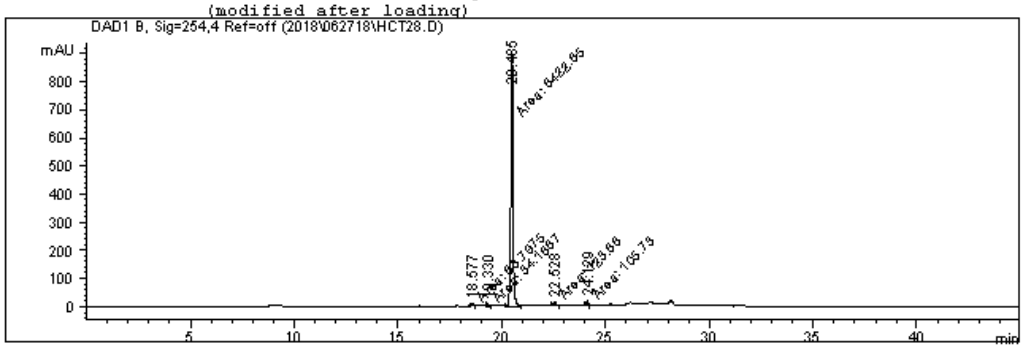


```
==================================================================
                        Area Percent Report
==================================================================

Sorted By             :      Signal
Multiplier            :      1.0000
Dilution              :      1.0000
Use Multiplier & Dilution Factor with ISTDs


Signal 1: DAD1 B, Sig=254,4 Ref=off

Peak RetTime Type  Width     Area      Height     Area
  #   [min]       [min]    [mAU*s]     [mAU]       %
----|-------|----|-------|----------|----------|--------|
   1  18.577 MM    0.1399   63.79748    7.60011   0.9451
   2  19.330 MM    0.0869   34.18670    6.55693   0.5065
   3  20.485 MM    0.1189 6422.64941  900.17096  95.1469
   4  22.528 MM    0.1418  123.87982   14.56061   1.8352
   5  24.129 MM    0.1046  105.72972   16.84713   1.5663

Totals :                  6750.24314  945.73574
```

\\Pmsl-analysis2\HP LaserJet P3015 on Ne00:
Letter 8 1/2 x 11 in/Portrait

Close | normal | Page 1 of 1

HPLC analysis of HCT14

Data File C:\HPCHEM\1\DATA\2018\082818\HCT33.D Sample Name: HCT33

```
==========================================================================
Injection Date  : 8/28/2018 11:11:26 AM          Seq. Line :   3
Sample Name     : HCT33                          Location : Vial 65
Acq. Operator   : JC                                Inj :   1
                                                 Inj Volume : 250 µl
Different Inj Volume from Sequence !     Actual Inj Volume : 20 µl
Acq. Method     : C:\HPCHEM\1\METHODS\JC-ISOQH.M
Last changed    : 8/24/2018 4:40:23 PM by JC
Analysis Method : C:\HPCHEM\1\METHODS\JV095.M
Last changed    : 12/12/2018 12:25:44 PM by Juno
                  (modified after loading)
```

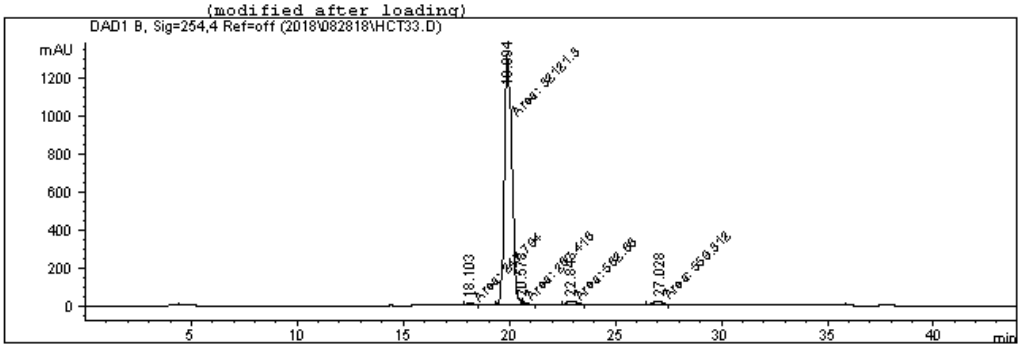


```
==========================================================================
                          Area Percent Report
==========================================================================

Sorted By             :      Signal
Multiplier            :      1.0000
Dilution              :      1.0000
Use Multiplier & Dilution Factor with ISTDs


Signal 1: DAD1 B, Sig=254,4 Ref=off

Peak RetTime Type  Width     Area      Height     Area
  #   [min]        [min]   [mAU*s]     [mAU]       %
----|-------|----|-------|----------|----------|--------|
   1  18.103 MM    0.3311  247.79393   12.47283   0.7331
   2  19.894 MM    0.4048 3.21213e4  1322.54614  95.0371
   3  20.578 MM    0.2189  287.41635   21.88802   0.8504
   4  22.843 MM    0.5525  582.85968   17.58376   1.7245
   5  27.028 MM    0.4419  559.31183   21.09399   1.6548
```

\\Pmsl-analysis2\HP LaserJet P3015 on Ne00:
Letter 8 1/2 x 11 in/Portrait

Close | normal | Page 1 of 1

HPLC analysis of HCT15

Data File C:\HPCHEM\1\DATA\121120 18\JVVBLNK.D Sample Name: JVV blank

```
==================================================================
Injection Date  : 12/11/2018 7:27:46 AM          Seq. Line :   2
Sample Name     : JVV blank                       Location : Vial 40
Acq. Operator   : Juno                               Inj :   1
                                                 Inj Volume : 250 µl
Different Inj Volume from Sequence !     Actual Inj Volume : 30 µl
Acq. Method     : C:\HPCHEM\1\METHODS\JV095.M
Last changed    : 12/11/2018 6:56:31 AM by Juno
                  (modified after loading)
Analysis Method : C:\HPCHEM\1\METHODS\JV095.M
Last changed    : 12/12/2018 12:25:44 PM by Juno
                  (modified after loading)
```

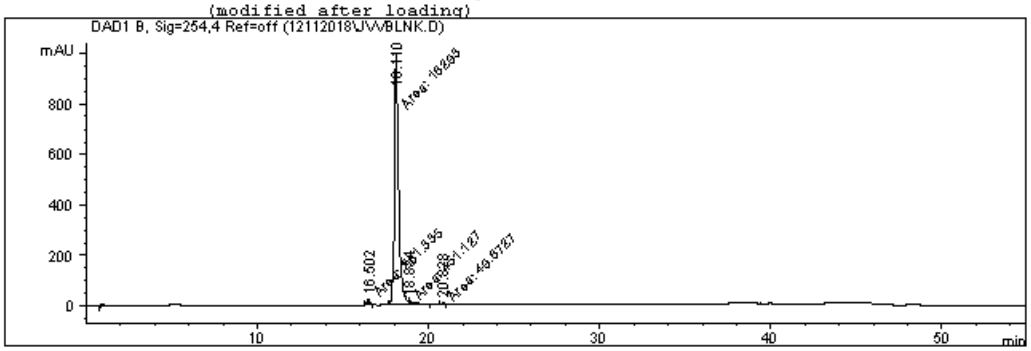


```
==================================================================
                        Area Percent Report
==================================================================

Sorted By             :      Signal
Multiplier            :      1.0000
Dilution              :      1.0000
Use Multiplier & Dilution Factor with ISTDs


Signal 1: DAD1 B, Sig=254,4 Ref=off

Peak RetTime Type  Width     Area      Height     Area
  #   [min]        [min]   [mAU*s]     [mAU]       %
----|-------|----|-------|----------|----------|--------|
   1  16.502 MM    0.1977  281.33484   23.71385   1.6476
   2  18.110 MM    0.2741 1.62930e4   990.64117  95.4195
   3  18.834 MM    0.3645  451.12701   14.48537   2.6420
   4  20.828 MM    0.2080   49.67268    3.98066   0.2909
```

\\Pmsl-analysis2\HP LaserJet P3015 on Ne00:
Letter 8 1/2 x 11 in/Portrait

Close | normal | Page 1 of 1

References

1. Agrawal, et al., J. Med. Chem. 1968, 11(4), 700-703.